ISSUES ON MANAGING SUSTAINABLE OPERATIONS

ZOU DING

PhD

The Hong Kong Polytechnic University

2022

The Hong Kong Polytechnic University
Department of Logistics and Maritime Studies

Issues on Managing Sustainable Operations

Zou Ding

A thesis submitted in partial fulfillment of the requirements for
the degree of Doctor of Philosophy
April 2022

CERTIFICATE OF ORIGINALITY

I hereby declare that this thesis is my own work and that, to the best of my knowledge and belief, it reproduces no material previously published or written, nor material that has been accepted for the award of any other degree or diploma, except where due acknowledgment has been made in the text.

Signature: _____

Name of Student: Zou Ding

Abstract

In this thesis, we explore two issues related to efficient resource utilization to support the sustainable development goal for our society. To achieve sustainable operations, firms are encouraged to positively impact customers as well as the environment in addition to pursue profit. For example, a last-mile transportation service provider can increase the utilization of limited vehicle resource, which provides customers a convenient alternative for short-distance travel in urban area and hence helps reduce the carbon emissions from automobiles. Another example is that, a firm selling consumer product can use recycled materials that saves production resource and waste to help citizens live in a better environment. Both of them save the resource and provide customers a more sustainable lifestyle. We further elaborate the two aforementioned aspects as follows.

In the first topic, we consider the efficient operations of limited amount of vehicles that can be allocated to urban area in a shared micromobility system. A micromobility service provider can crowdsource individual riders to conduct vehicle relocation with reward incentives and outsource relocation to a third-party logistics provider (3PL). The former performs vehicle relocation continuously while the latter runs the relocation following a certain schedule. We construct a time-space network with multiple regions and formulate a two-stage stochastic integer programming model incorporating riders' demand uncertainty. In the first stage, the micromobility operator plans the initial vehicle allocation across service regions, while in the second stage, he decides subsequent vehicle relocation across the regions over an operational horizon. To enable the practical significance of our model, we develop a temporal decomposition algorithm, which outperforms a state-of-the-art commercial solver in solution quality and computational time for solving large-scale problem instances based on real data. Numerical experiments show that 3PL outsourcing is

more efficient for mass relocation than rider crowdsourcing, while the latter is more efficient in handling sporadic relocation needs. Introducing rider crowdsourcing in addition to 3PL outsourcing can significantly increase the profit, reduce the demand loss, and improve the vehicle utilization rate of the system without affecting the existing commitment with the 3PL. The budget for acquiring vehicles and the budget for rider crowdsourcing significantly impact the vehicles' initial allocation and subsequent relocation. We also find that rider crowdsourcing relocates more vehicles under a unimodal demand pattern than a bimodal pattern, whereas the reverse holds for 3PL outsourcing.

In the second topic, we consider how the recycled materials in a sustainable product can be impacted by the recycling label. In practice, there are many different types of recycling label issued by NGOs. We consider two types of commonly observed recycling labels: 1) Percentage label that conducts a continuous grading assessment, from which consumers know exactly the fraction of recycled content; 2) Binary label that implements a pass/fail criterion, from which consumers only know whether the fraction of recycled content meets the standard or not. We establish a game-theoretical model wherein an NGO needs to decide the label type and a monopoly firm decides the fraction of recycled content and price for its product. The firm sells its product to consumers who cannot directly observe the fraction of recycled content used in the product but can obtain information from the label on the product. Some consumers are environmentally conscious who are willing to pay a premium for the recycled content; and others are environmentally unconscious who are indifferent in recycled and non-recycled content. We examine the impacts of different labelling schemes on a firm's recycling and pricing decisions as well as an NGO's payoff and consumer surplus. We highlight a few interesting findings. First, the firm weakly prefers the percentage label, while NGO and consumers weakly prefer the binary label. Second, more environmentally conscious consumers or lower fixed cost of recycling may not necessarily increase the firm's usage of recycled materials under the binary label, and may indeed hurt the consumer surplus under either label type. These findings can provide useful managerial insights for NGOs and firms who are concerned about recycled materials.

Publications Arising from the Thesis

Zou, D., Wang, Y.L., Lim, Y.F., Pan, K., Shen, Z.-J.M. 2022. Vehicle Rebalancing in A Shared Micromobility System with Rider Crowdsourcing. *Major Revision at MSOM.*

Guo, X.M., **Zou, D.** 2022. Impacts of Recycling Label Scheme on Firm's Recycling and Pricing Decisions. *Reject and Resubmission for POM.*

Acknowledgements

It has been five years since I enrolled in the PhD program in operations management. Looking back, I feel this journey like a roller coaster, full of ups and downs. I would not be able to successfully go through my PhD study and complete my thesis without the help and encouragement from my three supervisors, Dr. Xiaomeng Guo, Dr. Kai Pan and Professor Yulan Wang as well as my fellow students and family members. How time flies! At this moment and hereafter, I will always cherish whatever I have experienced, which witnesses my gradual growth in soul and body.

At the very beginning, I had shallow research experience in optimization for practical engineering problems. I gratefully thank my supervisors for training me from that fundamental stage. As a green hand who just embarked on the research in the field of operations management, I worked closely with my supervisors and raced against time to quickly absorb the most relevant research methodology used in my new projects. Meanwhile, I made up for my lack of knowledge in economics, game theory, combinatorial optimization and so on. The first year and a half filled my life with courses across campus, homework projects, trials and errors in the research projects. I felt many downs when I performed below my expectation. Fortunately, I was encouraged and understood by my supervisors. Although, honestly, I was not able to handle the course and research projects well enough, I made small and gradual progress day by day. I regarded it as a good sign to keep me sparing more effort to face and overcome the upcoming challenges. In the next two and a half years, I spent most of my time and energy on the formation of two working papers, which finally led to this thesis. Whenever I need help and discussions, I could easily reach my supervisors for advices. It was their patient guidance that I overcame many difficulties. It were those moments that I felt ups and moved to a little higher

stage. In the last year, I felt grateful that Dr. Guo and Dr. Pan continuously spent time improving and polishing my drafts. During this process, I gained more comprehensive view in improving the logic and consistency of my previous drafts. There are so many other periods that are crucial for my personal development and I want to thank again for whom offered kind help.

First, I deeply appreciate the step-by-step teaching by my three supervisors, especially Dr. Guo and Dr. Pan whom I worked with most frequently. We had meetings over once a week in my first year, which timely corrected my direction when I fell onto a wrong track. Second, I feel happy to have a crowd of senior and junior research students in MN037 and MN038. Thank Yanli Tang and Shuli Liu for sharing their research experiences and their encouragement for my research. Thank Hansin Zhang and Freya Liu for organizing fantastic activities indoors and outdoors, which filled my life with simple but happy hours outside the research. Thank Zepeng Chen for often accompanying my dinner and sharing academic and daily stories during the last two years. Thank Ziliang Jin for often discussing our difficulties in optimization.

Last but not least, I have always felt gratified that my parents and family members are so supportive of my PhD study. They always cared me and consoled me when I got stuck and their phone calls were so heartwarming. I also thank Betty Huang for encouraging me all the time during my last academic year. I wish all the best for those who love me and all those I love.

Table of Contents

List of Figures

List of Tables

Chapter 1

Introduction

Sustainable development is the international community's most urgent priority. In academia, the community of operations management is actively exploring what solutions can serve the sustainable goal. Being a major part in the business world, 90% of firms feel they need to change their core business models in some way to operate in a truly sustainable economy (Bain & Company 2018). Indeed, many decisions that determine a firm's sustainability impact also naturally intersect with established operations management streams such as product design and transportation system (Drake and Spinler 2013). Aiming to contribute to the sustainable development research from the lens of operations management, this thesis focuses on the two aforementioned streams regarding a sustainable last-mile mobility system and a green product with recycled materials, respectively. Particularly, the first study investigates the planning effectiveness and operational efficiency in the shared micromobility system with crowdsourcing relocation riders. The second study, regarding the sustainable use of natural resources, investigates the impact of different recycling label schemes on firms' recycling decisions. Both of them contribute to efficient resource utilization for the sustainable goal.

In Chapter 2, we focus on the planning and operational design for a sustainable shared micromobility system. In contrast to other mobility systems, the shared micromobility firm is burdened with physical assets (e.g., micromobility vehicles). It has flexible pick-up and drop-off spots and no self-regulated owner to ride the vehicle to meet the demand. These features intensify the supply-demand mismatch during operations. Thus, it is crucial to smartly allocate and relocate the vehicles

so that the firm can sustainably earn profit. We particularly investigate the micromobiliy vehicle rebalancing with third-party logistics (3PL) and/or crowdsourcing relocation riders. This part of the work was motivated by the innovative operations in the shared micromobility system. For example, *Bird* and *Mobike* provide customers with rewards to incentivize them to help relocate the vehicles. This innovative relocation method is in contrast to the traditional 3PL relocation. Then, we are interested in the following questions: How shall a shared micromobility firm allocate its vehicles and conduct the relocation to balance the supply and uncertain demand to improve its profit? How does the adoption of each relocation strategy (crowdsourcing and/or 3PL outsourcing) affect the system efficiency? How do the system parameters (e.g., demand patterns and the demand loss penalty) affect the performance of the two relocation methods? What is the optimal relocation strategy that a shared micromobility system shall adopt, and under what conditions?

We construct a time-space network with multiple regions and formulate a two-stage stochastic mixed-integer programming model that considers uncertain customer demands. In the first stage, the micromobility operator decides the initial vehicle allocation for the service regions, whereas in the second stage, he determines subsequent vehicle relocation across the regions over an operational horizon. We develop an efficient solution approach that incorporates scenario-based and time-based (temporal) decomposition ideas. Our approach outperforms a commercial solver in solution quality and computational time for solving large-scale problem instances based on real data. Our model and algorithm can help the micromobility firm make more comprehensive decisions towards the sustainable vehicle operations.

Then, we derive the following insights from numerical experiments with the dataset from Citi Bike. We first find that the 3PL outsourcing is more efficient for mass relocation than rider crowdsourcing, while the latter can be more efficient in handling sporadic relocation needs. Second, the budget for acquiring vehicles and the budget for rider crowdsourcing significantly impact the vehicles' initial allocation and subsequent relocation. Third, the 3PL often conducts relocation around peak hours of a day by moving vehicles in batches from faraway, low-demand regions, whereas rider crowdsourcing is engaged throughout the day to relocate a few

vehicles each time from neighboring regions. At last, rider crowdsourcing relocates more vehicles under a unimodal demand pattern than a bimodal pattern, whereas the reverse holds for 3PL outsourcing. These results inform how to improve the operational efficiency and profitability in shared micromobility systems.

In Chapter 3, we focus on the recycling label design for sustainable consumer products. We study the impacts of different recycling label schemes on a firm's recycling and pricing decisions as well as an NGO's payoff and consumers' surplus. This part of the work was based on observing diverse environmental labels in the current market, which convey different levels of recycled content information. The more the recycled material is used, the less waste is generated. However, when making recycling and pricing decisions, a profit-maximizing firm needs to be concerned about consumers' recognition of its green practice. Consumers usually do not have direct information regarding the recycled material in a product. A recycling label is one of the potential solutions that can serve the communication between the firm and consumers about the green efforts. Hence, the study on the labelling scheme contributes to waste reduction and sustainable product design. Specifically, we identify two types of labels issued by an NGO and they differ in the label information scheme for the recycled content. The first is a *binary label* with only one pass/fail standard. A product can apply the label if it contains the recycled material above the standard. The second, by contrast, is a *percentage label* that verifies and displays the actual percentage of the recycled material in a product. Then, we study the following three questions: (1) Under different labelling schemes, how are the firm's and NGO's payoffs influenced by the fraction of environmentally conscious consumers and the technology cost of recycling? (2) Which type of label benefits the firm? Which one is preferred by the NGO? (3) How is consumers' surplus influenced by the labelling scheme? For these questions, we establish a game-theoretical model wherein an NGO chooses the label type (binary or percentage) and a monopoly firm decides the fraction of the recycled material and price for its product.

We highlight our key insights as follows. First, we find that, as the fraction of environmentally conscious consumers increases or the fixed cost of recycling decreases, the firm's usage of recycled content increases under the percentage label, while it

may increase or decrease under the binary label. Second, the firm is always weakly better off under the percentage label than under the binary label. Third, NGO weakly prefers the binary label. Interestingly, under the percentage label, NGO can be worse off if more consumers become environmentally conscious or the technology cost of recycling reduces. Fourth, consumers weakly prefer the binary label to the percentage label. Noteworthily, under either percentage or binary label, more environmentally conscious consumers or lower fixed cost of recycling may hurt or benefit the consumer surplus. Our results can provide useful insights to facilitate an effective label design that helps convey information to consumers and also influences firms' recycling and pricing strategies.

In Chapter 4, we briefly summarize the main work in this thesis, and also point out some possible directions for future research relating to efficient resource utilization in the shared micromobility service or green products.

Chapter 2

Resource Utilization in A Shared Micromobility System: Vehicle Rebalancing with Rider Crowdsourcing

2.1 Introduction

A *shared micromobility system* consists of lightweight vehicles such as bikes, e-bikes, e-scooters, or e-mopeds. It offers an eco-friendly form of short-distance travel (e.g., last-mile transportation) and helps alleviate city congestion, achieving a sustainable urban transportation system (Simlett and Møller 2020, McKinsey 2021). During the COVID-19 pandemic, the shared micromobility system becomes even more popular as some people avoid taking crowded public transportation. In the U.S., around 60% of car trips are within 8 kilometers, making the shared micromobility system an excellent alternative. It is estimated that the micromobility market in the U.S. alone will reach 200 to 300 billion dollars by 2030 (McKinsey 2019).

A shared micromobility system differs from other *shared mobility systems* (e.g., car sharing and ride hailing) mainly because of the following three features. First, the shared micromobility system is asset heavy and its operator often bears high investment and operational costs of its physical assets (e.g., bikes) (Hasija et al. 2020). In a competitive market, these high costs cannot be covered by simply increasing rental prices because customers can easily switch to other mobility services (e.g., public transportation or car sharing). Thus, it is important for the operator to properly determine a total number of vehicles and allocate them to each service

region. Second, as there is no self-regulated owner for each micromobility vehicle, shared micromobility services are not provided on an on-demand basis like ride hailing because drivers do not ride a micromobility vehicle to search for customers. Third, customers of the shared micromobility system can pick up and drop off vehicles in any service region at any time. Such convenience often leads to a severe imbalance between the vehicle supply and demand in different regions, resulting in an oversupply of vehicles with few pick-ups in some regions and insufficient vehicles in others. Such imbalance can substantially undermine the system's operational efficiency, service quality, and profitability. As a result, the shared micromobility system requires efficient relocation of vehicles across the service regions.

The above three features draw special attention to the initial allocation and subsequent relocation of vehicles to help the shared micromobility system achieve economic viability and sustainability. In contrast to other mobility systems that adopt instruments such as increasing drivers' salaries or dynamic pricing to control the vehicle supply and demand, the operator of the shared micromobility system can first allocate and then relocate vehicles to balance their supply and demand for each service region. This allows the operator to boost profitability given the low profit margin of micromobility services.

Currently, many shared micromobility firms outsource the vehicle relocation to third-party logistics providers (3PLs). Each 3PL rebalances micromobility vehicles across service regions in batches of vehicles primarily by trucks to enjoy the economies of scale (Dell'Amico et al. 2014). Such 3PL relocation is often executed according to a certain schedule (e.g., in the early morning or late night) and may not meet all vehicle-relocation requirements. Each request for the 3PL relocation incurs a fixed setup cost. In fact, due to the high setup cost incurred in each request, it is too costly to frequently engage the 3PL to relocate vehicles across the service regions to rebalance the supply and demand.

To overcome this challenge, some shared micromobility firms adopt a crowdsourcing strategy to hire individual riders to relocate vehicles. Each crowdsourced rider relocates one vehicle at a time, and receives a reward from the operator upon completing the task. In addition to the financial rewards, the riders are motivated

by the fact that the relocation trips may be close to the riders' original travel routes or they use this opportunity to exercise. For example, Mobike rewards riders with coupons or cash to relocate bikes (Horwitz 2017) and Bird pays riders to charge and relocate e-scooters (Bird 2020). Such rider crowdsourcing can help relocate vehicles in a more flexible manner. In contrast to the 3PL relocation, rider crowdsourcing offers more flexibility by providing sporadic relocation. On the other hand, rider crowdsourcing increases the relocation cost because it loses the economies of scale and it relies on continuous tracking of the vehicle supply and demand for different service regions. Overall, the total cost of rider crowdsourcing may be higher than that of 3PL outsourcing if many vehicles are relocated.

To the best of our understanding, our work is the first to study the effectiveness and implications of combining 3PL outsourcing and rider crowdsourcing to rebalance shared micromobility vehicles. In particular, we are interested in the following research questions: How should a shared micromobility operator integrate the vehicle allocation and relocation decisions to match his finite supply with the uncertain demand to maximize his profit? Given a limited budget for acquiring vehicles, how does the budget affect the initial vehicle allocation for the regions and the subsequent vehicle relocation across the regions? Similarly, how does a budget for crowdsourcing individual riders affect the vehicle allocation and relocation? What is the best strategy for vehicle relocation (i.e., rider crowdsourcing only, 3PL outsourcing only, both of them, or none of them)? Under each relocation strategy, are there any interesting temporal or spatial features of the shared micromobility system? How do system parameters affect the performance of the system?

In this chapter, we consider an operator that provides a fleet of micromobility vehicles to satisfy customers' demands in a service area over an operational horizon with multiple periods. Due to government regulations, the entire service area is divided into multiple regions (He et al. 2017, Qi et al. 2018) with different vehicle allocation capacities. The customer demands in each period are uncertain. At the start of the horizon, the operator first decides the initial vehicle allocation for the different service regions without knowing the actual demands in each period. Subsequently, in each period, after the demands are realized, the operator determines

and executes the vehicle relocation across the regions (using rider crowdsourcing and 3PL outsourcing) to match the vehicles with the customer demands. Unsatisfied demands in each period are lost. The operator's objective is to maximize his expected profit over the operational horizon.

We make the following contributions for the work in this chapter:

(i) We formulate the operator's *integrated vehicle allocation and relocation problem* as a two-stage stochastic mixed-integer program (Birge and Louveaux 2011) on a time-space network. In the first stage, we decide the initial vehicle allocation for the service regions, whereas in the second stage we determine the subsequent vehicle relocation across the regions over the horizon. The vehicle relocation is modeled as recourse decisions after the demands are realized in each period.

(ii) We develop an efficient algorithmic approach that incorporates scenario-based and time-based (temporal) decomposition ideas to obtain high-quality solutions to the problem. Our numerical experiments based on data collected from Citi Bike (2021) suggest that our approach yields better solutions in a much shorter time than a commercial solver.

(iii) We obtain the following managerial insights for the micromobility operator. We find that the 3PL is more efficient in mass relocation than rider crowdsourcing, whereas the latter is more efficient in handling sporadic relocation needs. Introducing rider crowdsourcing in addition to the 3PL can significantly increase the profit, reduce the demand loss, and improve the vehicle utilization rate of the system without affecting the existing commitment with the 3PL. We also observe that the budget for acquiring vehicles and the budget for rider crowdsourcing have significant impact on the initial vehicle allocation and the subsequent vehicle relocation. We find that the 3PL often conducts relocation around peak hours of a day by moving vehicles in batches from faraway, low-demand regions, whereas rider crowdsourcing is engaged throughout the day to relocate a few vehicles each time from neighboring regions. Furthermore, rider crowdsourcing relocates more vehicles under a unimodal customer arrival pattern than a bimodal pattern, whereas the reverse holds for 3PL outsourcing.

After reviewing the related literature in Section 2.2, we formulate the problem

in Section 2.3. Section 2.4 studies structural results for the two-region case. Section 2.5 develops a solution approach for the general case with multiple regions. Section 2.6 performs extensive numerical experiments to examine the two vehicle-relocation methods based on the data from Citi Bike (2021). Section 2.7 concludes the chapter. All proofs are presented in Online Appendix.

2.2 Literature Review

Our work in this chapter is closely related to the Operations Management (OM) studies on shared mobility, a component of smart cities (Qi and Shen 2019, Mak 2022). The majority of literature on shared mobility focuses on vehicle-sharing systems, where people rent or hail cars from individual car owners or drivers for trips (e.g., Nair and Miller-Hooks 2014, Boyacı et al. 2015, and Feng et al. 2021). He et al. (2017) consider a service region design problem by incorporating fleet operations and the customer adoption rate for electric vehicles under uncertainty. Chang et al. (2017) optimize the car fleet location, size, and type via integer programming by considering a carbon emission constraint. Lu et al. (2018) optimize vehicle allocation under demand uncertainty and address the impact of one-way and round-way trips on the system's profit and service quality.

Shared micromobility, another type of shared mobility, further brings challenges and opportunities to OM researchers (Hasija et al. 2020). Recent work by Kabra et al. (2020) empirically investigates the impact of bike accessibility and availability on bike-share ridership by using a structural demand model. Our work is more related to Shu et al. (2013). Specifically, they build linear programming models with proportionality constraints to optimize the bicycle flows when the initial allocation of bicycles is given at each dock station and examine the impact of bicycle operations on the dock size. However, the decisions on initial allocation and fleet operations are inherently interdependent. Therefore, we consider an integrated allocation and relocation model in which an operator decides the initial vehicle allocation and subsequent vehicle relocation.

Our work also contributes to the literature on fleet operations on shared mobility. The existing studies extend the broader scope of inventory redistribution

or transshipment (Benjaafar et al. 2022), which has been widely investigated especially for the optimal stocking policy (Tagaras and Cohen 1992, Grahovac and Chakravarty 2001). Different approaches have been proposed to facilitate fleet operations for vehicle-sharing systems. Nair and Miller-Hooks (2011) minimize the cost of fleet redistribution by mixed-integer programming with chance constraints to ensure service level. Lu et al. (2018) implement dynamic vehicle relocation via a rolling horizon method. He et al. (2020) derive an optimal relocation policy for a two-region system and then use a linear decision rule to solve a distributionally robust model for a multi-region system.

Our work is more related to micromobility vehicle operations (e.g., fleet operations of bicycle-sharing systems). Dell'Amico et al. (2014) model bike relocation by trucks as a capacitated pickup-and-delivery vehicle routing problem and use a branch-and-cut algorithm to find solutions. Freund et al. (2020) consider truck- and trike-based rebalancing approaches for a bike-sharing system and formulate the underlying routing problems with integer programming to minimize expected customer dissatisfaction. Fu et al. (2022) build a two-stage robust model to optimize station location in the first stage and rebalancing vehicle assignment in the second stage, given the fixed number of stations and vehicles. The above studies often ignore the system operator's capacity design (e.g., bike allocation), which is more critical in shared micromobility than in vehicle-sharing as mentioned in Section 2.1. Furthermore, the above papers only consider bike relocation in batches and the corresponding route design problem. In contrast, our study considers different relocation strategies using rider crowdsourcing and 3PL outsourcing.

Finally, our work is related to OM studies on crowdsourcing. Crowdsourcing is widely studied in last-mile delivery operations, where independent car drivers (Qi et al. 2018, Fatehi and Wagner 2022) or cyclists (Kafle et al. 2017) are incentivized to provide customers with fast and on-time delivery services. Unlike goods that exit the delivery system once they are delivered, shared micromobility vehicles stay in the system after they are relocated. Such a difference inspires further studies that provide foundations for using crowdsourcing in micromobility vehicle relocation. According to a survey by Singla et al. (2015), customers are willing to alter their routes

to help relocate bikes given monetary incentives. Fricker and Gast (2016) analyze the steady-state performance of a bicycle-sharing system and show that incentivizing users to the least-loaded station leads to fewer problematic stations. He et al. (2021) formulate a model in which a two-sided matching platform (e.g., a free-float bike-sharing platform) determines both the spatial allocation of parking spaces and the design of incentive instruments (e.g., price and rewards to customers) that can affect the supply in each region. Huang et al. (2021) find that a sparse structure of a transshipment network can guide bike repositioning by crowdsourced volunteers and help reduce the rebalancing of workload without sacrificing much demand satisfaction. Unlike the above studies, our work in this chapter offers new insights by incorporating rider crowdsourcing and 3PL outsourcing in an integrated micromobility vehicle allocation and relocation model under different temporal demand patterns.

2.3 Problem Formulation

Consider a shared micromobility operator, who provides shared micromobility service for a set of regions $\mathcal{V} = \{1, 2, \ldots, V\}$ in each period $t \in \mathcal{T} = \{0, 1, \ldots, T-1\}$. We first describe the movement of micromobility vehicles across the service regions and then present our optimization model.

2.3.1 Vehicle Movement: A Time-Space Network

We model the vehicle movements among regions and across periods as flows in a time-space network $\mathcal{G} = (\mathcal{N}, \mathcal{A})$, where $\mathcal{N}$ is a set of nodes and $\mathcal{A}$ is a set of directed arcs on the network as shown in Figure 2.1. Service region $i \in \mathcal{V}$ in period $s \in \mathcal{T}$ is represented by node $n_{is} \in \mathcal{N}$. The *flow* on the directed arc $(n_{is}, n_{jt}) \in \mathcal{A}$ with $s \leq t-1$ represents the number of vehicles moving from node n_{is} to node n_{jt}. At the start of period 0, each node $n_{i0},\ i \in \mathcal{V}$, is allocated with an initial number of vehicles x_i. At the end of the operational horizon (period $T-1$), the number of vehicles in each node $n_{i,T-1},\ i \in \mathcal{V}$, is denoted as $\widetilde{x}_i$. We define column vectors $\mathbf{x} = (x_i,\ i \in \mathcal{V})^\top$ and $\widetilde{\mathbf{x}} = (\widetilde{x}_i,\ i \in \mathcal{V})^\top$ as the *inflow* and the *outflow* of the network $\mathcal{G}$.

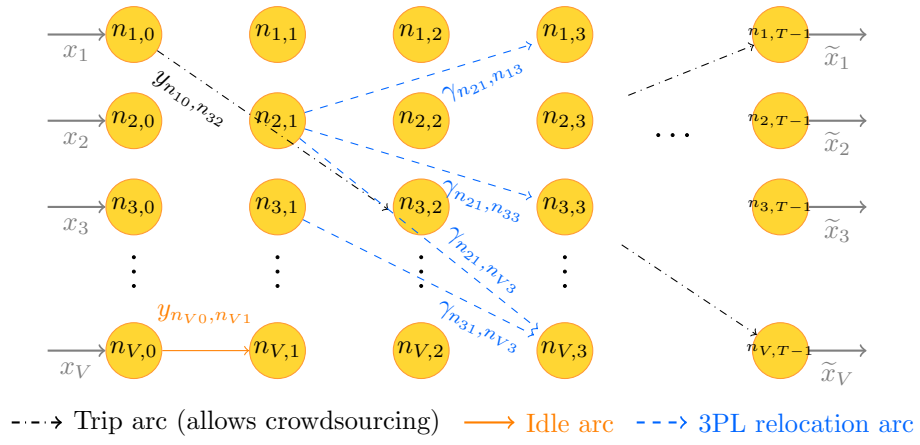

Figure 2.1: Time-space Network $\mathcal{G}$

Given regions $i, j \in \mathcal{V}$, we assume that a rider takes $l_{ij} \geq 1$ periods to ride a micromobility vehicle from region i to region j with $l_{ii} = 1$. In contrast, we assume the 3PL takes a fixed number of periods $l_{\mathrm{r}} \geq 1$ to relocate vehicles from region i to region j. This assumption is reasonable for a relatively compact geographical area in which the regions in $\mathcal{V}$ are near each other. To ensure that a rider has enough time to ride a micromobility vehicle from region i to region j before the end of the operational horizon, we consider the demands from region i to region j that occur only in period $t \in \mathcal{T}(l_{ij}) = \{0, 1, \ldots, T - l_{ij} - 1\}$. Similarly, to ensure that the 3PL can finish all the relocations before the end of the operational horizon, we consider only 3PL relocations that begin in period $t \in \mathcal{T}(l_{\mathrm{r}}) = \{0, 1, \ldots, T - l_{\mathrm{r}} - 1\}$.

Based on how micromobility vehicles are moved between two nodes, there are three types of arcs in $\mathcal{A}$ in the time-space network: (i) *Trip arcs*: The flow of each trip arc $(n_{is}, n_{jt}) \in \mathcal{A}^{\mathrm{t}}$ represents the number of trips from region i in period $s \in \mathcal{T}(l_{ij})$ to region $j \neq i$ in period $t = s + l_{ij}$, for all $i, j \in \mathcal{V}$. Each arc in $\mathcal{A}^{\mathrm{t}}$ may contain two types of trips: one corresponds to the customer demand and the other is induced by crowdsourced riders. (ii) *Idle arcs*: The flow of each idle arc $(n_{jt}, n_{j,t+1}) \in \mathcal{A}^{\mathrm{i}}$, represents the number of idling vehicles in region $j \in \mathcal{V}$ from period $t \in \mathcal{T} \backslash \{T - 1\}$ to period $t + 1$. (iii) *3PL relocation arcs*: The flow of each 3PL relocation arc $(n_{is}, n_{j,s+l_{\mathrm{r}}}) \in \mathcal{A}^{\mathrm{r}}$ represents the number of vehicles relocated by the 3PL from region i to region $j \neq i$ in period $s \in \mathcal{T}(l_{\mathrm{r}})$, for all $i, j \in \mathcal{V}$. Define $\mathcal{I} = \{\mathrm{t}, \mathrm{i}, \mathrm{r}\}$. Thus, we have $\mathcal{A} = \cup_{\forall e \in \mathcal{I}} \mathcal{A}^e$ and $\mathcal{A}^{e_1} \cap \mathcal{A}^{e_2} = \emptyset$, for $e_1 \neq e_2$, $e_1, e_2 \in \mathcal{I}$.

Given $i \in \mathcal{V}$ and $t \in \mathcal{T} \setminus \{T-1\}$, the sequence of events regarding vehicle movements and demand arrivals is depicted in Figure 2.2 and described as follows: (i) At the start of period t, vehicles idling in region i from period $t-1$ and incoming vehicles from any region $j \in \mathcal{V} \setminus \{i\}$ are realized, if any. (ii) Customer demands arrive. (iii) Knowing the realized demands, the operator determines and executes the numbers of vehicles relocated by crowdsourced riders and the 3PL. (iv) Any demand loss is observed and the system is updated for period $t+1$.

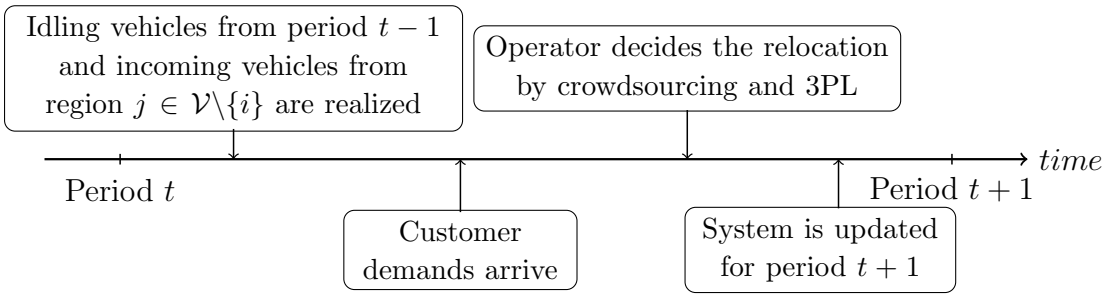

Figure 2.2: The sequence of events

By observing demand uncertainty, we can model such a process over multiple periods as a stochastic program in which decisions are made sequentially for each period t. To avoid the curse of dimensionality and enable efficient decision-making for large instances, we approximate the problem using a *two-stage stochastic programming model*. In the first stage, we decide the initial number of vehicles allocated to each region. In the second stage, we decide the vehicle relocation as a recourse for the entire operational horizon.

2.3.2 Mathematical Formulation

The shared micromobility operator is endowed with a budget that can afford at most N micromobility vehicles. In the first stage, the operator makes the vehicle allocation decisions $\mathbf{x}$ so that $\sum_{j\in\mathcal{V}} x_j \leq N$. A cost $c_j \geq 0$ is incurred for allocating a micromobility vehicle to region $j \in \mathcal{V}$. Due to government regulations on the parking space, we have $x_j \leq B_j$ for each region $j \in \mathcal{V}$.

In the second stage, time-dependent demands arrive at each region $i \in \mathcal{V}$ at the start of each period $t \in \mathcal{T}\setminus\{T-1\}$. For each arc $(n_{it}, n_{j,t+l_{ij}}) \in \mathcal{A}^{\mathrm{t}}$, let $\lambda_{n_{it},n_{j,t+l_{ij}}}$ denote the demand (number of customers) from region i in period t to region j with

travel time l_{ij}. The operator receives a revenue $R \geq 0$ for serving a customer per period. If the number of vehicles available in region i cannot meet the demands of the region in period t, the unsatisfied demand for $(n_{it}, n_{j,t+l_{ij}}) \in \mathcal{A}^{\mathrm{t}}$, denoted by $\eta_{n_{it},n_{j,t+l_{ij}}}$, is lost and the operator pays a penalty cost $C_{\mathrm{p}} \geq 0$ per customer lost.

Facing uncertain demands, the operator makes his initial vehicle allocation decisions and subsequent relocation decisions to maximize his expected profit. The profit equals the total revenue minus the total cost. The total cost includes the initial vehicle allocation cost $\sum_{j\in\mathcal{V}} c_j x_j$ in the first stage and demand-loss penalty and vehicle relocation costs in the second stage. Given the initial vehicle allocation $\mathbf{x}$, let $\Theta(\mathbf{x})$ denote the optimal expected net cost of the second stage (i.e., the total cost minus the total revenue of the second stage). Thus, maximizing the operator's expected profit is equivalent to minimizing the summation of $\sum_{j\in\mathcal{V}} c_j x_j$ and $\Theta(\mathbf{x})$. The operator optimizes his vehicle allocation decisions by solving the following problem:

$$\min_{\mathbf{x}} \sum_{j\in\mathcal{V}} c_j x_j + \Theta(\mathbf{x}) \quad \text{s.t.} \quad \mathbf{x} \in \mathcal{X} = \left\{ \mathbf{x} \in \mathbb{Z}_+^{|\mathcal{V}|} \;\middle|\; x_j \leq B_j,\ j \in \mathcal{V},\ \sum_{j\in\mathcal{V}} x_j \leq N \right\}, \quad (\mathcal{M})$$

where $\Theta(\mathbf{x})$ is realized in the second stage as the operator optimizes the vehicle relocation using rider crowdsourcing and 3PL across the regions. Problem ($\mathcal{M}$) is an *integrated vehicle allocation and relocation problem*. We discuss the vehicle relocation problem in the second stage in detail below.

Vehicle Relocation by Crowdsourced Riders: We assume riders are always available and can be crowdsourced in any period. For a given arc $(n_{it}, n_{j,t+l_{ij}}) \in \mathcal{A}^{\mathrm{t}}$, we introduce a continuous decision variable $\Lambda_{n_{it},n_{j,t+l_{ij}}}$ to represent the number of crowdsourced riders from region i in period t to region j. We assume the operator provides an incentive $\phi_{n_{it},n_{j,t+l_{ij}}}$ to motivate the riders to relocate the vehicles along arc $(n_{it}, n_{j,t+l_{ij}})$. We assume crowdsourcing riders follows the law of diminishing returns (Shephard and Färe 1974): The marginal reward for the crowdsourced riders increases as the number of crowdsourced riders increases. Specifically, we define a concavely increasing incentive function $g(\cdot)$ such that

$$\Lambda_{n_{it},n_{j,t+l_{ij}}} = g\left(\phi_{n_{it},n_{j,t+l_{ij}}}\right) = \bar{\Lambda}_{ij} \times \left(1 - e^{-\beta_{ij}\phi_{n_{it},n_{j,t+l_{ij}}}}\right),\ t \in \mathcal{T}(l_{ij}),\ j \neq i,\ i,j \in \mathcal{V}, \tag{2.1a}$$

where $\bar{\Lambda}_{ij} \geq 0$ represents the maximum number of riders that can be crowdsourced in region i to conduct trips to region j, and $\beta_{ij} \geq 0$ denotes the rate of diminishing return on rewards. Both $\bar{\Lambda}_{ij}$ and β_{ij} can be estimated from historical data.

The total incentive used by the operator to crowdsource riders is capped by a budget $B_{\mathrm{c}} \geq 0$:

$$\sum_{i \in \mathcal{V}} \sum_{j \in \mathcal{V}, j \neq i} \sum_{t \in \mathcal{T}(l_{ij})} \phi_{n_{it},n_{j,t+l_{ij}}} \leq B_{\mathrm{c}}. \tag{2.1b}$$

For each arc $(n_{it}, n_{j,t+l_{ij}}) \in \mathcal{A}^{\mathrm{i}} \cup \mathcal{A}^{\mathrm{t}}$, let $y_{n_{it},n_{j,t+l_{ij}}}$ denote its realized flow. We have the following equations:

$$y_{n_{it},n_{j,t+l_{ij}}} = \lambda_{n_{it},n_{j,t+l_{ij}}} + \Lambda_{n_{it},n_{j,t+l_{ij}}} - \eta_{n_{it},n_{j,t+l_{ij}}},\ t \in \mathcal{T}(l_{ij}),\ j \neq i,\ i,j \in \mathcal{V}. \tag{2.1c}$$

Vehicle Relocation by the 3PL: For each period $t \in \mathcal{T}(l_{\mathrm{r}})$, we define a decision variable z_t such that $z_t = 1$ if the 3PL is requested by the operator in period t to relocate vehicles and $z_t = 0$ otherwise. In practice, the operator can only request the 3PL for vehicle relocation for no more than $\bar{z}$ times over the entire operational horizon:

$$\sum_{t \in \mathcal{T}(l_{\mathrm{r}})} z_t \leq \bar{z}. \tag{2.2a}$$

For each request, the 3PL charges the operator a fixed fee $C_{\mathrm{r}} \geq 0$ to relocate vehicles across multiple regions. Note that no additional fees are required if it takes multiple periods to relocate the vehicles. Define a binary variable $\widetilde{z}_t$ to represent the status of the 3PL such that $\widetilde{z}_t = 1$ if the 3PL provides service in period t and $\widetilde{z}_t = 0$ otherwise. Since the 3PL provides service only if the operator has requested it, we have the following constraints:

$$z_t - \widetilde{z}_t \leq 0,\ t \in \mathcal{T}(l_{\mathrm{r}}). \tag{2.2b}$$

If a 3PL relocation is requested by the operator in period t (i.e., $z_t = 1$), then it implies that no 3PL relocation service is provided in period $t-1$ (i.e., $\widetilde{z}_{t-1} = 0$). We have the following constraints:

$$z_t + \widetilde{z}_{t-1} - 1 \leq 0,\ t \in \mathcal{T}(l_{\mathrm{r}}) \backslash \{0\}. \tag{2.2c}$$

If a 3PL relocation service is provided in period t (i.e., $\widetilde{z}_t = 1$) but not in period $t-1$ (i.e., $\widetilde{z}_{t-1} = 0$), then clearly the relocation service is initiated in period t (i.e., $z_t = 1$). This can be represented by the following constraints:

$$z_t - \widetilde{z}_t + \widetilde{z}_{t-1} \geq 0,\ t \in \mathcal{T}(l_{\mathrm{r}}) \backslash \{0\}. \tag{2.2d}$$

In practice, the 3PL can only serve a limited number of periods. Specifically, we assume that during any time interval of l_{f} periods, the 3PL operates for at most $\bar{\bar{z}}$ periods:

$$\sum_{i=t}^{t+l_{\mathrm{f}}-1} \widetilde{z}_i \leq \bar{\bar{z}},\ t \in \{0, 1, \ldots, T - l_{\mathrm{r}} - l_{\mathrm{f}} - 1\}. \tag{2.2e}$$

For each arc $(n_{it}, n_{j,t+l_{\mathrm{r}}}) \in \mathcal{A}^{\mathrm{r}}$, we define a continuous decision variable $\gamma_{n_{it},n_{j,t+l_{\mathrm{r}}}}$ to represent the number of vehicles relocated by the 3PL from region i in period t to region j. The total number of relocated vehicles in period t is constrained between a lower limit $\underline{q}$ and an upper limit $\bar{q}$:

$$\underline{q}\widetilde{z}_t \leq \sum_{i \in \mathcal{V}} \sum_{j \in \mathcal{V}, j \neq i} \gamma_{n_{it},n_{j,t+l_{\mathrm{r}}}} \leq \bar{q}\widetilde{z}_t,\ t \in \mathcal{T}(l_{\mathrm{r}}). \tag{2.2f}$$

At the beginning of period 0, we assume that the 3PL is requested if it provides relocation service:

$$z_0 - \widetilde{z}_0 \geq 0. \tag{2.2g}$$

Finally, the following constraints restrict $\widetilde{z}_t$ to be binary for $t \in \mathcal{T}(l_{\mathrm{r}})$:

$$\widetilde{z}_t \in \{0, 1\},\ t \in \mathcal{T}(l_{\mathrm{r}}), \tag{2.2h}$$

which, together with constraints (2.2b) – (2.2d) and (2.2g), guarantee z_t to be binary for $t \in \mathcal{T}(l_{\mathrm{r}})$.

Example. We show an example where the 3PL is requested in period s_1 and period s_2 with $s_1 < s_2$ (i.e., $z_{s_1} = z_{s_2} = 1$), as shown in Figure 2.3. Once requested in

period s_1, the 3PL provides services for two consecutive periods (i.e., $\widetilde{z}_{s_1} = \widetilde{z}_{s_1+1} = 1$ represented by orange circles). It then stops services in period $s_1 + 2$ until period $s_2 - 1$ (i.e., $\widetilde{z}_{s_1+2} = \cdots = \widetilde{z}_{s_2-1} = 0$ represented by gray circles). Once requested again in period s_2, the 3PL provides services for three consecutive periods (i.e., $\widetilde{z}_{s_2} = \widetilde{z}_{s_2+1} = \widetilde{z}_{s_2+2} = 1$). Figure 2.3 illustrates the detailed values of z_t and $\widetilde{z}_t$ for $t \in \{s_1 - 1, s_1, \ldots, s_2 + 3\}$, in which $z_t = 0$ if $t \neq s_1$ or $t \neq s_2$.

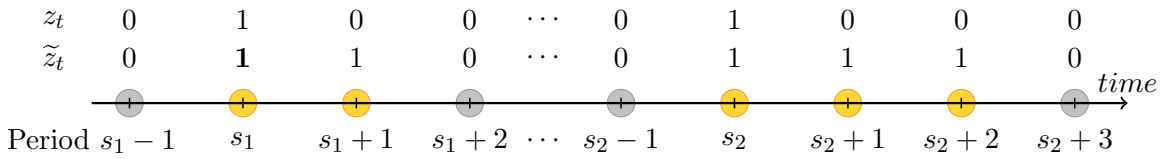

Figure 2.3: Service Status of the 3PL

We observe from the above Example 1 that the value of $\widetilde{z}_t$ can be different from that of z_t in each period $t \in \mathcal{T}(l_{\mathrm{r}})$, while their logical relationships are described by constraints (2.2b) – (2.2d) and (2.2g). Note that $\widetilde{z}_t$ is necessary to describe whether the 3PL provides services in each period t (i.e., service status), while z_t describes whether the 3PL is requested to *start* providing services in period t or not. Once starting to provide services, the 3PL can continue to provide services for several consecutive periods subject to constraints (2.2e). Technically the variable z_t is not necessary to describe the service status of the 3PL, but we define it for two purposes: (i) practically control the total number of requests that the operator submits to the 3PL, as described by constraints (2.2a); (ii) record the fixed fee C_{r} when the 3PL is requested because this fee is incurred once the 3PL starts providing services. Thus, the total fixed fee incurred over the entire operational horizon is $\sum_{t \in \mathcal{T}(l_{\mathrm{r}})} C_{\mathrm{r}} z_t^k$.

Flow Balance: Given any node $n_{it} \in \mathcal{N}$, the number of vehicles flowing into this node should be the same as the number of vehicles flowing out from this node:

$$\left(y_{n_{it},n_{i,t+1}} + \sum_{j \in \mathcal{V}, j \neq i} \left(y_{n_{it},n_{j,t+l_{ij}}} + \gamma_{n_{it},n_{j,t+l_{\mathrm{r}}}}\right)\right) - \left(y_{n_{i,t-1},n_{it}} + \sum_{j \in \mathcal{V}, j \neq i} \left(y_{n_{j,t-l_{ji}},n_{it}} + \gamma_{n_{j,t-l_{\mathrm{r}}},n_{it}}\right)\right)$$
$$= \begin{cases} x_i, & \text{if } t = 0; \\ 0, & \text{if } t = 1, \ldots, T-2; \\ -\widetilde{x}_i, & \text{if } t = T-1; \end{cases} \tag{2.3}$$

for $i \in \mathcal{V}$. Note that the constraints may contain some undefined arcs (n_{is}, n_{jt}) with $s < 0$ or $t \geq T$ for $j \neq i$, $i, j \in \mathcal{V}$ (see Figure A.1 in Appendix A.2.1). For

consistency, we set the realized flow $y_{n_{is},n_{jt}} = 0$ and the number of vehicles relocated by the 3PL $\gamma_{n_{is},n_{jt}} = 0$ on such arcs.

In the second stage, given the initial vehicle allocation $\mathbf{x}$, the operator relocates the vehicles to maximize his expected profit subject to uncertain demands $\lambda_{n_{it},n_{j,t+l_{ij}}}$. We assume that there is a finite support for the joint distribution of the uncertain demands in all the service regions across all the periods. Thus, we use a set $\mathcal{K}$ to include scenarios of uncertain demands in all the service regions across all the periods. Each scenario $k \in \mathcal{K}$ has a probability $p^k \geq 0$ with $\sum_{k\in\mathcal{K}} p_k = 1$. For each scenario $k \in \mathcal{K}$, the operator makes recourse decisions for all the periods in $\mathcal{T}$. We reuse the above notation for the second-stage problem and add a superscript k to each decision variable for each scenario. We use bold symbols to represent vectors. For example, $\widetilde{\mathbf{x}}^k = (\widetilde{x}_j^k,\ j \in \mathcal{V})^\top$ (see Appendix A.2.2 for the details). For each $k \in \mathcal{K}$, let $\mathbf{Y}^k = (\widetilde{\mathbf{x}}^k, \boldsymbol{\eta}^k, \mathbf{y}^k, \boldsymbol{\gamma}^k, \boldsymbol{\Lambda}^k, \boldsymbol{\phi}^k, \mathbf{z}^k, \widetilde{\mathbf{z}}^k)$ denote all the decision variables and let $\mathcal{Y}(\mathbf{x}, \boldsymbol{\lambda}^k) := \{\mathbf{Y}^k \in \mathbb{R}_+^{(|\mathcal{V}|+4|\mathcal{A}^{\mathrm{t}}|+|\mathcal{A}^{\mathrm{r}}|+2|\mathcal{T}(l_{\mathrm{r}})|)} \mid (2.1a)-(2.1c), (2.2a)-(2.2h), (2.3)\}$ denote the feasible region. Given the initial vehicle allocation $\mathbf{x}$, the expected net cost $\Theta(\mathbf{x})$ in the second stage can be determined by solving the following network flow optimization problem:

$$\Theta(\mathbf{x}) = \min_{\mathbf{Y}^k \in \mathcal{Y}(\mathbf{x},\boldsymbol{\lambda}^k),\ k\in\mathcal{K}} \left\{ \sum_{k\in\mathcal{K}} p^k \left(\sum_{a\in\mathcal{A}^{\mathrm{t}}} \left(C_{\mathrm{p}}\eta_a^k + \phi_a^k - Rl_a\left(y_a^k - \Lambda_a^k\right)\right) + \sum_{t\in\mathcal{T}(l_{\mathrm{r}})} C_{\mathrm{r}} z_t^k \right) \right\}. \quad (\mathcal{P})$$

Note that the flows on the idle arcs do not incur any costs and the flows corresponding to the 3PL and crowdsourcing relocation do not generate revenue.

Model Implementation: In practice, we can apply our model for the allocation planning on a seasonal or yearly basis. After deriving the amount of vehicles and the allocation, we can apply the second-stage model for daily relocation decisions given the estimated demand of the day. We may need to adjust the initial allocation in different regions at the beginning of the day to match the reality before we derive the relocation decisions.

Remark. We note that in practice the decision-makers can also use simulation methods for planning and operational policies for bike-sharing systems(Jian et al. 2016, Soriguera et al. 2018, Negahban 2019). It is preferred when the problem is difficult to be translated into an analytical expression. It can also handle the

problem with a high degree of uncertainty. However, simulation is often more time consuming and less accurate than the stochastic optimization (Amaran et al. 2016). Moreover, simulation is often regarded as a black box and may not be able to provide rich analytical insights as model-based mathematical programming. Therefore, we prefer to investigate our problem by stochastic optimization.

2.4 Analysis of Two-region Case

We consider a special case of problem ($\mathcal{M}$) with two service regions. To obtain some structural results, we focus on a scenario in $\mathcal{K}$ with demands $\lambda_{n_{it},n_{3-i,t+L}}$. We assume that the numbers of vehicles initially allocated to the two regions x_1 and x_2 are given so that we can study the optimal relocation strategy for problem ($\mathcal{P}$) in detail. We use the following problem setting: (i) The travel time and the 3PL relocation time between the two regions are a constant L. (ii) To relocate vehicles from region i and period t to the other region by crowdsourcing, the total reward provided increases linearly with the number of crowdsourced riders: $\phi_{n_{it},n_{3-i,t+L}} = \alpha\Lambda_{n_{it},n_{3-i,t+L}} + b$, where $\alpha \geq 0$ represents a variable cost of crowdsourcing an additional rider and $b \geq 0$ represents a fixed cost of crowdsourcing. (iii) We set $\underline{q} = 0$ and $\bar{q} = \max\left\{\lambda_{n_{it},n_{3-i,t+L}} \;\middle|\; i \in \{1,2\}, t \in \{0,1,\ldots,T-L-1\}\right\}$. Problem ($\mathcal{P}$) becomes

$$\Theta(x_1,x_2) = \min_{(\mathbf{\Lambda},\mathbf{y},\boldsymbol{\eta},\mathbf{z},\boldsymbol{\gamma})\in\mathcal{Y}(x_1,x_2,\boldsymbol{\lambda})} \left\{ \sum_{t=0}^{T-L-1} \left(\sum_{i=1}^{2} \Big(C_{\mathrm{p}}\eta_{n_{it},n_{3-i,t+L}} + \alpha\Lambda_{n_{it},n_{3-i,t+L}} + b - RL\left(y_{n_{it},n_{3-i,t+L}} - \Lambda_{n_{it},n_{3-i,t+L}}\right)\Big) + C_{\mathrm{r}} z_t \right) \right\}, \tag{2.4}$$

where $\mathcal{Y}(x_1,x_2,\boldsymbol{\lambda})$ is described in detail in Appendix A.3.1. Note that there are no incoming vehicles for any region in the first L periods and no demands in the last L periods. Thus, it is sufficient to consider periods $t \in \{0,1,\ldots,T-L-1\}$ in the objective.

Proposition 2.1. *Given any $i \in \{1,2\}$ and $t \in \{0,1,\ldots,T-L-1\}$, the optimal relocation strategy satisfies the following three conditions: (a) $\Lambda^*_{n_{it},n_{3-i,t+L}}\gamma^*_{n_{it},n_{3-i,t+L}} = 0$; (b) $C_r \geq \alpha\Lambda^*_{n_{it},n_{3-i,t+L}}$; and (c) if $z^*_t = 1$ and $\gamma^*_{n_{it},n_{3-i,t+L}} > 0$, then $C_r \leq \alpha\gamma^*_{n_{it},n_{3-i,t+L}}$.*

Part (a) of Proposition 2.1 shows that under the optimal relocation strategy, the 3PL and crowdsourcing are not used simultaneously in any region i and period t. Part (b) shows that if crowdsourcing is used (i.e., $\Lambda^*_{n_{it},n_{3-i,t+L}} > 0$), then its unit cost of relocating one vehicle is less than that by the 3PL (i.e., $\alpha \leq C_{\mathrm{r}}/\Lambda^*_{n_{it},n_{3-i,t+L}}$). Similarly, Part (c) shows that if the 3PL is used in a given period t (i.e., $z^*_t = 1$ and $\gamma^*_{n_{it},n_{3-i,t+L}} > 0$), then its unit cost of relocating one vehicle is less than that by crowdsourcing (i.e., $C_{\mathrm{r}}/\gamma^*_{n_{it},n_{3-i,t+L}} \leq \alpha$). Such insights imply that the unit cost of each relocation method serves as a critical instrument for the micromobility operator to decide which method to use for each arc in the time-space network. Section 2.6 considers a more practical setting in industry by solving the general problem ($\mathcal{M}$). We first introduce a solution approach to problem ($\mathcal{M}$) in the following section.

2.5 Solution Approach for Multiple Regions

We will develop a decomposition-based solution approach to efficiently solve the *integrated vehicle allocation and relocation problem* ($\mathcal{M}$). To accomplish that, we first propose a piecewise-linear approximation of the nonlinear crowdsourcing incentive function $g(\cdot)$ in (2.1a) and then develop a solution algorithm to solve problem ($\mathcal{M}$).

2.5.1 Piecewise-Linear Approximation of the Incentive Function

In constraints (2.1a), given any scenario $k \in \mathcal{K}$ and arc $(n_{it}, n_{i,t+l_{ij}}) \in \mathcal{A}^{\mathrm{t}}$, the number of crowdsourced riders is $\Lambda^k_{n_{it},n_{i,t+l_{ij}}} = g(\phi^k_{n_{it},n_{i,t+l_{ij}}}) = \bar{\Lambda}_{ij}(1 - e^{-\beta_{ij}\phi^k_{n_{it},n_{j,t+l_{ij}}}})$, which is a concavely increasing function of the reward amount $\phi^k_{n_{it},n_{i,t+l_{ij}}}$. To facilitate algorithmic development for solving problem ($\mathcal{M}$), we approximate the function $g(\cdot)$ with a piecewise-linear function, as illustrated in Figure 2.4, such that the nonlinear constraints (2.1a) can be replaced by a set of linear constraints. Since the same approximation is applicable for any two given regions i and j in each period t for any scenario k, we drop the superscript and subscripts from $\Lambda^k_{n_{it},n_{j,t+l_{ij}}}$, $\phi^k_{n_{it},n_{j,t+l_{ij}}}$, $\bar{\Lambda}_{ij}$, and β_{ij} when describing our approximation. That is, we have $\Lambda = g(\phi) = \bar{\Lambda}(1 - e^{-\beta\phi})$, where $\phi \in [0, \infty)$.

Given an arbitrarily small number $\epsilon > 0$, define $\bar{\phi} = g^{-1}\left(\bar{\Lambda} - \epsilon\right)$. We divide the

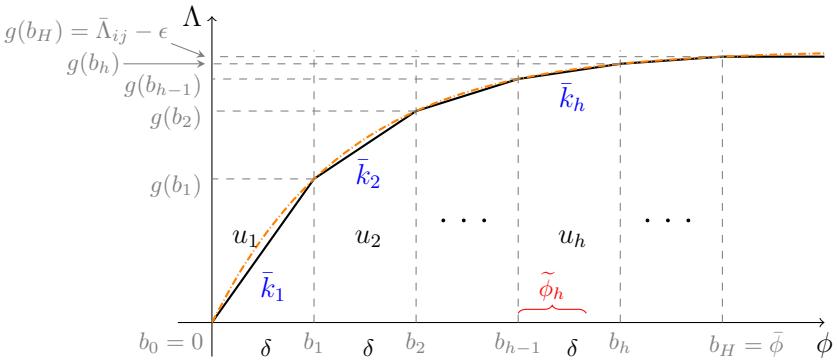

Figure 2.4: Piecewise-Linear Approximation of the Incentive Function

interval $[0, \bar{\phi}]$ into H segments, each with length $\delta = \bar{\phi}/H$. Given any $h \in \mathcal{H} = \{1, 2, \ldots, H\}$, we approximate the function $g(\cdot)$ in the hth segment $[(h-1)\delta, h\delta]$ (denoted as $[b_{h-1}, b_h]$ in Figure 2.4) with a linear function passing through points $((h-1)\delta, g((h-1)\delta))$ and $(h\delta, g(h\delta))$. Let $\bar{k}_h = (g(h\delta) - g((h-1)\delta))/\delta$ denote the slope of this linear function. For ϕ in $[\bar{\phi}, \infty)$, we approximate the function $g(\cdot)$ with a constant $\bar{\Lambda} - \epsilon$. For each $h \in \mathcal{H}$ in the above approximation, the number of crowdsourced riders Λ linearly increases with the reward ϕ, while the slope $\bar{k}_h$ is decreasing in h and becomes 0 as ϕ reaches $\bar{\phi}$. Clearly, having more segments (i.e., a larger H) leads to a more accurate approximation.

For each $h \in \mathcal{H}$, define a binary decision variable u_h such that $u_h = 1$ if the optimal reward ϕ falls in the hth segment, and $u_h = 0$ otherwise. Since we minimize the objective of problem ($\mathcal{M}$), no binary variables are needed for $[\bar{\phi}, \infty)$ because no more crowdsourced riders will be attracted when ϕ becomes larger than $\bar{\phi}$ (i.e., the optimal ϕ will not exceed $\bar{\phi}$). We thus restrict $\phi \in [0, \bar{\phi}]$. For each $h \in \mathcal{H}$, define a continuous decision variable $\widetilde{\phi}_h \in [0, \delta]$ such that the optimal reward $\phi = (h-1)\delta + \widetilde{\phi}_h$ and the optimal number of crowdsourced riders $\Lambda = g((h-1)\delta) + \bar{k}_h \widetilde{\phi}_h$ in the hth segment. Thus, the constraint $\Lambda = g(\phi)$ can be approximated by the following set of constraints:

$$\phi = \sum_{h=1}^{H} u_h \left((h-1)\delta + \widetilde{\phi}_h \right), \tag{2.5a}$$

$$\Lambda = \sum_{h=1}^{H} u_h \left(\sum_{m=1}^{h-1} \bar{k}_m \delta + \bar{k}_h \widetilde{\phi}_h \right), \tag{2.5b}$$

$$\sum_{h=1}^{H} u_h = 1, \tag{2.5c}$$

$$0 \le \widetilde{\phi}_h \le \delta, \ h \in \mathcal{H}, \tag{2.5d}$$

$$u_h \in \{0, 1\}, \ h \in \mathcal{H}. \tag{2.5e}$$

Note that there are bilinear terms (i.e., $u_h\widetilde{\phi}_h$) in (2.5a) and (2.5b). Since u_h is binary for $h \in \mathcal{H}$, such bilinear terms can be exactly reformulated as the following linear constraints:

$$\begin{aligned}&\phi = \sum_{h=1}^{H}\big((h-1)u_h\delta + \omega_h\big),\ \Lambda = \sum_{h=1}^{H} u_h \sum_{m=1}^{h-1}\bar{k}_m\delta + \sum_{h=1}^{H}\bar{k}_h\omega_h,\\ &u_h\delta - \omega_h \geq 0,\ \widetilde{\phi}_h - \omega_h \geq 0,\ \delta - u_h\delta - \widetilde{\phi}_h + \omega_h \geq 0,\ \omega_h \geq 0,\ h \in \mathcal{H},\end{aligned} \tag{2.6}$$

where ω_h replaces $u_h\widetilde{\phi}_h$ in (2.5a) and (2.5b) for $h \in \mathcal{H}$.

By adopting the approximation in (2.5c) – (2.5e) and (2.6), we are ready to reformulate the relocation problem ($\mathcal{P}$) by approximating nonlinear constraints (2.1a) for each scenario $k \in \mathcal{K}$. For each arc $a = (n_{it}, n_{j,t+l_{ij}}) \in \mathcal{A}^{\mathrm{t}}$, we add a subscript a to the decision variables $\phi, u_h, \widetilde{\phi}_h$, and ω_h, and add subscripts ij to the parameters δ and $\bar{k}_h$ in (2.5c) – (2.5e) and (2.6). Given any first-stage solution $\mathbf{x}$, problem ($\mathcal{P}$) can be decomposed to $|\mathcal{K}|$ independent problems, each corresponds to scenario $k \in \mathcal{K}$. Let $\mathcal{P}^k$ denote the relocation problem that corresponds to scenario $k \in \mathcal{K}$ with its net cost equals

$$\Psi\left(\widetilde{\mathbf{Y}}^k\right) = \sum_{a\in\mathcal{A}^{\mathrm{t}}}\left(C_{\mathrm{p}}\eta_a^k + \phi_a^k - Rl_a\left(y_a^k - \Lambda_a^k\right)\right) + \sum_{t\in\mathcal{T}(l_{\mathrm{r}})} C_{\mathrm{r}} z_t^k, \tag{2.7}$$

where $\widetilde{\mathbf{Y}}^k = (\widetilde{\mathbf{x}}^k, \boldsymbol{\eta}^k, \mathbf{y}^k, \boldsymbol{\gamma}^k, \boldsymbol{\Lambda}^k, \mathbf{u}^k, \boldsymbol{\phi}^k, \widetilde{\boldsymbol{\phi}}^k, \mathbf{z}^k, \widetilde{\mathbf{z}}^k, \boldsymbol{\omega}^k) \in \mathbb{R}_+^{(|\mathcal{V}|+(4+3H)|\mathcal{A}^{\mathrm{t}}|+|\mathcal{A}^{\mathrm{r}}|+2|\mathcal{T}(l_{\mathrm{r}})|)}$, $\mathbf{u}^k = ((u_{1,a}^k, \ldots, u_{H,a}^k),\ a \in \mathcal{A}^{\mathrm{t}})^\top$, $\widetilde{\boldsymbol{\phi}}^k = ((\widetilde{\phi}_{1,a}^k, \ldots, \widetilde{\phi}_{H,a}^k),\ a \in \mathcal{A}^{\mathrm{t}})^\top$, and $\boldsymbol{\omega}^k = ((\omega_{1,a}^k, \ldots, \omega_{H,a}^k), a \in \mathcal{A}^{\mathrm{t}})^\top$. We obtain the final formulation of the relocation problem ($\mathcal{P}$) as follows:

$$\begin{aligned}\Theta'(\mathbf{x}) = \min_{\widetilde{\mathbf{Y}}^k,\ k\in\mathcal{K}}\Big\{&(2.7)\ \Big|\ (2.1\mathrm{b}), (2.1\mathrm{c}), (2.2\mathrm{a}) - (2.2\mathrm{h}), (2.3),\\ &\big((2.5\mathrm{c}) - (2.5\mathrm{e}), (2.6),\ a \in \mathcal{A}^{\mathrm{t}}\big),\ k \in \mathcal{K}\Big\}.\end{aligned} \tag{$\mathcal{Q}_0$}$$

By relaxing $u_{h,a}^k$ to be continuous for $k \in \mathcal{K}$, $h \in \mathcal{H}$, and $a \in \mathcal{A}^{\mathrm{t}}$, the above problem becomes

$$\begin{aligned}\Theta''(\mathbf{x}) = \min_{\widetilde{\mathbf{Y}}^k,\ k\in\mathcal{K}}\Big\{&(2.7)\ \Big|\ (2.1\mathrm{b}), (2.1\mathrm{c}), (2.2\mathrm{a}) - (2.2\mathrm{h}), (2.3),\\ &\Big((2.5\mathrm{c}) - (2.5\mathrm{d}), (2.6), \big(u_{h,a}^k \in [0,1],\ h \in \mathcal{H}\big),\ a \in \mathcal{A}^{\mathrm{t}}\Big),\ k \in \mathcal{K}\Big\}.\end{aligned} \tag{$\mathcal{Q}$}$$

Proposition 2.2. *Given any initial vehicle allocation* $\mathbf{x} \in \mathcal{X}$*, we have* $\Theta'(\mathbf{x}) = \Theta''(\mathbf{x})$.

Proposition 2.2 shows that for each scenario $k \in \mathcal{K}$, the optimal objective value of problem ($\mathcal{Q}_0$) is not affected if binary variables $u^k_{h,a}$ ($h \in \mathcal{H}, a \in \mathcal{A}^{\mathrm{t}}$) are relaxed to continuous ones. Thus, we can use ($\mathcal{Q}$) to approximate the original second-stage problem ($\mathcal{P}$) to reduce the computational burden. Hereafter, we replace ($\mathcal{P}$) with the reformulated relocation problem ($\mathcal{Q}$) in the integrated allocation and relocation problem ($\mathcal{M}$).

2.5.2 Solution Algorithm

We propose an algorithm that can efficiently solve large-scale instances of problem ($\mathcal{M}$). The algorithm consists of three steps: First, to increase computational efficiency, we reduce the number of binary variables in the relocation problem ($\mathcal{Q}$). Second, as problem ($\mathcal{Q}$) is difficult to solve when considering the entire time-space network $\mathcal{G}$, we derive a temporal decomposition approach by iteratively solving a series of subproblems. Each subproblem considers only a part of the time-space network covering several consecutive periods. Third, based on initial vehicle allocations obtained in the second step, we design a heuristic to further improve the solution quality. To facilitate the algorithm description, we first refine the notation defined in Section 2.3.

Algorithm Notation. Recall from Section 2.3.2 that the starting periods of trip arcs and 3PL relocation arcs are in the sets $\mathcal{T}(l_{ij})$ and $\mathcal{T}(l_{\mathrm{r}})$, respectively, where l_{ij} and l_{r} represent the trip and relocation durations, respectively. For recording purposes, we rename the sets as $\mathcal{T}(l_{ij}, 0, T) = \{0, 1, \ldots, T - l_{ij} - 1\}$ and $\mathcal{T}(l_{\mathrm{r}}, 0, T) = \{0, 1, \ldots, T - l_{\mathrm{r}} - 1\}$. Likewise, we rename the relocation problem ($\mathcal{Q}$) as $\mathcal{Q}(0, T)$ and the integrated allocation and relocation problem ($\mathcal{M}$) as $\mathcal{M}(0, T)$. Generally, given a starting period $s \in \mathcal{T}$, an ending period $e \in \mathcal{T} \cup \{T\}$ ($e \geq s + 1$), and a time duration $l \in \{1, 2, \ldots, e - s\}$, define $\mathcal{T}(l, s, e) = \{s, s + 1, \ldots, e - l - 1\}$. For a part of the time-space network with a starting period s and an ending period e, let $\mathcal{Q}(s, e)$ denote the corresponding relocation problem, which has a vector of variables $\widetilde{\mathbf{Y}}^k_{(s,e)}$ and a feasible region $\mathcal{Y}_{(s,e)}(\mathbf{x}, \boldsymbol{\lambda}^k) := \{(\text{A.9a}) - (\text{A.9s})\}$ for $k \in \mathcal{K}$

(see Appendix A.4.2 for details). Let $\mathcal{M}(s,e)$ denote the integrated allocation and relocation problem with $\mathcal{Q}(s,e)$ as the relocation problem in its second stage.

When we relax the binary variables $\widetilde{\mathbf{z}}^k, k \in \mathcal{K}$, to continuous ones, we denote the resulting feasible region in the second stage as $\mathcal{Y}_{\mathrm{LP}(s,e)}(\mathbf{x}, \boldsymbol{\lambda}^k) := \{(\text{A.9a}) - (\text{A.9r}),\ \widetilde{z}_t^k \in [0,1],\ t \in \mathcal{T}(l_{\mathrm{r}}, s, e)\},\ k \in \mathcal{K}$. The relaxed relocation problem is $\mathcal{Q}_{\mathrm{LP}}(s,e) := \{\Theta''(\mathbf{x}) |\ \widetilde{\mathbf{Y}}^k_{(s,e)} \in \mathcal{Y}_{\mathrm{LP}(s,e)}(\mathbf{x}, \boldsymbol{\lambda}^k),\ k \in \mathcal{K}\}$ and the overall relaxed two-stage problem is denoted by $\mathcal{M}_{\mathrm{LP}}(s,e)$. Note that as the second-stage problem of $\mathcal{M}_{\mathrm{LP}}(s,e)$, problem $\mathcal{Q}_{\mathrm{LP}}(s,e)$ is a linear programming (LP) relaxation of $\mathcal{Q}(s,e)$. By using the starting period s as a superscript, let $\mathbf{x}^s = (x_i^s,\ i \in \mathcal{V})^\top$ denote the first-stage solution of $\mathcal{M}_{\mathrm{LP}}(s,e)$ and let v^s denote its corresponding objective value. Similarly, we add a superscript s to the second-stage decision variables to denote the second-stage solution.

Step 1: Reducing The Number of Binary Variables. Due to constraints (2.2a) – (2.2e), in an optimal solution, only a limited number of $\widetilde{z}_t^k,\ k \in \mathcal{K}, t \in \mathcal{T}$, will be 1, and the others equal 0. This means that the 3PL relocation service is provided only in several periods. To reduce the number of binary variables, we design Algorithm 1 (see Appendix A.4.3) with some $\widetilde{z}_t^k$ fixed at 0, while the others are optimized. Specifically, for any $s \in \mathcal{T}$ and $e \in \mathcal{T} \cup \{T\}$ such that $e - s \geq 3$, we solve the LP relaxation problem $\mathcal{M}_{\mathrm{LP}}(s,e)$ to find $\widetilde{z}_t^{ks}$ for each scenario $k \in \mathcal{K}$. If the values of $\widetilde{z}_t^{ks}$ and $\widetilde{z}_t^{ks} + \widetilde{z}_{t+1}^{ks}$ are almost zero, then we fix $\widetilde{z}_t^k = 0$ in $\mathcal{Q}(s,e)$.

Step 2: Temporal Decomposition. Our original relocation problem $\mathcal{Q}(0,T)$ can have a huge number of variables and constraints. By splitting the time-space network along the operational horizon into M sub-networks, each sub-network $m \in \{1,2,\ldots,M\}$ has a shorter time horizon with $T_{\mathrm{sub}} = \lfloor T/M \rfloor$ periods. Solving the problem $\mathcal{Q}(s,e)$ with $s = (m-1)T_{\mathrm{sub}}$ and $e = mT_{\mathrm{sub}}$, which corresponds to the mth sub-network, is more computationally efficient. Thus, we will solve a sequence of smaller two-stage stochastic programs, each corresponding to a sub-network, in a backward manner, from sub-network M to sub-network 1.

For each sub-network m, we follow a four-step solution procedure. First, we apply Algorithm 1 to reduce the number of binary variables. Second, based on the initial vehicle allocation of sub-network $m+1$, we add new constraints to balance the vehicle

flows between sub-networks m and $m+1$, and obtain the initial vehicle allocation of sub-network m. Third, we re-solve the relaxed two-stage problem $\mathcal{M}_{\text{LP}}(s,e)$ several times by perturbing the initial vehicle allocation of sub-network m to yield several candidate allocations. Fourth, if $m \geq 2$, then we choose the vehicle allocation with the best objective of $\mathcal{M}_{\text{LP}}(s,e)$ as the vehicle allocation of sub-network m. If $m = 1$, then given an initial vehicle allocation of sub-network m, we solve the two-stage problem $\mathcal{M}(0,T)$ over the original time-space network with the first-stage decisions fixed at this initial vehicle allocation and the number of binary variables reduced. We choose the vehicle allocation with the best objective of $\mathcal{M}(0,T)$ as the initial vehicle allocation of the entire network. Algorithm 2 in Appendix A.4.4 presents the above decomposition approach in detail to solve problem $(\mathcal{M})$.

Step 3: Heuristic Search. With several initial vehicle allocations of sub-network 1 obtained from the above temporal decomposition approach, we introduce Algorithm 3 in Appendix A.4.5 to further search for better solutions. Algorithm 3 is based on the following intuition: If the objective value under a vehicle allocation monotonically decreases as the total number of allocated vehicles increases (resp. decreases), then likely a smaller objective can be found by further increasing (resp. decreasing) the total number of allocated vehicles. We observe this phenomenon in our numerical experiments.

2.6 Numerical Experiments: A Case Study

We conduct numerical experiments using real operational data from Citi Bike (2021). We first discuss parameter settings of the problem and then obtain managerial insights from various numerical experiments based on these settings.

2.6.1 Parameter Settings

We have collected data from Citi Bike (2021) in New York City (NYC) from January 1, 2018 to December 31, 2019. Figure 2.5 shows the overview of daily demands of different locations of Manhattan in 2018. We focus on Midtown Manhattan between the 20th Street and the 57th Street, and divide the area into nine rectangular service regions (i.e., $|\mathcal{V}| = 9$). Each region covers an area of about 1-kilometer square, as

shown in Figure 2.6.[2.1] The travel distance between any two regions is measured by the Manhattan distance (L1 norm) between their centers. Based on the data in 2018, we find that the average riding speed is 9 kilometers per hour.[2.2] Thus, the average trip duration from one region to a neighboring region is 6.7 minutes. For simplicity, we assume the traveling speed between any two regions is the same and set each period as 6 minutes (leading to $T = 240$ periods per day). As a result, the longest trip (e.g. from region 1 to region 9) takes four periods. This is evidenced in the data as 96.5% of the trips in the studied area finish within 24 minutes.

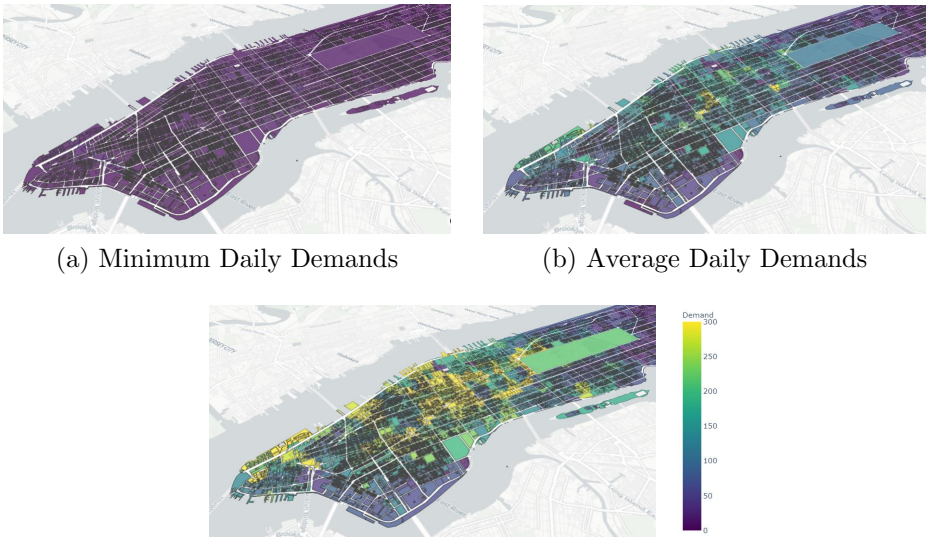

(a) Minimum Daily Demands

(b) Average Daily Demands

(c) Maximum Daily Demands

Figure 2.5: Daily Demands of Manhattan in 2018

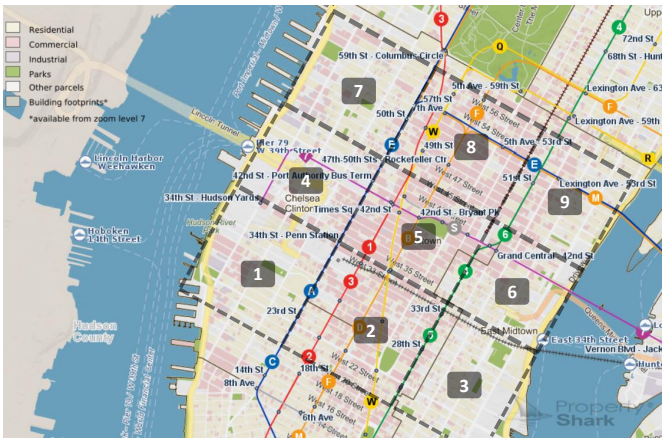

Figure 2.6: Service Regions in Midtown Manhattan

[2.1] Source: https://www.propertyshark.com/mason/ny/New-York-City/Maps?map=nyc2.

[2.2] Similar user behavior for urban commuters in NYC can be found in NYC DOT (2019).

The upper bound N of the total number of vehicles allocated to the studied area is not available in the data set. We estimate such an upper bound as follows:

$$N = \frac{\text{No. of all the trips in the studied area}}{\text{No. of all the trips in NYC}} \times \text{No. of vehicles in NYC},$$

where the number of vehicles in NYC is obtained by counting unique bike IDs in the data set. Based on the above calculation, we have $N = 1,206$. Similarly, we estimate the upper bound B_j of the total number of vehicles allocated to region j as follows:

$$B_j = \frac{\text{No. of all the trips from region } j}{\text{No. of all the trips in the studied area}} \times N, \ j \in \mathcal{V}.$$

Note that the total number of vehicles allocated by our model is much smaller than N. This indicates that there are many redundant bikes allocated to the studied area — a phenomenon commonly seen among shared micromobility systems in practice. The reasons can be (i) the firm believes that allocating more bikes will provide more convenient services and attract more customers; (ii) the firm may want to increase its market share by increasing their vehicle supply. Nevertheless, allocating redundant bikes creates traffic congestion or chaos on the streets and leads to more complicated vehicle relocation operations. To tighten the number of bikes, we reduce N to 500 in our numerical experiments. As N is scaled from 1,206 down to 500, the upper bound B_j of region $j \in \mathcal{V}$ is also scaled down by multiplying $500/1,206$.

The cost parameters are estimated (in USD) on a daily basis. The vehicle allocation cost is $c_j = 0.5$ for each $j \in \mathcal{V}$.[2.3] The revenue per bike trip per period is $R = 0.2$ and the penalty cost $C_{\text{p}} = 0.5$ for an unfulfilled trip demand.[2.4] As for relocation costs, we use $C_{\text{r}} = 15$ for 3PL relocation per request with volume lower capacity $\underline{q} = 0$ and upper capacity $\bar{q} = 100$.[2.5] In addition, the 3PL can be requested at most $\bar{z} = 10$ times per day. In any given $l_{\text{f}} = 10$ consecutive periods, the 3PL

[2.3] The vehicle allocation cost is estimated by dividing 150 dollars (the normal price of a bicycle offered on Amazon.com) over 300 operational days per year (we exclude some days due to vehicle maintenance and weather conditions).

[2.4] Given that the annual membership costs 15 dollars per month, the revenue is estimated by assuming that each customer has 30 rides per month with 2.5 periods (15 minutes) per ride, leading to $R = 0.2$.

[2.5] According to American Transportation Research Institute (Murray and Glidewell 2019), the average service cost of motor carriers from 2015 to 2018 is 1.67 dollars per mile. We assume that the 3PL relocation charges the same price and covers 9 miles of a route through nine regions, which leads to about 15 dollars per relocation request.

can operate at most $\bar{\bar{z}} = 2$ consecutive periods.

The parameters of the incentive function $g(\cdot)$ are obtained as follows. Given any pair of regions $i, j \in \mathcal{V}$, we may estimate the maximum number of crowdsourced riders $\bar{\Lambda}_{ij}$ and the rate β_{ij} of the incentive function in (2.1a) from the historical data. Unfortunately, the available data is insufficient for such an estimation. Instead, we construct the piecewise-linear approximation of the incentive function in (2.5a) – (2.5e) using three parameters $\bar{\Lambda}_{ij}$, $\bar{k}_{hij}$, and $\bar{\phi}_{ij}$. We estimate these parameters as follows. (i) We first solve the two-stage optimization problem ($\mathcal{M}$) over the entire network $\mathcal{G}$ without any relocations. Denote its solution with superscript "**", and set $\bar{\Lambda}_{ij} = \max\{\eta^{**}_{n_{it},n_{j,t+l_{ij}}} \mid t \in \mathcal{T}(l_{ij})\}$. (ii) Next, we generate H slopes $\bar{k}_{hij},\ h \in \{1, 2, \ldots, H\}$, of the piecewise-linear function by obtaining the corresponding unit reward $1/\bar{k}_{hij}$. The H unit rewards are sampled from a uniform distribution $U(\underline{u}_{ij}, \bar{u}_{ij})$, where $\underline{u}_{ij} = 0.1 + 0.1 l_{ij}$ and $\bar{u}_{ij} = 0.2 + 0.1 l_{ij}$ are estimated by using the data of the Citi Bike's Bike Angels Rewards Program.[2.6] We then sort the H slopes in decreasing order to fit the incentive function in Figure 2.4. (iii) Finally, we can derive the length of each segment in Figure 2.4 by $\delta_{ij} = (\bar{\Lambda}_{ij} - \epsilon)/\sum_{h=1}^{H} \bar{k}_{hij}$ and the reward threshold by $\bar{\phi}_{ij} = H\delta_{ij}$. The trip duration between any two regions $i, j \in \mathcal{V}$ ranges from 1 to 4 periods. The maximum reward for crowdsourcing one rider is 0.6 dollar (i.e., $\max\{\bar{u}_{ij}\} = \max\{0.2 + 0.1 l_{ij} \mid l_{ij} \in \{1, \ldots, 4\}\} = 0.6$). We set the crowdsourcing budget $B_c = 500$ as we note that the actual crowdsourcing costs in our experiments are always lower than this value.

The data reveals that the hourly total demand of the studied area exhibits different patterns on weekdays and weekends. The former has a bimodal pattern with morning and evening peak hours, while the latter has a unimodal pattern with afternoon peak hours. Thus, we conduct the case study for the weekdays and the weekends separately. In the experiments, we use the 2018 data for training to com-

[2.6] This program has a hierarchical reward scheme. One can earn 1-6 points for one crowdsourcing trip depending on the origin and destination. The value of 1 point also varies. When a rider has accumulated points less than 80 in one month, every 20 points worth a one-week membership (i.e., 15 dollars per month). Thus we round the value of one point as 0.2 dollar. When more points are collected, every 10 points worth 1.2 dollar and we simply take one point as 0.1 dollar. Thus, we assume that on average, a 6-minute trip (i.e., one period) will reward the rider 1-1.5 point (i.e., 0.2-0.3 dollar) and every additional 6-minute will increase the range bounds by 1 more point (i.e., 0.1 dollar). In summary, the reward cost corresponding to trip duration l_{ij} is between $\underline{u}_{ij} = 0.1 + 0.1 l_{ij}$ and $\bar{u}_{ij} = 0.2 + 0.1 l_{ij}$ for any $i, j \in \mathcal{V}$.

pute the first-stage allocation $\mathbf{x}$ by solving problem ($\mathcal{M}$). Given $\mathbf{x}$, we use the 2019 data to perform out-of-sample tests by solving problem ($\mathcal{Q}$). We use 350 days of trip records each year as 350 different scenarios (i.e., a one-day sample corresponds to one scenario) to capture the demand uncertainty, where 250 scenarios correspond to the weekday demands and 100 scenarios correspond to the weekend demands. In our algorithm, we set the number of sub-networks $M = 8$.

Note that an efficient shared micromobility system should have a low total unsatisfied demand (also known as demand loss) $\sum_{a\in\mathcal{A}^{\mathrm{t}}} \eta_a$ and a high expected vehicle utilization rate defined as $\sum_{a\in\mathcal{A}^{\mathrm{t}}}(y_a - \Lambda_a)/\sum_{i\in\mathcal{V}} x_i$. We use these two measures to evaluate the service quality.

2.6.2 Computational Performance of the Solution Approach

We demonstrate the computational efficiency of our proposed solution approach in Section 2.5.2 for solving the integrated allocation and relocation problem ($\mathcal{M}$) by benchmarking it against CPLEX 12.71 with C++ API.[2.7] Our solution approach is implemented in parallel on 24 threads with C++ OpenMP. The computational experiments are performed on a computing node with 24 2.3-GHz Intel Xeon E5-2670 processors and 32 GB of memory in a high performance computing cluster.

It is worth noting that considering more scenarios ensures a higher solution quality but increases the computational time. Since both approaches above cannot solve any of the weekday training instances with 250 scenarios (because of out of memory), we need to reduce the number of scenarios for each weekday instance. Figure 2.7 shows how the computational time and the relative error of the total allocation[2.8] vary with the number of scenarios $|\mathcal{K}|$ under our solution algorithm. In general, as $|\mathcal{K}|$ decreases, the computational time decreases whereas the relative error first decreases and then increases. To strike a balance between the computational time

[2.7] We also implement the benchmark problems in the recent version CPLEX 12.10, but the solution performance only slightly improved for our instances. Note that the presolver, the dynamic search, the various cuts, and heuristics are turned on by default and decided by CPLEX internally.

[2.8] The relative error is defined as $(|x_{\mathrm{sum},|\mathcal{K}|=k} - x_{\mathrm{sum},|\mathcal{K}|=250}|)/x_{\mathrm{sum},|\mathcal{K}|=250} \times 100\%$, where $x_{\mathrm{sum},|\mathcal{K}|=250}$ and $x_{\mathrm{sum},|\mathcal{K}|=k}$ represent the numbers of allocated vehicles under the 250 scenarios and k scenarios respectively. To compute $x_{\mathrm{sum},|\mathcal{K}|=250}$, we implement our solution algorithm in a single thread by handling each scenario of the second-stage problem ($\mathcal{Q}$) sequentially (rather than in parallel), which requires much less memory.

and the relative error, we reduce the number of scenarios for each weekday instance from 250 to 80. We sample three 80-scenario instances (by randomly selecting 80 out of the 250 scenarios) and observe that the resulting relative error is only 1.18% on average. Note that the benchmark CPLEX approach cannot even solve any weekday training instance with 80 scenarios.

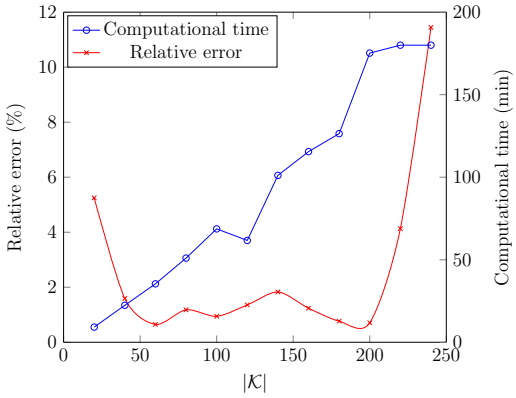

Figure 2.7: The Trade-off between the Computational Time and the Relative Error

Furthermore, our solution approach can efficiently solve all the weekend training instances, while the benchmark CPLEX approach struggles to get a high-quality solution. Thus, we do not reduce the number of scenarios for the weekend training instances. Finally, we set 180 minutes as the time limit for all the instances in our later experiments.

We further demonstrate the computational efficacy of our solution approach by varying several parameters. First, as the price varies with the vehicle type and quality, we consider the vehicle allocation cost $c_j \in \{0.5, 0.8, 1.0\}$, for $j \in \mathcal{V}$.[2.9] Second, we consider the fluctuation in the logistics market such that the 3PL relocation cost is $C_{\mathrm{r}} \in \{13, 15, 17\}$.[2.10] We consider the penalty cost $C_{\mathrm{p}} \in \{0.1, 0.3, 0.5, 0.7\}$ to represent the potential revenue loss of losing a customer under different market competition levels. This results in 36 ($= 3 \times 3 \times 4$) problem instances for a given

[2.9]For example, Mobike provides both the 'Lite' version bike (which incurs low cost) and the electric bike (which incurs high cost). The corresponding yearly allocation costs are estimated as 150, 210, and 300, leading to $c_j \in \{0.5, 0.8, 1.0\}$ for all $j \in \mathcal{V}$, respectively. Such costs are representative for most bikes, e-bikes and e-scooters according to their prices listed on Amazon.com; see https://www.amazon.com/s?k=bike&ref=nb_sb_noss.

[2.10]The average marginal cost (in US dollar) of trucking per mile ranges from 1.5-1.8 during 2010-2019 (Murray and Glidewell 2019). We assume that the 3PL runs 9 miles per request and thus the total cost per request is 13.5-16.2. We consider a slightly larger range 13-17.

weekday or weekend demand setting. For each instance, we run three experiments and report the average result in Table A2 in Appendix A.5.1, where each experiment is created by randomly sampling the demand values from the historical data.

For all the instances, our solution approach performs significantly better than the benchmark CPLEX approach for solving problem ($\mathcal{M}$) in terms of the solution quality ("Profit" in Table A2) and computational time. Note that the CPLEX approach cannot provide any feasible solution within the time limit of 180 minutes for the weekday instances, and can only provide a solution $x_j = 0,\ j \in \mathcal{V}$, for the weekend instances. In contrast, our solution approach produces high-quality solutions within 37.7 minutes on average for each weekday instance with 80 scenarios, and within 45.9 minutes on average for each weekend instance with 100 scenarios (see Table A2). These results suggest that our solution approach can potentially support urban shared micromobility operations well. We investigate its out-of-sample performance and obtain managerial insights from different perspectives in the following sections.

2.6.3 Impact of Allocation Upper Bound N on Vehicle Allocation and Relocation

We examine the impact of the vehicle allocation upper bound (UB) on the system's vehicle allocation and relocation under the parameter settings stated in Section 2.6.1. We vary the allocation upper bound N between 120 and 720, while keeping other parameters unchanged. We use the weekday demands for illustration. Similar insights are obtained for the weekend situation. Specifically, we examine how N affects the initial vehicle allocation in Figure 2.8 and the average number of relocated vehicles in Figure 2.9.

Figure 2.8 suggests that when the upper bound N is large (i.e., $N > 210$), it is economical to allocate fewer vehicles to each region than its upper bound. There is no need to allocate too many vehicles if demands can be well satisfied. It is interesting to see that more vehicles are allocated to regions 1 to 5, where public transportation and commercial blocks are distributed more densely than other regions (see Figure

2.6).[2.11]

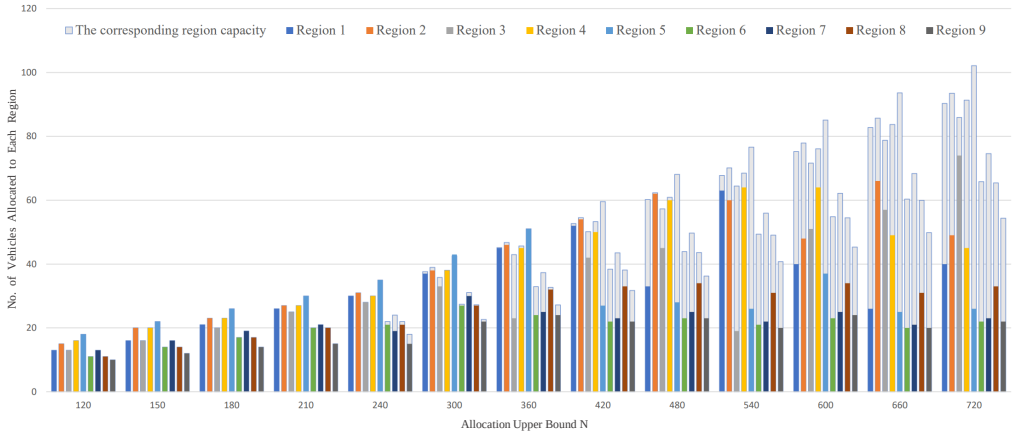

Figure 2.8: The Impact of Allocation UB on Vehicle Allocation for Different Regions

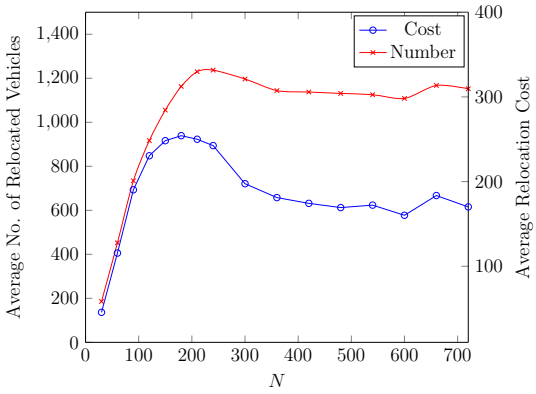

Figure 2.9: The Impact of Allocation UB on Vehicle Relocation

Figure 2.9 suggests that as N increases, both the average number of relocated vehicles and the average relocation cost first increase and then decrease. When the upper bound is low (i.e., $N \leq 210$), the initially allocated vehicles are not enough to satisfy the demands. Increasing the upper bound increases the initial allocation (as shown in Figure 2.8) and leads to more relocated vehicles. Thus, the number of relocated vehicles increases as the initial allocation increases. When the allocation upper bound is moderate (i.e., $210 < N \leq 480$), a larger upper bound N decreases both the average number of relocated vehicles and the average relocation cost. This is because a larger N leads to a higher initial allocation (see Figure 2.8) and the allocated vehicles are sufficient to satisfy most of the demands, which requires less vehicle relocation subsequently. This suggests that a higher initial allocation can

[2.11] The ridership ranking of the subway stations in NYC is referred to MTA (2020).

reduce the need for subsequent relocation. When the allocation upper bound is large (i.e., $N > 480$), both the initial allocation and subsequent relocation stabilize and are less affected by the upper bound.

Finally, we choose a sufficiently large upper bound $N = 500$ for the training instances. The optimal total number of allocated vehicles for the weekdays is 338 and that for the weekends is 253. Such vehicle allocations will be used for the later experiments.

2.6.4 Impact of Relocation Strategies

We examine four different relocation strategies for problem ($\mathcal{Q}$): (i) No micromobility vehicle relocation, i.e., $\phi_{n_{it},n_{j,t+l_{ij}}} = \Lambda_{n_{it},n_{j,t+l_{ij}}} = 0$, for $(n_{it}, n_{j,t+l_{ij}}) \in \mathcal{A}^{\mathrm{t}}$, and $z_t = 0$, for $t \in \mathcal{T}(l_{\mathrm{r}})$; (ii) relocation only by rider crowdsourcing, i.e., $z_t = 0$, for $t \in \mathcal{T}(l_{\mathrm{r}})$; (iii) relocation only by the 3PL, i.e., $\phi_{n_{it},n_{j,t+l_{ij}}} = \Lambda_{n_{it},n_{j,t+l_{ij}}} = 0$, for $(n_{it}, n_{j,t+l_{ij}}) \in \mathcal{A}^{\mathrm{t}}$; and (vi) relocation by both rider crowdsourcing and the 3PL. To demonstrate their operational performance, we conduct experiments over various instances by varying the penalty cost C_{p}.

Table 2.1 shows that demand loss can be effectively reduced by vehicle relocation. Compared to the case without any relocation, the demand loss can be significantly reduced by 98% through rider crowdsourcing alone and 50% through 3PL relocation alone, and can be further reduced when both relocation methods are used. Furthermore, relocation only by rider crowdsourcing yields a higher utilization rate and profit compared to relocation only by the 3PL. A more detailed observation on Table 2.1 indicates that rider crowdsourcing alone relocates more vehicles than the 3PL alone. Thus, compared to the 3PL, rider crowdsourcing is a more effective way to match supply with demand for the shared micromobility system.

To understand the above results, it is helpful to distinguish two types of relocation needs: mass relocation needs (i.e., many vehicles to be relocated, such as in rush hours) and sporadic relocation needs (i.e., only a few vehicles to be relocated, such as in non-rush hours). It is worth noting that rider crowdsourcing serves both the mass and sporadic relocation needs, while the 3PL generally only serves the mass relocation needs. For the sporadic relocation, the average cost per relocated

Table 2.1: Impact of Relocation Strategies and Penalty Cost

	C_p	Relocation Strategies	Crowdsourcing		3PL		Demand Loss	Utilization Rate	Profit ($)
			No. of Vehicles Relocated	Cost ($)	No. of Vehicles Relocated	Cost ($)			
Weekdays	0.1	No relocation	–	–	–	–	953.0	17.892	2,209.9
		Crowdsourcing	928.8	238.6	–	–	24.2	20.640	2,407.8
		3PL	–	–	650.7	63.5	473.3	19.311	2,398.2
		Combination	484.0	111.7	660.1	57.0	14.8	20.668	**2,481.4**
	0.3	No relocation	–	–	–	–	947.2	17.909	2,019.9
		Crowdsourcing	960.6	247.8	–	–	1.9	20.706	2,406.1
		3PL	–	–	665.1	66.7	457.0	19.359	2,309.5
		Combination	492.1	115.2	673.2	56.9	0.3	20.711	**2,482.5**
	0.5	No relocation	–	–	–	–	942.8	17.922	1,830.9
		Crowdsourcing	964.2	248.7	–	–	0.1	20.711	2,405.9
		3PL	–	–	673.3	67.6	455.3	19.364	2,217.1
		Combination	491.5	114.8	673.2	57.3	0	20.711	**2,482.7**
	0.7	No relocation	–	–	–	–	942.7	17.922	1,642.3
		Crowdsourcing	964.2	248.8	–	–	0.1	20.711	2,405.9
		3PL	–	–	677.6	69.1	451.1	19.377	2,129.9
		Combination	489.4	113.9	674.1	57.6	0	20.711	**2,483.3**
Weekends	0.1	No relocation	–	–	–	–	494.5	11.383	1,008.7
		Crowdsourcing	492.0	133.9	–	–	0.4	13.336	1,130.0
		3PL	–	–	318.5	33.8	218.1	12.475	1,128.4
		Combination	228.5	53.9	320.2	30.2	0.8	13.334	**1,179.8**
	0.3	No relocation	–	–	–	–	492.7	11.390	910.0
		Crowdsourcing	492.4	134.1	–	–	0.1	13.337	1,130.0
		3PL	–	–	319.8	34.5	219.2	12.471	1,082.8
		Combination	235.3	56.3	305.6	29.1	0	13.337	**1,178.6**
	0.5	No relocation	–	–	–	–	491.2	11.396	811.6
		Crowdsourcing	492.5	134.1	–	–	0	13.337	1,130.0
		3PL	–	–	309.3	34.8	228.5	12.434	1,030.4
		Combination	246.9	58.8	302.3	27.8	0	13.337	**1,177.5**
	0.7	No relocation	–	–	–	–	491.2	11.396	713.4
		Crowdsourcing	492.5	134.1	–	–	0	13.337	1,130.0
		3PL	–	–	301.1	34.5	227.1	12.440	985.0
		Combination	245.6	59.1	302.9	27.9	0	13.337	**1,177.0**

vehicle by using the 3PL is much higher than the cost of losing a customer. Thus, the 3PL is not cost effective for the sporadic relocation. For the mass relocation, the 3PL achieves a lower average cost per relocated vehicle because of the economies of scale in relocating vehicles in batches. Furthermore, Table 2.1 shows that when both relocation methods are used, the 3PL relocates more vehicles with a lower cost than rider crowdsourcing. The number of vehicles relocated by the 3PL is similar to that when only 3PL relocation is used. This suggests that the 3PL satisfies mostly the mass relocation needs, while rider crowdsourcing mainly serves the sporadic relocation needs.

In general, as the penalty cost per customer lost C_p increases, it becomes more likely to relocate vehicles to avoid demand losses. Interestingly, we observe the opposite effect for relocation only by the 3PL (strategy (iii)) on weekends: Increasing C_p may decrease the number of vehicles relocated by the 3PL.[2.12] Figure 2.10 shows

[2.12]To leave out the numerical errors, we test with different values of C_p in a finer scale and a

a typical scenario on weekends: When the penalty cost is low ($C_p = 0.1$), the 3PL relocates some vehicles (47 in this example) around 5pm. Surprisingly, when the penalty cost is high ($C_p = 0.5$), it does not relocate any vehicles. We explain this counter-intuitive result below.

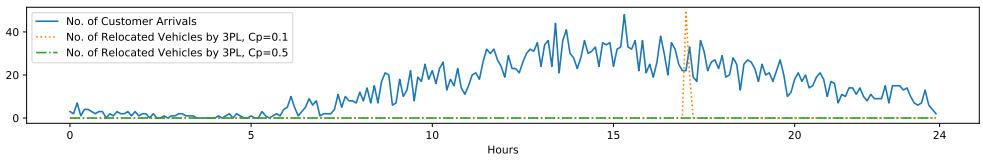

Figure 2.10: Customer Arrivals and Vehicles Relocated by The 3PL in A Day during Weekends

This counter-intuitive situation only happens on weekends rather than on weekdays. Since demands are lower on weekends, the need for relocation is lower. The unimodal pattern of customer arrivals in Figure 2.10 over a day shows that there are fewer rush hours. This reduces the need for the 3PL to relocate vehicles in batches. For example, when $C_p = 0.5$, the 3PL is requested 4.5 times per day on weekdays ($\approx$ total relocation cost by the 3PL/$C_r = 67.6/15$) and is requested only 2.3 times per day on weekends ($\approx 34.8/15$). Furthermore, relocating vehicles from region i to region j can increase the profit from region j, but may incur demand losses in region i. As C_p increases, the profit gain may be less than the penalty cost, causing the number of vehicles relocated by the 3PL to decrease. This reduces the overall profit of the 3PL. Table 2.1 shows that as C_p increases on weekends, the profit gap between relocation by combining both methods and relocation only by the 3PL increases. In fact, as C_p increases, the profit gap between relocation only by rider crowdsourcing and relocation only by the 3PL also increases. Therefore, the operator should use either only rider crowdsourcing or the combination of both methods instead of using the 3PL alone to relocate vehicles on weekends.

2.6.5 Impact of Rider Crowdsourcing Budget

If a shared micromobility operator wants to thrive in the market, his operational budget for relocation should be carefully planned. The shared micromobility op-

wider range from 0.1 to 1 with step length 0.1. We observe that the number of vehicles relocated by the 3PL remains decreasing while the demand loss shows an increasing trend.

erator often contracts with the 3PL for its relocation service, and thus the total relocation fee paid to the 3PL often remains stable. In addition, the operator can introduce rider crowdsourcing with a more adjustable budget to support his daily operations. When the operator is new in rider crowdsourcing, he can experiment and gradually adjust the budget to learn the effect. We examine the impact of rider crowdsourcing budget B_c on the system performance in Table 2.2.

Table 2.2: Impact of Rider Crowdsourcing Budget

	B_c	Crowdsourcing		3PL		Demand Loss	Utilization Rate	Profit ($)
		No. of Vehicles Relocated	Cost ($)	No. of Vehicles Relocated	Cost ($)			
Weekdays	0	0	0	673.3	67.6	455.3	19.365	2,217.1
	30	140.0	29.0	693.4	67.0	315.7	19.777	2,310.5
	50	223.4	46.9	689.5	66.2	234.4	20.018	2,357.9
	80	323.5	69.8	694.2	64.4	140.6	20.296	2,409.3
	100	373.7	82.1	685.8	62.9	95.2	20.430	2,433.4
	∞	491.5	114.8	673.2	57.3	0	20.711	2,482.7
Weekends	0	0	0	309.3	34.8	228.5	12.435	1,030.4
	10	47.7	9.7	316.0	34.2	181.4	12.621	1,064.6
	20	89.4	18.4	312.4	33.8	140.9	12.780	1,091.6
	30	125.4	26.4	313.3	32.4	108.2	12.910	1,112.5
	50	176.6	38.7	307.3	30.8	61.8	13.093	1,140.7
	∞	246.9	58.8	302.3	27.8	0	13.337	1,177.5

For weekdays or weekends, as the rider crowdsourcing budget B_c increases, more riders are crowdsourced and the number of vehicles relocated by these riders significantly increases. Meanwhile, the demand loss decreases and the vehicle utilization rate increases, leading to a higher profit. In contrast, as the crowdsourcing budget B_c increases, the number of vehicles relocated by the 3PL first increases and then decreases in general. The above results lead to the following phenomenon: Rider crowdsourcing complements (benefits) the 3PL when the crowdsourcing budget is low. On the other hand, when the budget is high, rider crowdsourcing substitutes the 3PL.

Figure 2.11 illustrates how rider crowdsourcing can complement the 3PL. Both the demands in region j in period t and that in region i in period $t + l_{jm} + l_{mi}$ are greater than the corresponding vehicle supply. If rider crowdsourcing is provided in region m, then the 3PL can relocate vehicles from region i in period $t - l_r$ to region j so that these vehicles can satisfy the demand of customers in region j in period t that move to region m. Crowdsourced riders help relocate these vehicles back to

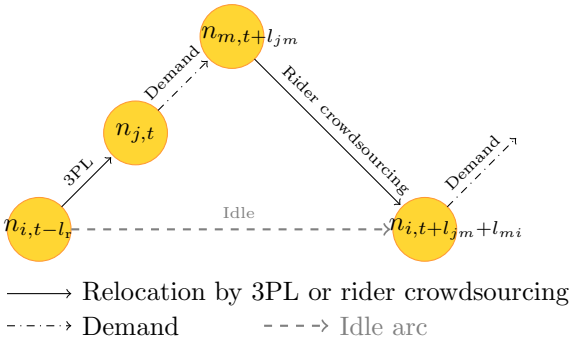

Figure 2.11: Rider Crowdsourcing Benefits The 3PL

region i to meet the demand in period $t + l_{jm} + l_{mi}$. Conversely, if no crowdsourcing is provided in region m because of an insufficient budget, then the 3PL may not relocate vehicles from region i in period $t - l_{\mathrm{r}}$ to region j. The vehicles remain idle in region i until period $t + l_{jm} + l_{mi}$. Thus, rider crowdsourcing can complement the 3PL.

As the crowdsourcing budget becomes larger, the 3PL relocation with a relatively high average cost per relocated vehicle can be substituted by the cheaper rider crowdsourcing, manifesting the substitutional effect. Although the above complementary and substitutional effects can potentially exist, rider crowdsourcing has limited impact on the number of vehicles relocated by the 3PL. Table 2.2 shows that as the crowdsourcing budget B_{c} increases, the number of vehicles relocated by the 3PL fluctuates only within 3.1% on weekdays and 4.5% on weekends. This suggests that introducing rider crowdsourcing to the micromobility system with 3PL relocation may significantly increase the system's profit without affecting the existing commitment with the 3PL.

2.6.6 Operational Features of Relocation

Table 2.1 shows that the micromobility system generates more profit if both relocation methods are adopted. Here, we examine the operational features of relocation in detail on three representative scenarios for weekdays, where the daily demand is low (4,744 trips), medium (7,967 trips), and high (12,294 trips). We observe similar relocation results on weekends.

Temporal Features of Relocation. Figure 2.12 shows the number of relocated

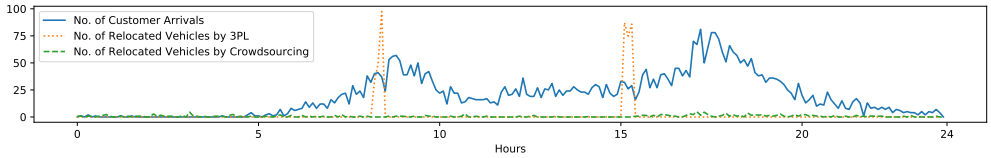

(a) Low-demand Scenario

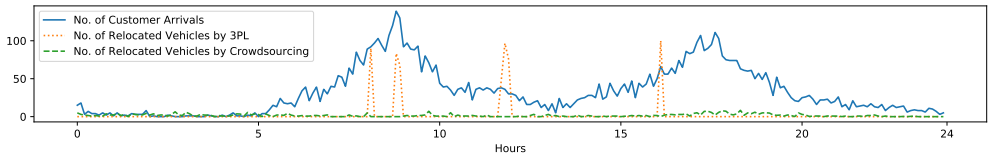

(b) Medium-demand Scenario

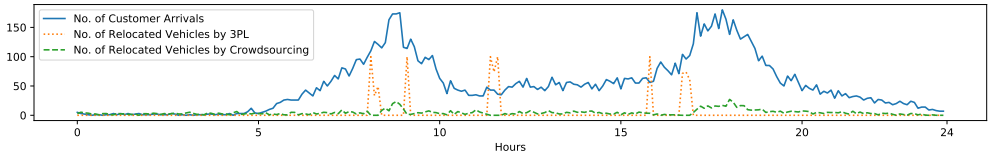

(c) High-demand Scenario

Figure 2.12: Customer Arrivals and Vehicles Relocated by 3PL and Rider Crowdsourcing during A Weekday

vehicles compared to the number of customer arrivals over the operational horizon. Clearly, the 3PL often relocates vehicles in batches during 8am-10am, 11am-1pm, and 3pm-5pm (i.e., around peak hours). As the 3PL relocates vehicles to adjust the supply across multiple regions to match potential demands in the upcoming periods, the number of relocated vehicles can be larger than the demand per period. Note that the 3PL is usually not engaged after the evening demand peak because of fewer customer arrivals that do not need batch relocation. In contrast, rider crowdsourcing is conducted throughout the day to relocate a much smaller number of vehicles per period.

Spatial Features of Relocation. Figure 2.13 displays the weekday demands during rush hours in the morning (top row) and evening (bottom row). Specifically, regions 2, 4, 5, 6, and 8 represent Midtown South, West, Center, East, and North, respectively, whereas regions 1, 3, 7, and 9 represent Midtown Southwest, Southeast, Northwest, and Northeast, respectively (see Figure 2.6).

According to a ridership report of subway traffic in Manhattan (MTA 2020), region 5 (Midtown Center) is the busiest region with the largest passenger flow.

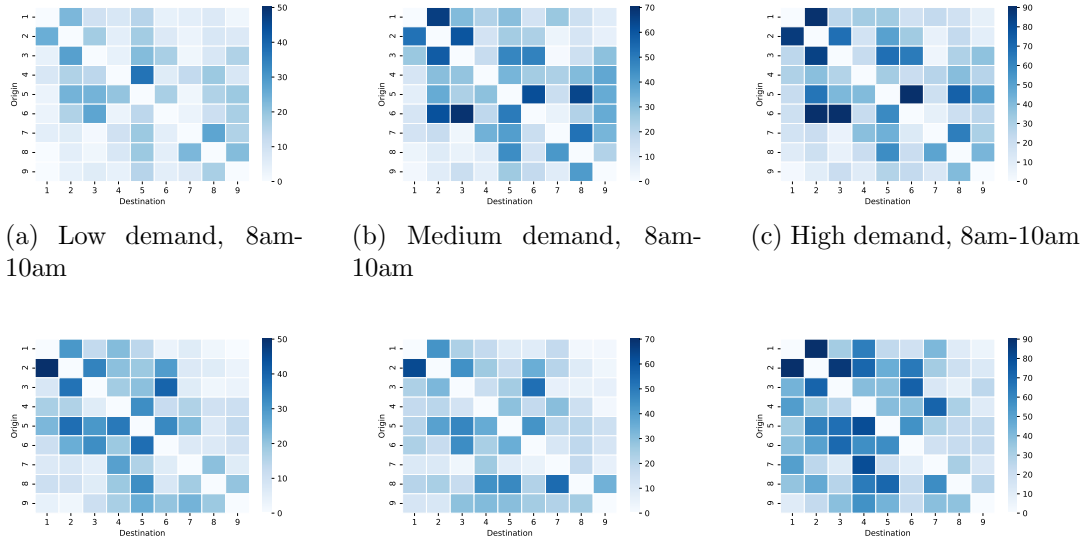

(a) Low demand, 8am-10am

(b) Medium demand, 8am-10am

(c) High demand, 8am-10am

(d) Low demand, 5pm-7pm

(e) Medium demand, 5pm-7pm

(f) High demand, 5pm-7pm

Figure 2.13: Spatial Features of Demands in Rush Hours

It covers Times Square, Herald Square, and the north part of Broadway, and has multiple subway lines passing through. Region 6 (Midtown East) has an important transportation hub, the Grand Central Terminal. Region 2 (Midtown South) has high-traffic subway stations, 34St Herald and 34St Penn Station, and is slightly busier than region 8 (Midtown North) where Rockefeller Center is located. Region 1 (Midtown Southwest) covers a few entrances of 34St Penn Station and hence can be a busy region. Region 9 (Midtown Northeast) has one high-traffic station, Lexington Av/53St. Figure 2.13 suggests that the shared micromobility demand is closely related to the ridership of subway traffic. The demand for short-range trips ($l_{ij} \leq 2$) is higher than that for long-range trips ($l_{ij} \geq 3$).

Figures 2.14 and 2.15 show the relocation by the 3PL and rider crowdsourcing, respectively. We focus on the demand features in two clusters of regions and the corresponding relocation features. In the first cluster, the busiest pick-up regions are regions 1, 2, and 3 (respectively, Midtown Southwest, South, and Southeast) during both 8am-10am and 5pm-7pm (see Figure 2.13), as most customers travel from one of these regions to a neighboring one. Thus, they are also among the busiest destinations. To maintain the vehicle supply, the operator relocates many vehicles to regions 1, 2, and 3 rather than from them. In particular, the 3PL may

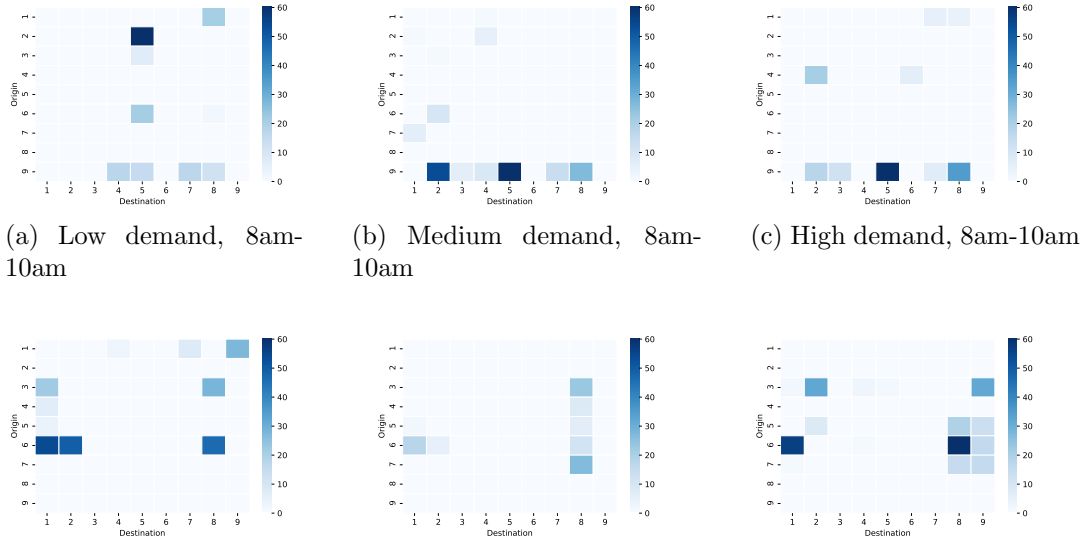

(a) Low demand, 8am-10am

(b) Medium demand, 8am-10am

(c) High demand, 8am-10am

(d) Low demand, 3pm-5pm

(e) Medium demand, 3pm-5pm

(f) High demand, 3pm-5pm

Figure 2.14: Spatial Features of 3PL Relocation

relocate vehicles from a faraway region (e.g., from region 9 to region 2 in Figure 2.14(b)). In contrast, rider crowdsourcing relocates from nearby regions (e.g., from region 5 to region 2 in Figure 2.15(i)).

In the second cluster, many customers pick up vehicles from region 5 (Midtown Center) and travel to regions 6 and 8 (respectively, Midtown East and North) in the morning (see Figures 2.13(b) and (c)). Thus, many vehicles are relocated to region 5 (Midtown Center) from other regions before the customers arrive. In particular, the 3PL relocates batches of vehicles mostly from the low-demand region 9 (Midtown Northeast) to region 5 (see Figures 2.14(b) and (c)). In contrast, rider crowdsourcing relocates only a few vehicles from each neighboring region to region 5 (see Figures 2.15(b) and (c)).

These observations suggest that the destinations of relocation by rider crowdsourcing and the 3PL are similar, indicating their common goal to match supply with demand. The 3PL relocates many vehicles per request from faraway regions, whereas rider crowdsourcing often incentivizes a few riders each time from neighboring regions. Thus, their origins of relocation are often different, resulting in the substitutional effect at each origin. This is consistent with Proposition 2.1.

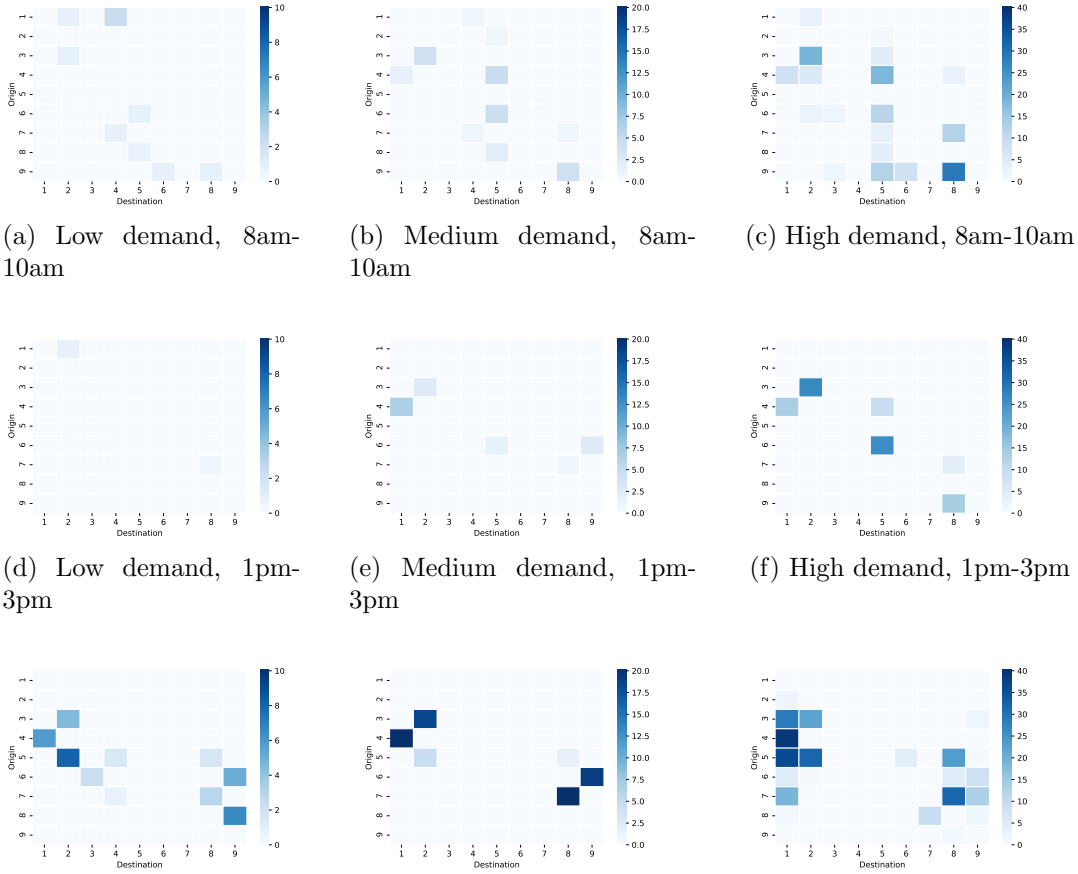

(a) Low demand, 8am-10am

(b) Medium demand, 8am-10am

(c) High demand, 8am-10am

(d) Low demand, 1pm-3pm

(e) Medium demand, 1pm-3pm

(f) High demand, 1pm-3pm

(g) Low demand, 5pm-7pm

(h) Medium demand, 5pm-7pm

(i) High demand, 5pm-7pm

Figure 2.15: Spatial Features of Rider Crowdsourcing Relocation

2.6.7 Impact of Temporal Demand Patterns

In this section, we investigate the impact of the demand pattern on vehicle relocation by comparing the unimodal customer arrival pattern on weekends and the bimodal pattern on weekdays. Note that the demand per day during weekends is lower than that during weekdays. To focus on the demand pattern's impact, we process our data using ARIMA models (Hamilton 2020) so that the demand per day during weekends is on the same scale as the demand per day during weekdays (see Appendix A.5.2 for the details). After training with the new data by solving problem ($\mathcal{M}$), the optimal total number of vehicles allocated under the unimodal pattern is 159, and that under the bimodal pattern is 170. We then solve problem ($\mathcal{Q}$) using testing data to obtain out-of-sample results. Table 2.3 presents the optimal vehicle relocation under the two demand patterns.

Table 2.3: Impact of Demand Patterns

Demand Pattern	C_p	Crowdsourcing		3PL		Demand Loss	Utilization Rate	Profit ($)
		No. of Vehicles Relocated	Cost ($)	No. of Vehicles Relocated	Cost ($)			
Bimodal (Weekdays)	0.05	254.8	60.4	130.4	17.1	8.4	29.861	1,590.2
	0.1	271.8	65.5	113.5	14.8	3.8	29.888	1,588.4
	0.3	274.1	65.9	113.3	15.0	0.2	29.901	1,588.9
	0.5	264.5	63.3	127.1	17.5	0	29.911	1,589.1
Unimodal (Weekends)	0.05	279.5	64.7	93.7	11.9	9.1	31.879	1,594.9
	0.1	278.6	64.5	101.0	12.8	6.0	31.898	1,594.8
	0.3	291.5	67.9	82.4	10.6	2.8	31.918	1,593.8
	0.5	293.3	68.2	81.9	10.8	2.0	31.923	1,593.4

We obtain the following insights. First, the total number of vehicles relocated by rider crowdsourcing together with the 3PL remains similar under the two demand patterns. However, the 3PL relocates more vehicles under the bimodal pattern than under the unimodal pattern. This is because the bimodal pattern has two demand peaks, for which batch relocation is more needed from the 3PL than the unimodal case. In contrast, rider crowdsourcing relocates more vehicles under the unimodal pattern than under the bimodal pattern.

Second, in contrast to Tables 2.1 and 2.2, the number of vehicles relocated by the 3PL is significantly smaller than that by rider crowdsourcing. This surprising result is because of the newly sampled demand that has slightly lower peak values as shown in Figure 2.16. Although the demand peak values are slightly lower, batch relocation by the 3PL is substantially less needed, while rider crowdsourcing is used more often.

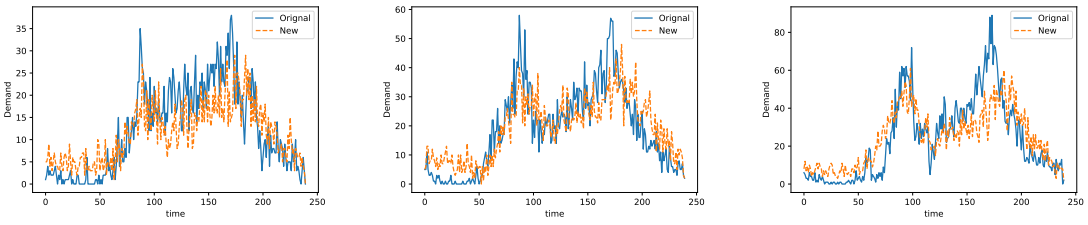

(a) Low-demand Scenario (b) Medium-demand Scenario (c) High-demand Scenario

Figure 2.16: Representative Demand Patterns during A Weekday

Third, the system has more vehicles allocated initially for the bimodal demand pattern (i.e., 170) than that for the unimodal pattern (i.e., 159). However, the profit under the bimodal pattern is lower than that under the unimodal pattern,

indicating that it is more challenging to manage the operations under the bimodal demand pattern. Since the total costs under the two demand patterns are similar, the higher utilization rate under the unimodal pattern leads to a higher profit.

2.7 Conclusion

Among shared mobility systems, a shared micromobility system presents a unique challenge because its operator often bears the cost of physical assets (i.e., micromobility vehicles). A proper initial vehicle allocation for different service regions is especially crucial for satisfying customer demands. In addition, the system offers the convenience of vehicle pick-ups and drop-offs, which may lead to a severe mismatch between supply and demand under uncertain customer arrivals. To better match supply with demand, it is necessary for the operator to constantly relocate the micromobility vehicles across the regions. When the system operator decides on how many vehicles to be initially allocated to different service regions, he also needs to consider the future relocation decisions. Thus, it is critical to integrate the initial allocation and subsequent relocation decisions to maximize the operator's profitability. The problem becomes especially complex when the operator adopts both rider crowdsourcing and 3PL outsourcing for vehicle relocation.

We formulate an integrated vehicle allocation and relocation problem under demand uncertainty as a two-stage stochastic integer programming model on a time-space network. In the first stage, the system operator decides the initial vehicle allocation before the demands are realized. In the second stage where various demand realizations are considered, the operator decides the relocation of vehicles across the regions to match supply with demand in each period. To maintain a financially sustainable micromobility system, the operator maximizes his expected profit.

For a special case with two service regions, we derive basic insights for the relocation strategy with both rider crowdsourcing and the 3PL. We find that under the optimal relocation strategy, rider crowdsourcing and the 3PL are not used simultaneously in any region and period. Instead, the optimal relocation strategy will choose a relocation method with a lower relocation cost per vehicle (see Proposition

2.1).

For a more general case with multiple service regions, we first approximate the incentive function, which determines the number of crowdsourced riders given a reward amount, using a piecewise-linear function. The approximation introduces some binary variables, which can be relaxed to continuous variables without affecting the optimal objective value of the second-stage relocation problem (see Proposition 2.2). We then propose an algorithmic approach that incorporates both scenario-based and time-based (temporal) decomposition ideas to efficiently solve the two-stage model. Numerical experiments suggest that our approach significantly outperforms the CPLEX solver in both solution quality and computational time (see Section 2.6.2).

Based on a data set from Citi Bike, we investigate the critical role of rider crowdsourcing in micromobility vehicle relocation for different parameter settings and demand patterns. We first solve the integrated vehicle allocation and relocation problem to obtain an initial vehicle allocation for different service regions. Based on the initial allocation, we then solve the second-stage relocation problem to determine out-of-sample relocation decisions. We uncover the following insights that may shed light on the successful operations of shared micromobility systems.

(i) If the vehicle allocation budget is tight, the number of relocated vehicles in the second stage increases as the number of allocated vehicles in the first stage increases. In contrast, if the vehicle allocation budget is sufficiently large, the number of relocated vehicles decreases as the number of allocated vehicles becomes larger. This is because if there are sufficiently many micromobility vehicles available initially, the need to relocate vehicles to match supply with demand subsequently becomes smaller (see Section 2.6.3).

(ii) If only one relocation method is adopted, rider crowdsourcing often outperforms the 3PL for matching supply with demand (see Table 2.1). If both relocation methods are used, the number of vehicles relocated by the 3PL dominates that by rider crowdsourcing because of the 3PL's lower average cost per relocated vehicle. The 3PL satisfies mostly mass relocation needs, while rider crowdsourcing mainly serves sporadic relocation needs. We find that investing in rider crowdsourcing

can increase the profit, reduce the demand loss, and improve the vehicle utilization rate of a shared micromobility system with an existing 3PL relocation method. Therefore, in high-traffic areas with dense populations, combining the two relocation methods leads to a higher profit. It is also interesting to note that as the penalty cost per customer lost increases, the number of vehicles relocated by the 3PL alone may decrease (see Figure 2.10).

(iii) We also investigate the impact of the rider crowdsourcing budget. As the rider crowdsourcing budget increases, the number of vehicles relocated by rider crowdsourcing increases, while the number of vehicles relocated by the 3PL first increases and then decreases. This suggests that rider crowdsourcing complements (benefits) the 3PL when the crowdsourcing budget is low, but substitutes the 3PL when the budget is high. Overall, introducing rider crowdsourcing to the micromobility system with 3PL relocation may significantly increase the system's profit without affecting the existing commitment with the 3PL (see Section 2.6.5).

(iv) Through studying the temporal and spatial relocation features, we find that the 3PL often conducts relocation around demand peak hours (e.g., 8am-10am, 11am-1pm, and 3pm-5pm), while rider crowdsourcing is conducted throughout the day. Moreover, to increase the supply in high-demand pick-up regions, the 3PL may relocate vehicles in batches from faraway, low-demand regions, while rider crowdsourcing tends to relocate a few vehicles each time from neighboring regions (see Section 2.6.6).

(v) Temporal demand patterns also have a significant impact on vehicle allocation and relocation. The operator allocates more vehicles initially under a bimodal customer arrival pattern. Besides, rider crowdsourcing relocates more vehicles under a unimodal customer arrival pattern than a bimodal pattern, whereas the reverse holds for 3PL outsourcing (see Section 2.6.7).

Although our numerical experiments are based on Citi Bike (2021), our proposed model and solution approach are sufficiently general for any typical shared micromobility systems. As the Citi Bike's data is quite representative, we believe the above insights shall hold for other micromobility systems with similar operational features as well.

Chapter 3

Resource Utilization in Green Products: Impacts of Recycling Label Scheme on Firm's Recycling and Pricing Decisions

3.1 Introduction

The promotion of recycled materials is one of the key missions in establishing Circular Economy, which is a model of production and consumption that involves sharing, leasing, reusing, repairing, refurbishing and recycling existing materials and products as long as possible. However, the current adoption of recycled materials in manufacturing is insufficient to meet these sustainability goals. Per an EU report, recycled materials during 2008-2016 met less than 12% of EU demand for materials (European Commision 2019). To aid the situation, for example, the New Plastics Economy Global Commitment was endorsed by over 400 organizations in 2018 to promote the circular use of plastics.[3.1] Other similar efforts are on the way, such as Make Fashion Circular, which promotes the use of recycled inputs for apparel in the fashion industry.[3.2] The environmental benefit of using recycled materials is multi-faceted, such as reducing the post-consumer waste to be landfilled or incinerated, reducing the need for raw materials and thus conserving natural resources.

Many consumers also care about the greenness of a product and are willing to

[3.1] Source: https://www.newplasticseconomy.org/ (Last accessed on September 1, 2020)
[3.2] Source: https://www.ellenmacarthurfoundation.org/our-work/activities/make-fashion-circular (Last accessed on September 1, 2020)

pay more for it. A UL Environment survey in 2014 shows 58% of respondents are willing to pay up to 10% more for a certified green product.[3.3] In spite of consumers' growing concern about sustainability, there are potential barriers that prevent consumers from knowing the extent of recycled materials used in a product. Hence, there is a strong demand for trustworthy environmental labels. The PEFC Global Consumer Survey reveals that more than 80% of consumers want product labels to communicate sustainable practices and content.[3.4] On the one hand, the labels help firms to communicate green efforts to consumers. On the other hand, they allow consumers to assess and compare the environmental performance of similar products without being an expert.

There are diverse environmental labels in the current market, and some are voluntary and some are mandatory.[3.5] This chapter studies voluntary recycling labels offered by non-governmental organizations (NGOs) that can independently evaluate and verify the product's recycled content. Furthermore, we focus on two different types of labels for recycled content. (For the sake of brevity, we often refer to recycling label as "label", and refer to the proportion of the recycled material used in a product as "recycled content".) First, we consider a *binary label* with only one pass/fail standard, such as the *PEFC recycled* label that requires the labeled product to contain at least 70% recycled material (PEFC Council 2008), as shown in Figure 3.1(a).[3.6] When observing such a binary label, consumers know that the product contains at least 70% recycled material. Second, we consider a *percentage label* that verifies and displays the actual percentage of the recycled material in a product, such as the *SCS Kingfisher* label (SCS Global Services 2014), the *Verus*

[3.3] Source: https://www.ul.com/news/study-proves-influence-green-product-claims-purchase-intent-and-brand-perception (Last accessed on September 1, 2020)

[3.4] Source: https://pefc.org/news/consumers-trust-certification-labels-and-expect-companies-to-label-products-pefc-research-shows (Last accessed on September 1, 2020)

[3.5] Voluntary labels are those that firms can choose to adopt or not. Mandatory labels impose regulations that firms must obey. In addition, the form of environmental labels can be versatile. We consider a general situation, in which the labels may appear directly on the product, indirectly in the advertisement, or in the online product display page, etc., subject to the marketing strategy.

[3.6] For example, 3M applies this label for some of its paper product *Post-it*, see https://www.3mireland.ie/3M/en_IE/p/d/v101312060/ (Last accessed on September 1, 2020). Note that in the latest PEFC standard released in February 2020, the standard for recycled content has been lifted to 100% to be eligible for the *PEFC recycled* label on the product. More information at www.pefc.org

label (Verus Carbon Neutral 2019), the *UL Recycled Content* label (UL 2019), and the *GreenCircle Certified* label (GreenCircle Certified 2019).[3.7] The examples of percentage labels are shown in Figure 3.1(b). When observing such a percentage label, consumers can discern the exact proportion of the recycled material.

(a) Example of Binary Label: PEFC Recycled Label

(b) Examples of Percentage Labels: GreenCircle Certified (left) and SCS Kingfisher Labels (right)

Figure 3.1: Label Examples

Different recycling label schemes will affect a firm's decisions regarding recycled content usage and price, which will in turn influence product demand, consumer surplus, and environmental impact. It remains unclear how different labels' designs influence the firm's decisions and profitability. Moreover, from the NGO's perspective, the focal question is how to design a recycling label that can incentivize sustainable practices and induce greater usage of recycled materials.

Motivated by the above observations, this chapter targets to study the impacts of different recycling label schemes on a firm's recycling and pricing decisions, as well as an NGO's payoff and consumers' surplus. To this end, we establish a game-theoretical model, wherein an NGO chooses a label type (binary or percentage) to maximize the total usage of recycled materials and a monopoly firm decides the fraction of the recycled material and price for his product. The market consists of two types of consumers: A fraction of consumers are environmentally conscious

[3.7]For example, the NORAMCO plastic bags with *SCS* label, see https://www.noramcobag.com/products/recycled-pgb-series; one type of HP printers is verified with 9% recycled content by *UL* label, see https://www.ul.com/news/ul-2809-recycled-content-validation-earned-hp-designjet-t200t600-printer-series. According to *SCS* standard for percentage-based recycled content claim, the term "minimum content" refers to the total recycled content (possibly for multiple components) in the final product rather than the recycled content of a particular component. The nature of this term is different from the minimum standard used by a binary label. For more details, please see https://cdn.scsglobalservices.com/files/standards/scs_stn_recycledcontent_v7-0_070814.pdf.

and willing to pay more for the recycled content; the rest are environmentally unconscious and indifferent between the recycled or non-recycled content. We aim to answer the following questions: (1) Under different labelling schemes, how are the firm's recycling and pricing decisions influenced by the fraction of environmentally conscious consumers and the technology cost of recycling? (2) Which type of label is preferred by the firm? Which one is preferred by the NGO? (3) How is consumer surplus influenced by the labelling scheme?

We highlight some of our findings. First, we derive the firm's optimal decisions under the percentage and binary labeling schemes, respectively. We find that as the fraction of environmentally conscious consumers increases or as the technology cost of recycling decreases, the firm's recycled content increases under the percentage label, while it may either increase or decrease under the binary label.

Second, the firm is always weakly better off under the percentage label than under the binary label. This is because the firm can choose the optimal recycled content and fully reveal the information by applying the percentage label. By contrast, the firm is constrained by the binary label standard and cannot fully reveal information to consumers, which reduces the firm's profitability.

Third, in contrast to the firm's preference, the NGO always weakly prefers the binary label. Moreover, under the percentage label, the NGO might even be worse off as more consumers become environmentally conscious or as the technology cost of recycling declines. This is because the NGO's payoff is associated with the total usage of recycled materials, which depends on both the recycled content in each product and the total demand of the product. As more consumers are willing to pay a premium for recycled content or as the fixed cost of recycling declines, the firm may change his strategy by increasing the price to only target the environmentally conscious consumers, which will lead to lower demand and thus reduce the total usage of recycled content.

Finally, we study the impact of different labeling schemes on consumers' total surplus. We find that, in contrast to the firm's preference, consumers weakly prefer the binary label to the percentage label. Because the binary label conveys only partial information, the NGO may set a low label standard that induces the firm to

compromise on price in exchange for more demand, which in turn allows consumers to extract more surplus. Noteworthily, under either a percentage or binary label, more environmentally conscious consumers or a lower fixed cost of recycling may hurt or benefit consumer surplus, as the firm's price strategy may change.

The remainder of this chapter is organized as follows. We review the literature in Section 3.2 and describe the game-theoretical model in Section 3.3. Section 3.4.1 analyzes the case of the percentage label; Section 3.4.2 analyzes the case of the binary label; Section 3.4.3 compares the outcomes in the two cases. The consumer surplus is discussed in Section 3.4.4. Section 3.5 concludes the chapter.

3.2 Literature Review

Our study is related to three streams of literature in economics and management operations areas: voluntary certification/labeling, recycling/remanufacturing, and corporate social responsibility (CSR). Certification is important in disclosing product information to consumers. Traditionally in economic literature, many papers study the information disclosure of a pass/fail certification (Lizzeri 1999, Garella and Petrakis 2008, Stahl and Strausz 2017, Zapechelnyuk 2020), and they mainly concern mandatory certifications for non-green products. This study, on the other hand, is closely related to voluntary certification/labeling concerning environmental issues. The literature related to this topic often focuses on the impact of competition, including competition among firms (Youssef and Lahmandi-Ayed 2008), competition among label certifiers (like NGOs) with the same interest (Heyes and Martin 2016), competition between conflicting interests, such as between NGOs and industry (Fischer and Lyon 2014, Li 2020) or between industry and regulator (Heyes and Maxwell 2004). These papers also examine the pass/fail standard for label design. In particular, some papers consider the information uncertainty of the label standard that results from certification error (Mason 2011) or consumers' lack of trust (Harbaugh et al. 2011). Moreover, there are some papers study multi-tier label design: Li and van 't Veld (2015) compare a multi-tier label with many competing single-tier labels under different objectives. Nadar and Ertürk (2020) compare the effects of a multi-tier label with a single-tier label in reducing environmental impact

and resource consumption. Fischer and Lyon (2019) study the environmental consequences when two sponsors, NGO and industry, compete with single-tier labels and multi-tier labels. Yenipazarli (2015) studies the impact of label standard and price under a full information label with a special labelling cost structure. Different from the above papers, this study mainly focuses on the NGO's voluntary recycling label and compares the percentage label of full information with the binary label of partial information.

Our work is also related to the literature on recycling or remanufacturing (see Souza 2013 for a comprehensive review). Chen and Liu (2014) study how price leadership impacts price and quality decisions for the green product in a duopoly market. They show that the brown firm as the price leader can lead to more recycled content in the product. Schlosser et al. (2021) develop an optimal control model to study dynamic pricing and recycling investment over time. For remanufacturing papers, many relevant ones focus on the impact of remanufacturing on product design. For example, Debo et al. (2005) study how a product's remanufacturing level and price are influenced by consumer distribution and cost structure. Atasu and Souza (2013) compare quality and pricing choices under three recovery schemes. They also compare mandatory and voluntary recovery rates, and find the quality is higher under mandate recovery legislation. Örsdemir et al. (2014) study how an OEM can compete with a remanufacturer in both quantity and quality. They find remanufacturing may not benefit the environment and consumers. Papers in this stream often assume perfect information and do not consider labels. We differ by considering different recycling label designs that can convey different information to consumers.

Finally, our work is relevant to the literature on CSR in operations area (see Lee and Tang (2018) for a comprehensive review). One stream of the literature examines how firms' strategies impact socially responsible behaviors (Plambeck and Taylor 2016, Chen and Lee 2017, Iyer and Singh 2018). We are more relevant to the studies on how regulation standards can induce social and environmental benefits. For example, a large body of papers investigate the impact of Extended Producer Responsibility (EPR), a policy that mandates manufacturers support the take-back,

recycling and final disposal of their products (see Atasu and Van Wassenhove 2012 and Kunz et al. 2018 for the overview). The literature of this stream considers diverse issues, such as the efficient design of EPR to improve environmental and/or economic impact (Atasu et al. 2009, Alev et al. 2020), the comparison of regulation standards facing channel competition (Esenduran et al. 2020), and the comparison of regulations with different cost allocations (Atasu and Subramanian 2012, Esenduran and Kemahlıoğlu-Ziya 2015, Gui et al. 2016, Huang et al. 2019, Rahmani et al. 2021). These studies mainly focus on mandatory regulation, rather than on the voluntary label as we consider. In particular, Murali et al. (2019) compare a self-label with full information and an external label with a pass/fail standard, and they aim to investigate the credibility of self-label and whether the government should intervene. In contrast to this and other studies within this stream, our work contributes to this body of work by studying voluntary recycling labels with different schemes that convey different information. We focus on the interaction between the label design and a firm's usage of recycled materials in a product.

3.3 Model Framework

We construct a single-period game to analyze the interactions among an NGO (referred to as "she"), a firm (referred to as "he"), and consumers (referred to as "they") in the context of label design and product design with recycled materials. The details of each player and the game sequence are explained below, and the notations used in this chapter are summarized in Table 3.1.

Firm: We consider a profit-maximizing firm selling a single product to consumers. The product can be produced from two types of materials: virgin material and recycled material. The firm can decide what percentage of recycled material to use for the product. Let $q \in [0, 1]$ denote the percentage of recycled material (also referred to as "recycled content") and $1 - q$ denote the percentage of virgin material.[3.8] To produce a product with recycled content q, the firm needs to incur fixed cost kq^2 and marginal cost $c(q)$, where $k > 0$ (referred to as "technology cost

[3.8]The recycled content is calculated by the ratio of the weight of the recycled material to that of the overall product. This definition of recycled content follows ISO 14021.

Table 3.1: Summary of Notations

Notation	Description
α	The fraction of environmentally conscious consumers
d	Consumer demand
v	Consumers' base valuation of the product
v_r	Environmentally conscious consumers' marginal valuation of recycled content
c_n	The marginal cost of the virgin material
c_r	The marginal cost of the recycled material
k	The fixed cost related to recycling technology
p	The product price
q	The percentage of recycled content, $q \in [0, 1]$
$\bar{q}$	The recycled content standard for the binary label, which is determined by the NGO, $\bar{q} \in (0, 1]$
π	The firm's profit
Π	The NGO's payoff
CS	Consumer surplus

of recycling"). The fixed cost kq^2 is associated with the facility or technology set-up for processing and integrating recycled materials into the product. The marginal cost $c(q) = c_r q + c_n(1 - q)$ is the sum of the costs of the two types of materials, where $c_r > 0$ and $c_n > 0$ represent the marginal costs of recycled and virgin material, respectively. The cost of the recycled material can be higher or lower than that of the virgin material in practice. For example, the recycled paper and carpet can be cheaper than their virgin counterparts (Biddle 1993); the recycled aluminum is cheaper than the newly processed aluminum (Goman 2021); and the recycled plastic was cheaper than its virgin counterpart during 2012-2019 but began to be more expensive since 2019 (Judith Evans and Hook 2020). Hence, we consider both the cases of $c_n > c_r$ and $c_n \leq c_r$ to cover the diverse cost scenarios in practice. The product has a base valuation $v > \max\{c_r, c_n\}$, regardless of its recycled content. In addition, we consider the recycled content in the product (i.e., q) to be the firm's

private information and unobservable to consumers. However, the recycled content can be verified by an NGO and certified with a label (if it meets the requirement), from which consumers can obtain some information regarding the recycled content, which will be elaborated later. The firm's problem is to choose recycled content q and retail price p to maximize his profit $\pi(p,q) = d\,(p - c(q)) - kq^2$, where d denotes the firm's demand and will be discussed later.

Consumers: Without loss of generality, we normalize the total number of consumers to one. There are two types of consumers with respect to their attitude towards recycled materials. A fraction $\alpha \in [0,1]$ of consumers are environmentally conscious (denoted by C-type), who appreciate recycled materials and are willing to pay more for greater recycled content; the rest of them $1-\alpha$ are environmentally unconscious (denoted by N-type), who are indifferent between recycled and virgin materials when making purchase decisions. The C-type consumers have additional marginal valuation $v_r > 0$ for the usage of recycled materials.[3.9] Consumers cannot observe the recycled content q directly, but can obtain information from the label certified by the NGO if the firm obtains one. Each N-type consumer's utility of purchasing the product is given by $u_N(p) = v - p$, which only depends on the base valuation v and price p but not on the recycled content. By contrast, each C-type consumer's utility is given by $u_C(p,\phi) = v + v_r\phi - p$, where ϕ denotes C-type consumers' belief about the recycled content based on the label information and will be discussed in details later when we introduce the label types. Each consumer will purchase one unit of the product if and only if the utility is non-negative. That is, C-type consumers will purchase the product if and only if $p \le v + v_r\phi$, and N-type consumers will purchase if and only if $p \le v$. Thus, the product demand is given by

$$d \doteq d(p,\phi) = \begin{cases} 1, & \text{if } p \in [0, v] \\ \alpha, & \text{if } p \in (v, v + v_r\phi] \\ 0, & \text{otherwise} \end{cases} . \tag{3.1}$$

Note that we assume that there exist some outside options which are made of pure virgin material and can provide consumers zero utility. That is, consumers who do

[3.9] The additional marginal valuation is a kind of premium that reflects the recognition of environmental benefits believed only by C-type consumers, as noted by Chen (2001) and Heyes and Martin (2016). The linear form of benefits that consumers obtain from recycled content is also adopted by Li and van 't Veld (2015), Lim et al. (2019), and Fischer and Lyon (2019).

not purchase this product will switch to the outside options that are made of pure virgin material.

NGO: We model an NGO as a third-party certifier that can provide a voluntary and credible label of recycled content for products. The NGO is able to verify the recycled content used in the product once the firm chooses to apply her label. For the sake of simplicity, we consider that there are two types of labels for the NGO to choose between: the percentage label (denoted as P) and the binary label (denoted as B). The percentage label shows exactly the percentage of the recycled material used in a product and can provide perfect information to consumers. By contrast, the binary label sets one pass/fail standard, denoted by $\bar{q} \in (0, 1]$,[3.10] and the product can only obtain the label if its recycled content meets the standard (i.e., $q \geq \bar{q}$) and cannot obtain the label otherwise (i.e., $q < \bar{q}$). To simplify the NGO's problem and derive clear insights from label comparison, we consider that the NGO can only choose one type of label to offer, and that there is no cost for the firm to apply the label as in Murali et al. (2019).

We focus on the case where the NGO is an environmental proactivist that cares about product waste management and aims to minimize environmental damage. Note that in our setting, all consumers will either purchase the focal product or switch to the outside options that made of pure virgin material. Therefore, the more total amount of recycled material used by the firm, the less total amount of virgin material to be exploited, and thus the less environmental damage there will be. Hence, we consider that the objective of the NGO is to maximize the overall usage of recycled material, which is equivalent to minimize the total amount of virgin material used in the whole market and hence reduce environmental damage.[3.11] As such, the NGO's payoff is given by $\Pi = dq$, where d is the total demand of the product and q is the percentage of the recycled material in the product.

Next, we discuss how C-type consumers' belief about the recycled content, ϕ, is influenced by the product's label. The percentage label provides them full informa-

[3.10] We assume $\bar{q} > 0$ in the binary case to avoid the trivial discussion on $\bar{q} = 0$.

[3.11] We remark that there is no consensus on an NGO's objective. Some NGOs may care more about environmental damage or benefit, and some may care more about profit performance. Our paper focuses on the former case, similar as that considered in Heyes and Martin (2016).

tion about the recycled content q, and thus $\phi = q$. By contrast, the binary label only indicates that the content q is no less than the standard $\bar{q}$. We assume that C-type consumers are willing to pay for the certified content $\bar{q}$ (i.e., $\phi = \bar{q}$) when the product obtains the binary label, and not willing to pay for the recycled content (i..e, $\phi = 0$) when the product fails to have a binary label. It is clear that the firm will always choose to apply the label, given that the label is free of cost and can provide necessary information to enhance C-type consumers' willingness-to-pay. We further remark that including the cost of applying the label will not qualitatively affect our main insights. Thus, for the sake of simplicity, we assume the labeling cost is zero.

Game sequence: The sequence of events is given as follows. In Stage 1, the NGO decides which type of label to offer, and sets the label standard $\bar{q}$ if the binary label is chosen. In Stage 2, given the NGO's label type, the firm decides the percentage of the recycled material q and retail price p. Given that applying the label is free, the firm will try to apply the label and may or may not obtain it. In Stage 3, consumers make purchase decisions after observing retail price p and the firm's label information.

Tie-breaking rules: We make the following tie-breaking rules: (1) When the firm is indifferent between setting a high or low price, the firm sets a low price so as to benefit consumers and the NGO. (2) When the NGO is indifferent between setting a high or low standard under the binary label, she will choose a high standard that benefits the firm.

3.4 Analysis

We solve the game through backward induction. We first analyze the case of the percentage label in Section 3.4.1, and then study the binary label in Section 3.4.2. The comparisons regarding the firm's profits and the NGO's payoffs under the two different labels are provided in Section 3.4.3. Finally, we further examine consumer surplus in Section 3.4.4.

3.4.1 Percentage Label

Given that the NGO offers the percentage label, the firm needs to decide the recycled content $q \in [0,1]$ and the product's price $p \geq 0$. Since we assume a zero cost for label registration, the firm will always apply for the label. In this case, consumers can perfectly know q by observing the label, i.e., $\phi = q$. Note that only if the firm's recycled content $q = 0$, he fails to obtain a label, and $\phi = 0$ accordingly. The firm's problem is to choose the recycled content and retail price to maximize his profit, i.e.,

$$\max_{p,q} \ \pi(p,q) = \begin{cases} \alpha(p - c(q)) - kq^2, & \text{if } p \in (v, v + v_r q] \\ p - c(q) - kq^2, & \text{if } p \in [0, v] \end{cases}.$$

Given any recycled content q, we first show the firm's optimal pricing strategy, denoted by $p_P^*(q)$, in Lemma 3.1. Note that we use subscript "P" to denote the case of the percentage label.

Lemma 3.1. *Under the percentage label, given recycled content q, the firm's optimal price decision is given by*

$$p_P^*(q) = \begin{cases} v + v_r q, & \text{if } \alpha > \tilde{\alpha} \text{ and } q > \tilde{q} \\ v, & \text{otherwise} \end{cases},$$

where $\tilde{\alpha} = \frac{v - c_r}{v + v_r - c_r}$ *and* $\tilde{q} = \frac{(1-\alpha)(v - c_n)}{v_r \alpha - (1-\alpha)(c_n - c_r)}$.

Obviously, the firm will either set $p_P^*(q) = v + v_r q$ to serve only C-type consumers (i.e., $d = \alpha$) or set $p_P^*(q) = v$ to serve all consumers (i.e., $d = 1$). We refer to the former as high price strategy and the latter as low price strategy. Lemma 3.1 provides us with the following insights. When there is a large fraction of C-type consumers (i.e., $\alpha > \tilde{\alpha}$) and the product contains a high percentage of the recycled material (i.e., $q > \tilde{q}$), the firm prefers to set a high price to only serve C-type consumers; otherwise, he prefers to set a low price and sell to all consumers. Next, we characterize the optimal recycled content q_P^* and the corresponding price $p_P^* \doteq p_P^*(q_P^*)$ in Proposition 3.1 and Table 3.2. The details are referred to Appendix B.1.2.

Proposition 3.1. *Given the percentage label, there exist parameter regions P_{1H}, P_{HH}, P_{LL}, P_{1L}, and P_{0L} in terms of the fraction of C-type consumers (α) and fixed cost factor (k), such that the firm's optimal recycled content (q_P^*) and the corresponding price (p_P^*) are given in Table 3.2.*

Table 3.2: The Firm's Decisions under the Percentage Label

Region	$c_n > c_r$				$c_n \leq c_r$		
	P_{1H}	P_{HH}	P_{LL}	P_{1L}	P_{1H}	P_{HH}	P_{0L}
q_P^*	1	$\frac{\alpha(v_r+c_n-c_r)}{2k}$	$\frac{c_n-c_r}{2k}$	1	1	$\frac{\alpha(v_r+c_n-c_r)}{2k}$	0
p_P^*	$v+v_r$	$v+v_r q_P^*$	v	v	$v+v_r$	$v+v_r q_P^*$	v

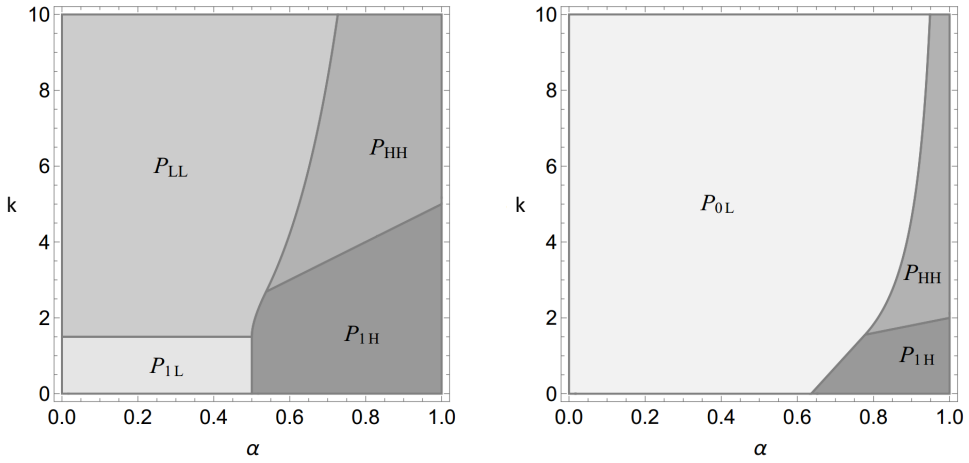

(a) When $c_n > c_r$ (b) When $c_n \leq c_r$

Figure 3.2: The Firm's Decision Regions under the Percentage Label
Note: In (a): $c_n = 4, c_r = 1, v = 8, v_r = 7$; In (b): $c_n = 1, c_r = 4, v = 8, v_r = 7$.

We define five regions ($P_{1H}, P_{HH}, P_{LL}, P_{1L}$, and P_{0L}) in terms of (α, k), in which the firm's decisions are different. Each region P_{ij} has two subscripts: The first subscript i denotes the recycled content decision and the second subscript j represents the price decision. Specifically, $i = 1$ means 100% recycled content (i.e., $q_P^* = 1$), $i = H$ means a high percentage of recycled content (i.e., $q_P^* = \frac{\alpha(v_r+c_n-c_r)}{2k}$), $i = L$ means a low percentage of recycled content (i.e., $q_P^* = \frac{c_n-c_r}{2k}$), and $i = 0$ means no recycled content (i.e., $q_P^* = 0$); $j = H$ means high-price strategy (i.e., $p_P^* = v+v_r q_P^*$), while $j = L$ indicates low-price strategy (i.e., $p_P^* = v$). These regions are depicted in Figure 3.2.

We explain Proposition 3.1 in two different cases, depending on whether the recycled material has a cheaper marginal cost than that of virgin material. First, we consider the case where the marginal cost of the recycled material is strictly cheaper than that of virgin material ($c_n > c_r$), as shown in Figure 3.2(a). Although the recycled material has a cheaper marginal cost, integrating the recycled material

will still incur an additional fixed cost. Thus, only when the fixed cost factor of recycling (k) is low (i.e., in regions P_{1H} and P_{1L}), the firm would use purely recycled materials (i.e., $q_P^* = 1$); otherwise, the firm would choose a high percentage of the recycled material if the fraction of C-type consumers is high (i.e., in region P_{HH}) and a low percentage of the recycled material if the fraction of C-type consumers is low (i.e., in region P_{LL}). Moreover, as previously discussed in Lemma 3.1, when the fraction of C-type consumers is high (i.e., in regions P_{1H} and P_{HH}), the firm would charge a high price such that only C-type consumers are willing to buy; otherwise (i.e., in regions P_{1L} and P_{LL}), he will charge a low price to serve all consumers. Next, we consider the case where the marginal cost of the recycled material is higher ($c_n \leq c_r$), as shown in Figure 3.2(b). The firm's price decision is similar to the previous case, but the recycled content decision is different. Since the recycled material is more expensive, the firm will not use any recycled material if the fraction of C-type consumers is not sufficiently high (i.e., in region P_{0L}). If there are sufficient C-type consumers, the firm will use purely recycled materials (i.e., $q_P^* = 1$) only when the fixed cost of recycling (k) is low (i.e., in region P_{1H}), and adopt a high percentage of recycled materials when the fixed cost is high (i.e., in region P_{HH}).

Let π_P^* and Π_P^* denote the firm's equilibrium profit and the NGO's equilibrium payoff in the percentage label case, respectively, which are given by:

$$(\pi_P^*, \Pi_P^*) = \begin{cases} (\alpha(v + v_r - c_r) - k, \alpha), & (\alpha, k) \in P_{1H} \\ (\frac{v_r^2\alpha + \alpha(c_n - c_r)(c_n - c_r + 2v_r) + 4k(v - c_n)}{4k}, \frac{\alpha^2(v_r + c_n - c_r)}{2k}), & (\alpha, k) \in P_{HH} \\ (\frac{4k(v - c_n) + (c_n - c_r)^2}{4k}, \frac{c_n - c_r}{2k}), & (\alpha, k) \in P_{LL} \\ (v - c_r - k, 1), & (\alpha, k) \in P_{1L} \\ (v - c_n, 0), & (\alpha, k) \in P_{0L} \end{cases} . \quad (3.2)$$

We further conduct sensitivity analysis to study how the fraction of C-type consumers (α) and the technology cost of recycling (k) affect the firm's optimal recycled content and profit as well as the NGO's payoff. The results are summarized in Corollary 3.1.

Corollary 3.1. *Under the percentage label: (1) The firm's optimal recycled content (q_P^*) and the corresponding profit (π_P^*) are (weakly) increasing in α and (weakly)*

decreasing in k. (2) The NGO's payoff (Π_P^*) may increase or decrease in α and in k.

Corollary 3.1(1) shows the firm will (weakly) increase the recycled content and earn a (weakly) higher profit as more consumers become C-type or as the technology cost of recycling decreases. This implies that when the percentage label is offered to reveal full information, the firm would have incentive to help popularize environmental education and increase the environmental consciousness of the public, or to improve the technology level to pursue a lower cost of processing recycled materials. Our findings are consistent with some practical observations. For example, Hewlett-Packard adopted *UL Recycled Content* label (an example of percentage labels) for some of its products, and it also actively engaged in the practices that could encourage consumers to recycle and enhance their awareness of environmental issues.[3.12]

Moreover, interestingly, we find that as the fraction of C-type consumers increases or the fixed cost of recycling becomes lower, the NGO can be better off within each decision region (see Figure 3.2) but may be even worse off in the entire region, as shown in Corollary 3.1(2). Specifically, when α increases or k decreases such that the region switches from $P_{LL} \cup P_{1L} \cup P_{0L}$ to $P_{1H} \cup P_{HH}$, the NGO's payoff could even be reduced. This is because although the firm adopts a higher percentage of recycled materials as α increases or k decreases, his pricing strategy may change from low to high, and thus the total demand becomes lower. This may lead to either a higher or lower total usage of recycled materials, and thus may benefit or hurt the NGO's payoff.

3.4.2 Binary Label

We study the case of the binary label in this section. Given that the binary label is chosen, the NGO needs to further decide the label standard $\bar{q} \in (0, 1]$. Then, the firm decides the recycled content q and price p. Different from the percentage

[3.12] See https://www.recyclingtoday.com/article/hp-striving-higher-recycled-plastics/; https://www.siliconrepublic.com/science/hp-encourages-consumers-to-print-and-recycle-like-the-lorax.

label, the firm can only obtain the binary label if $q \geq \bar{q}$, and cannot obtain the label otherwise. The C-type consumers are willing to pay for the certified recycled material (i.e., $\phi = \bar{q}$) when the product has a binary label, and are not willing to pay any premium (i.e., $\phi = 0$) for the product without a label. Given the binary label with standard $\bar{q}$, the firm's profit is:

$$\pi(p, q|\bar{q}) = \begin{cases} \alpha(p-c) - kq^2, & \text{if } p \in (v, v + v_r\bar{q}] \text{ and } q \geq \bar{q} \\ -kq^2, & \text{if } p \in (v, v + v_r\bar{q}] \text{ and } q < \bar{q} \\ p - c - kq^2, & \text{if } p \in [0, v] \end{cases}.$$

Note that if $p > v + v_r\bar{q}$, the product demand will be zero; similarly, if $p > v$ and $q < \bar{q}$, the firm has zero demand and negative profit. Thus, it is easy to see that in the equilibrium, the firm would either obtain a binary label ($q \geq \bar{q}$) and charge a high price $p = v + v_r\bar{q}$ to target C-type consumers only, or charge a low price $p = v$ to target all consumers. Lemma 3.2 characterizes the firm's optimal pricing strategy, denoted by $p_B^*(q, \bar{q})$, given the recycled content q and the label standard $\bar{q}$. Note that we use subscript "B" to denote the binary label case.

Lemma 3.2. *Given the binary label with standard $\bar{q}$ and the firm's recycled content q, the firm's optimal price decision is given by*

$$p_B^*(q, \bar{q}) = \begin{cases} v + v_r\bar{q}, & \text{if } \frac{(\alpha-1)[c_r q + c_n(1-q) - v]}{\alpha v_r} < \bar{q} \leq q \\ v, & \text{otherwise} \end{cases}.$$

This lemma shows that the firm prefers the high-price strategy (i.e., $p_B^*(q, \bar{q}) = v + v_r\bar{q}$) when the binary label standard is relatively high and he obtains the label, and he prefers the low-price strategy (i.e., $p_B^*(q, \bar{q}) = v$) otherwise. Next, given label standard $\bar{q}$, we show the firm's optimal recycled content, denoted by $q_B^*(\bar{q})$, and the corresponding price, denoted by $p_B^*(q_B^*(\bar{q}), \bar{q})$, in Lemma 3.3 and Table 3.3. A visualization of the equilibrium outcomes as a function of k and $\bar{q}$ is shown in Figure 3.3. The details are referred to Appendix B.2.2.

Lemma 3.3. *Given the binary label standard $\bar{q}$, there exist parameter regions Q_{ij} for $i \in \{1, H, M, L, 0\}$ and $j \in \{H, L\}$, such that the firm's optimal recycled content ($q_B^*(\bar{q})$) and the associated price ($p_B^*(q_B^*(\bar{q}), \bar{q})$) are given in Table 3.3. Specifically, in region Q_{0L} or Q_{LL}, the firm cannot obtain the binary label, i.e., $\bar{q} > q_B^*(\bar{q})$; otherwise, he can obtain the label, i.e., $\bar{q} \leq q_B^*(\bar{q})$.*

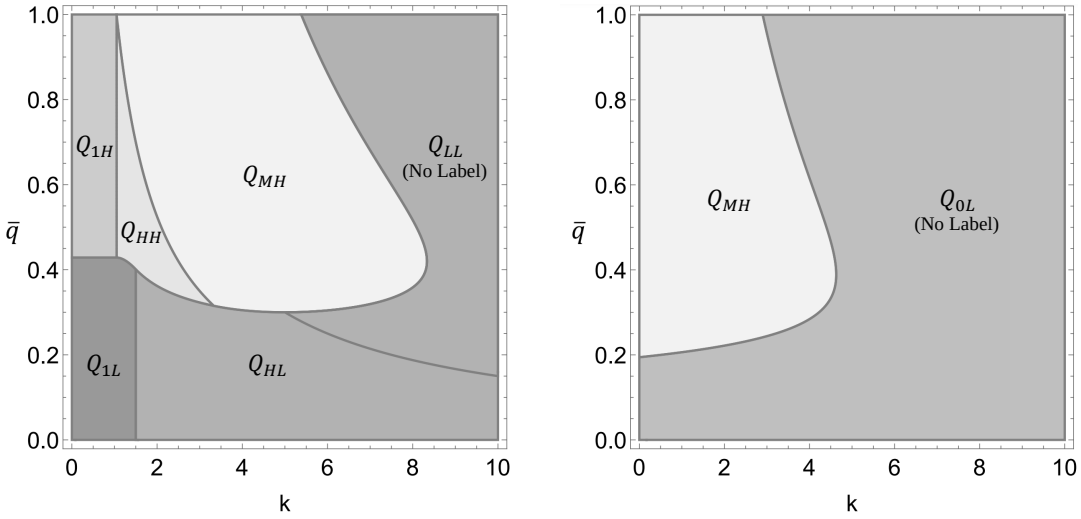

(a) When $c_n > c_r$ (b) When $c_n \leq c_r$

Figure 3.3: The Firm's Decision Regions under the Binary Label

Note: In (a): $c_n = 4, c_r = 1, v = 8, v_r = 7, \alpha = 0.7$; In (b): $c_n = 1, c_r = 4, v = 8, v_r = 7, \alpha = 0.9$. In $Q_{0L} \cup Q_{LL}$, the firm cannot obtain the label. Otherwise, the firm can obtain the label.

Table 3.3: The Firm's Decisions Given the Binary Label Standard

	$c_n > c_r$						$c_n \leq c_r$	
Region	Q_{1H}	Q_{HH}	Q_{MH}	Q_{1L}	Q_{HL}	Q_{LL}	Q_{MH}	Q_{0L}
$q_B^*(\bar{q})$	1	$\frac{\alpha(c_n-c_r)}{2k}$	$\bar{q}$	1	$\frac{c_n-c_r}{2k}$	$\frac{c_n-c_r}{2k}$	$\bar{q}$	0
$p_B^*(q_B^*(\bar{q}), \bar{q})$	$v + v_r\bar{q}$	$v + v_r\bar{q}$	$v + v_r\bar{q}$	v	v	v	$v + v_r\bar{q}$	v
Label	✓	✓	✓	✓	✓	×	✓	×

We define the regions Q_{ij} for $i \in \{1, H, M, L, 0\}$ and $j \in \{H, L\}$, in which the firm's decisions are different. Each region Q_{ij} has two subscripts: The first subscript i describes the recycled content decision and the second subscript j represents the price decision. Specifically, $i = 1$ means 100% recycled content (i.e., $q_B^*(\bar{q}) = 1$), $i = H$ means the recycled content is greater than the label standard (i.e., $q_B^*(\bar{q}) > \bar{q}$), $i = M$ means the recycled content exactly equals the label standard (i.e., $q_B^*(\bar{q}) = \bar{q}$), $i = L$ means the recycled content is less than the label standard (i.e., $q_B^*(\bar{q}) < \bar{q}$), and $i = 0$ means no recycled content (i.e., $q_B^*(\bar{q}) = 0$); $j = H$ means high-price strategy, while $j = L$ means low-price strategy. The visualization of these regions is given in Figure 3.3.

Similarly, we explain the firm's optimal recycled content in two different cases, depending on the marginal cost of the recycled material. The first case, in which

the recycled material is cheaper than the virgin material (i.e., $c_n > c_r$), is shown in Figure 3.3(a). Note that integrating recycled material will incur an additional fixed cost. Thus, although the recycled material has a cheaper marginal cost, the firm will adopt purely recycled materials only when the fixed cost k is small, and switch to high, medium, and low level of recycled content as k increases. Particularly, when both fixed cost k and the label standard $\bar{q}$ are large (i.e., in region Q_{LL}), the firm's recycled content will be lower than the label standard and will have to set a low price since he fails to obtain the label. In the second case, in which recycled material is more expensive (i.e., $c_n \leq c_r$), the firm will either adopt a medium percentage of recycled content and a high price when the fixed cost factor k is low, or adopt zero recycled content and a low price when k is large, as shown in Figure 3.3(b).

Finally, we remark that, in contrast to the percentage label case in which the firm can always obtain a label, the firm may or may not obtain the binary label. As shown in Lemma 3.3, the firm will choose not to meet the label standard in two regions: 1) When the recycled material is cheaper and both the fixed cost of recycling and the label standard are high (i.e., in region Q_{LL}); 2) When the virgin material is cheaper and the fixed cost of recycling is high (i.e., in region Q_{0L}).

Next, we turn to the NGO's problem. Given the firm's decisions, the NGO sets the binary label standard $\bar{q}$ to maximize her payoff:

$$\max_{\bar{q}} \ \Pi(\bar{q}) = \begin{cases} \alpha \cdot q_B^*(\bar{q}), & \text{if } p_B^*(q_B^*(\bar{q}), \bar{q}) \in (v, v + v_r\bar{q}] \\ q_B^*(\bar{q}), & \text{if } p_B^*(q_B^*(\bar{q}), \bar{q}) \in [0, v] \end{cases}.$$

The NGO obtains payoff $\alpha q_B^*(\bar{q})$ when the firm sets a high price that only attracts C-type consumers (i.e., $d = \alpha$), and payoff $q_B^*(\bar{q})$ when the firm sets a low price to target all consumers (i.e., $d = 1$). Let $\bar{q}^*$ denote the NGO's optimal binary label standard, and let $q_B^* \doteq q_B^*(\bar{q}^*)$ and $p_B^* \doteq p_B^*(q_B^*, \bar{q}^*)$ denote the firm's corresponding recycled content and price, respectively. Then, the NGO's optimal label standard $\bar{q}^*$ and the firm's optimal recycled content q_B^* and price p_B^* are described in Proposition 3.2 and Table 3.4. The NGO's corresponding payoff is provided in Appendix B.2.5.

Proposition 3.2. *Given the binary label, the NGO's optimal label standard ($\bar{q}^*$) and the firm's optimal decisions are given in Table 3.4.*

Table 3.4: NGO's and the Firm's Decisions under the Binary Label

	$c_n > c_r$						$c_n \leq c_r$		
Region	B_{1H}	B_{MH}	B_{1L}	B'_{1L}	B_{ML}	B_{HL}	B_{1H}	B'_{MH}	B_{0L}
$\bar{q}^*$	1	$\bar{q}_{MH}$	1	$\bar{q}_{1L}$	$\frac{c_n-c_r}{2k}$	$\bar{q}_{HL}$	1	$\bar{q}'_{MH}$	$(0,1]$
q^*_B	1	$\bar{q}_{MH}$	1	1	$\frac{c_n-c_r}{2k}$	$\frac{c_n-c_r}{2k}$	1	$\bar{q}'_{MH}$	0
p^*_B	$v+v_r\bar{q}^*$	$v+v_r\bar{q}^*$	v	v	v	v	$v+v_r\bar{q}^*$	$v+v_r\bar{q}^*$	v
Label	✓	✓	✓	✓	✓	✓	✓	✓	×

Note: $\bar{q}_{MH}=\frac{\alpha(v_r-c_r+c_n)+\sqrt{\alpha^2(v_r-c_r+c_n)^2+4k(v-c_n)(\alpha-1)-(c_n-c_r)^2}}{2k}$, $\bar{q}'_{MH}=\frac{\alpha(v_r-c_r+c_n)+\sqrt{\alpha^2(v_r-c_r+c_n)^2+4k(v-c_n)(\alpha-1)}}{2k}$, and $\bar{q}_{1L}$ and $\bar{q}_{HL}$ are given in Appendix B.2.3.

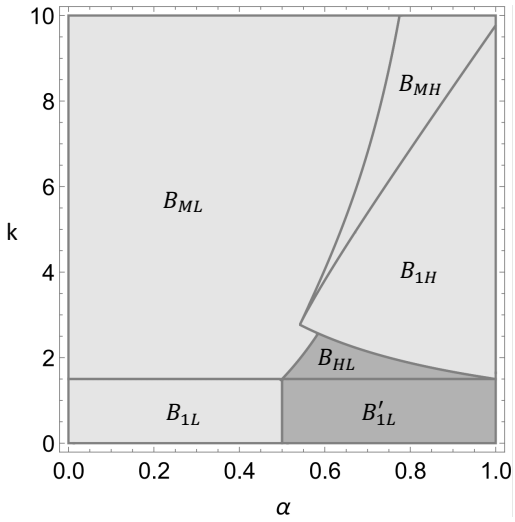

(a) When $c_n > c_r$

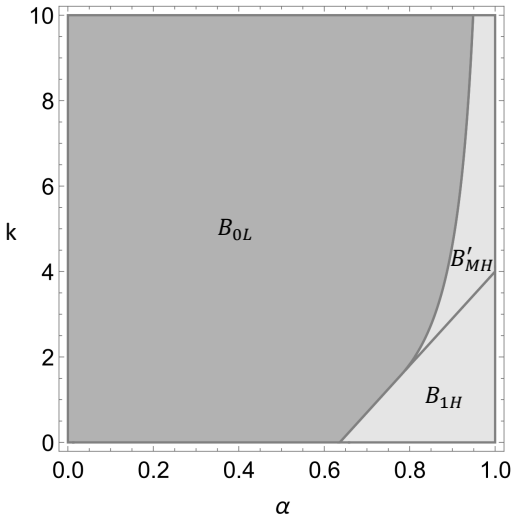

(b) When $c_n \leq c_r$

Figure 3.4: The NGO's Decision Regions under the Binary Label

Note: In (a): $c_n = 4, c_r = 1, v = 8, v_r = 7$; In (b): $c_n = 1, c_r = 4, v = 8, v_r = 7$.

Similarly, we define the regions B_{ij} for $i \in \{1, H, M, L, 0\}$ and $j \in \{H, L\}$ in terms of (α, k) to differentiate the equilibrium outcomes. The subscript i represents recycled content and j indicates the price strategy, which are defined similarly to those for region Q_{ij}. Those regions are depicted in Figure 3.4, and the details are referred to Appendix B.2.3.

First, we consider the case in which the recycled material has a higher marginal cost (i.e., $c_n \leq c_r$), as shown in Figure 3.4(b). Since the recycled material is more expensive, when the fraction of C-type consumers is small (i.e., in region B_{0L}), the firm is not interested in using any recycled content and will set a low price regardless of the NGO's label standard. In this region, the NGO will gain zero

payoff and become indifferent to any label standard between 0 and 1. When the fraction of C-type consumers (α) becomes larger, the firm will have more incentive to use recycled materials and the NGO will induce more usage of recycled content through the design of its label standard. Specifically, when α is large and the technology cost of recycling (k) is low (i.e., in region B_{1H}), the NGO will set the label standard to 100%, and the firm will use purely recycled content to obtain the label and set a high price to target only C-type consumers. When both α and k are high (i.e., in region B_{MH}), the NGO will set a moderate label standard, and the firm will just meet the standard and set a high price.

Second, we consider the case in which the recycled material has a lower marginal cost (i.e., $c_n > c_r$), as shown in Figure 3.4(a). Since the recycled material is cheaper, the firm has an incentive to adopt some recycled material in order to lower the total marginal cost; and the NGO's label standard would also influence the firm's recycled content and price decisions. When the fixed cost factor k is low or the fraction of C-type consumers α is high (i.e., in regions B_{1L}, B'_{1L}, B_{HL} and B_{1H}), the firm will either choose purely recycled content or a proportion of recycled content that is strictly higher than the label standard (i.e., $q_B^* > \bar{q}^*$); otherwise (i.e., in regions B_{MH} and B_{ML}), he will choose the recycled content that just meets the label standard (i.e., $q_B^* = \bar{q}^*$). Interestingly, in regions B'_{1L} and B_{HL}, the firm's recycled content will be strictly higher than the label standard. Given that the NGO can anticipate the firm's recycled content decision, why would she set a label standard strictly lower than the firm's choice? The reason is as follows. In these two regions, the firm faces a low fixed cost and a high fraction of C-type consumers; thus, he has incentive to adopt high percentage of recycled materials and set a high price to only serve C-type consumers. While the NGO wants to encourage high demand so that the total usage of recycled materials can be improved. Note that the binary label can only partially reveal the information of recycled content to consumers, that is, a firm's high price strategy is constrained by the label standard. Thus, to induce greater usage of recycled materials, the NGO will set a relatively low label standard in these regions, so that charging a high price to serve only C-type consumers becomes less profitable for the firm. Hence, given the low label standard, the firm will choose a

strictly higher recycled content but a low price to serve all consumers, and the NGO can benefit from the larger demand.

We further summarize different situations of the firm's label outcome in the following proposition.

Proposition 3.3. *Given the binary label:*
(1) The firm will not obtain the label (i.e., $\bar{q}^* > q_B^*$) in the region B_{0L};
(2) The firm sets the level of recycled content strictly higher than the label standard (i.e., $\bar{q}^* < q_B^*$) and obtains the label in the regions B_{HL} and $B_{1L}^{'}$;
(3) The firm sets recycled content exactly the same as the label standard (i.e., $\bar{q}^* = q_B^*$) and obtains the label in the other regions.

As previously discussed, in most cases the NGO will set a label standard at the level such that the firm will just meet it (i.e., $\bar{q}^* = q_B^*$). However, when the recycled material is more costly than virgin material and the technology cost of recycling is high (i.e., in region B_{0L}), the firm will not use any recycled content regardless of the label standard, and thus will not obtain the label. Moreover, when the recycled material is cheaper, the firm would prefer to use a percentage of the recycled material that is even strictly higher than the label standard (i.e., $\bar{q}^* < q_B^*$) if the technology cost of recycling is low and the fraction of C-type consumers is high (i.e., in regions B_{HL} and $B_{1L}^{'}$). This situation is not uncommon in practice. For example, 3M claims that its product, Post-it Recycled Notes, is made with pure recycled paper and certified by *PEFC Recycled* label (an example of binary labels) which only requires a minimum of 70% recycled content.[3.13]

Next, we will show how the fraction of C-type consumers and the fixed cost of recycling affect the NGO's and the firm's decisions and payoffs. The results are summarized in Corollary 3.2 and depicted in Figure 3.5.

Corollary 3.2. *Under the binary label, in the equilibrium: (1) The NGO's label standard ($\bar{q}^*$) may increase or decrease in α and in k. (2) The firm's recycled content (q_B^*) (weakly) increases in α and may increase or decrease in k. (3) Both the firm's profit and the NGO's payoff (weakly) increase in α and (weakly) decrease*

[3.13] See https://www.3m.co.uk/3M/en_GB/p/d/v101054008/

in k.

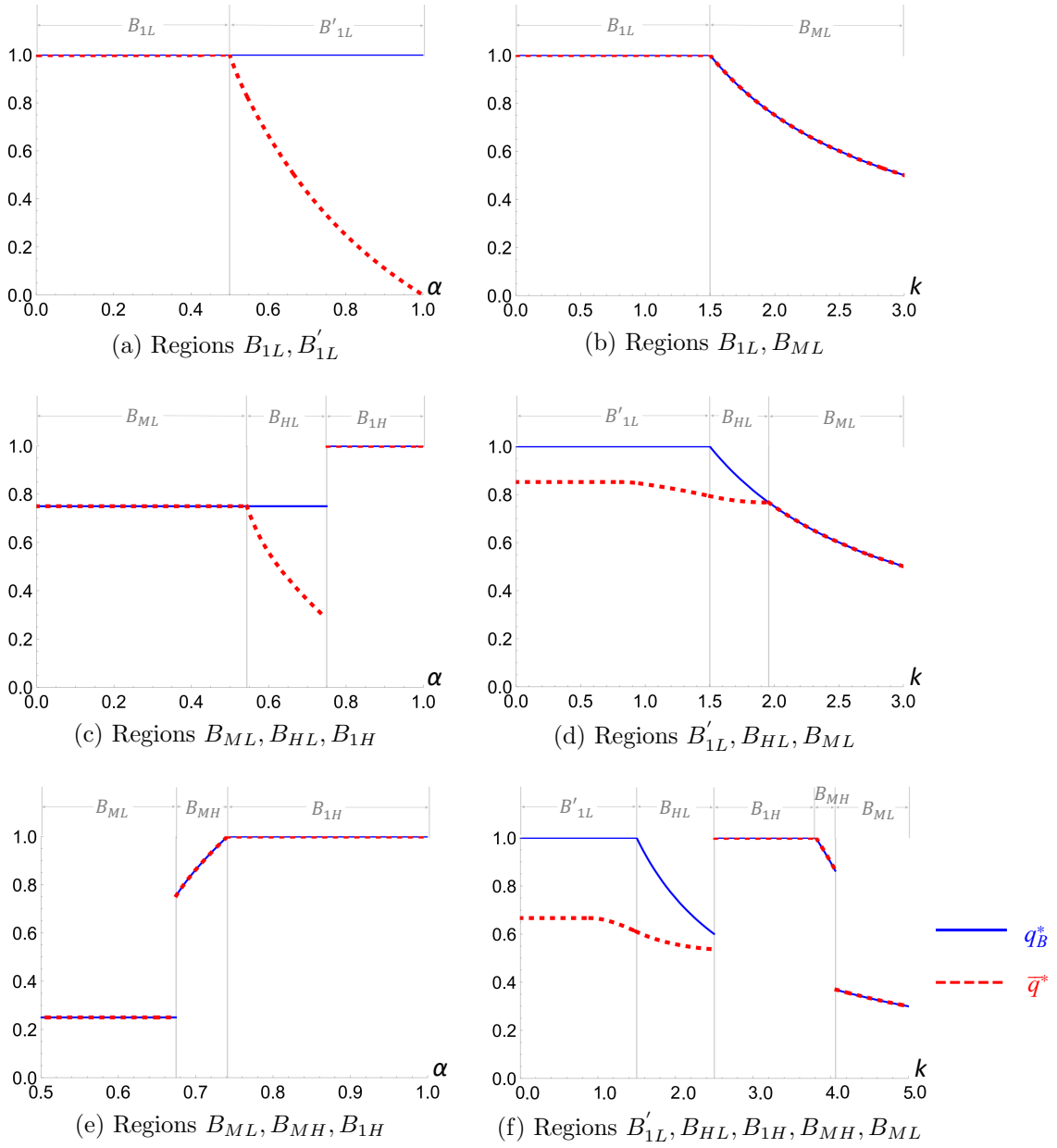

(a) Regions B_{1L}, B'_{1L} (b) Regions B_{1L}, B_{ML}

(c) Regions B_{ML}, B_{HL}, B_{1H} (d) Regions B'_{1L}, B_{HL}, B_{ML}

(e) Regions B_{ML}, B_{MH}, B_{1H} (f) Regions $B'_{1L}, B_{HL}, B_{1H}, B_{MH}, B_{ML}$

Figure 3.5: Impact of α and k under the Binary Label when $c_n > c_r$

Note: $(a), (c), (e)$ show the impact of α where (a) $k = 1$, (c) $k = 2$, and (e) $k = 6$. $(b), (d), (f)$ show the impact of k where (b) $\alpha = 0.2$, (d) $\alpha = 0.54$, and (f) $\alpha = 0.6$. $(a) - (f)$ are based on $c_n > c_r$ where $c_n = 4, c_r = 1, v = 8, v_r = 7$.

Intuitively, the firm should use more recycled content and the NGO should raise the label standard as the fraction of C-type consumers (α) grows or as the technology cost of recycling (k) drops. Interestingly, we find that i) the NGO's label standard may actually decrease as α increases (e.g., see region B'_{1L} in Figure 3.5(a)), and ii)

the firm's recycled content and the NGO's label standard may also increase as k increases (e.g., see Figure 3.5(f) when the region switches from B_{HL} to B_{1H}). Both of these two situations occur in the case when the recycled content has a lower marginal cost (i.e., $c_n > c_r$). The reason is as below. For point i), as α increases from region B_{1L} to B'_{1L} (see Figure 3.5(a)), the firm has incentive to switch his price strategy from low to high, which in turn would lead to low demand. To prevent this, the NGO would decrease the label standard, which makes serving only C-type consumers less profitable and forces the firm to maintain a low price that serves all consumers. For point ii), as k increases from region B_{HL} to B_{1H} (see Figure 3.5(f)), the firm prefers to reduce the recycled content and set a low price. As the recycled content becomes too low, the NGO has incentive to increase the label standard, which encourages the firm to adopt high recycled content to obtain the label and set high price to only target C-type consumers. Thus, both the label standard and the firm's recycled content will jump up as k increases from region B_{HL} to B_{1H}. Moreover, Corollary 3.2(3) shows that both the firm and the NGO can benefit from a higher fraction of C-type consumers or a lower technology cost of recycling.

3.4.3 Comparison between Percentage and Binary Labels

We have so far examined the equilibrium outcomes under the percentage and binary labels, respectively. In this section, we compare the outcomes of the two labels. We show the results in Proposition 3.4 and Figures 3.6-3.7. The intersection of the decision regions under the two labeling schemes in Proposition 3.4 is depicted in Figure 3.8.

Proposition 3.4. *The firm always weakly prefers the percentage label, while the NGO always weakly prefers the binary label. Moreover, the recycled content may be higher or lower under the binary label than that under the percentage label. Specifically:*

(1) When $c_n \leq c_r$*:* $q_P^* < q_B^*$ *if* $(\alpha, k) \in R_B$*; otherwise (i.e.,* $(\alpha, k) \in R_I$*),* $q_P^* = q_B^* = 0$ *and the outcomes of the two labels are identical.*

(2) When $c_n > c_r$*:* $q_P^* < q_B^*$ *if* $(\alpha, k) \in R_B$*;* $q_P^* > q_B^*$ *if* $(\alpha, k) \in R_P$*; otherwise (i.e.,*

$(\alpha, k) \in R_I$), $q_P^* = q_B^*$ *and the outcomes of the two labels are identical.*[3.14]

As shown in Proposition 3.4 and Figure 3.7, the binary label either leads to an identical outcome as that of the percentage label, or strictly benefits the NGO but hurts the firm. This is due to the factor that the binary label can only partially reveal the firm's recycling information, and thus the firm may not be able to select his most preferred recycled content and price as he could under the percentage label. At the same time, under the binary label, the NGO could influence the firm's decision through setting the label standard to enhance the total usage of recycled materials. Thus, the NGO always weakly prefers the binary label, while the firm weakly prefers the percentage label.

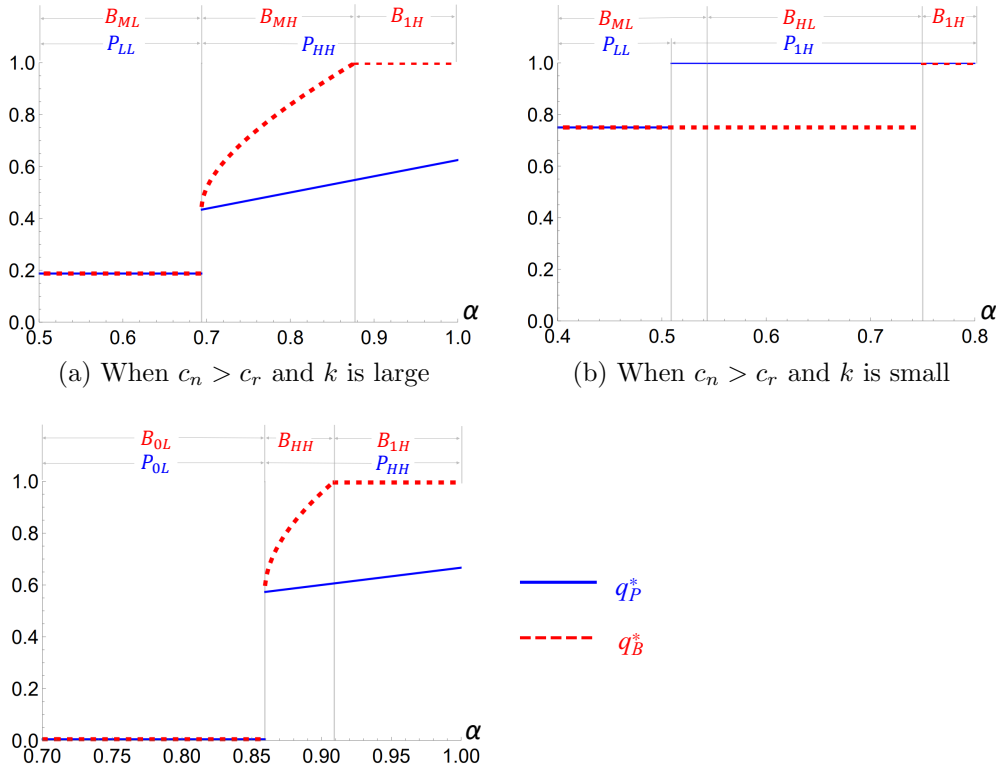

(a) When $c_n > c_r$ and k is large

(b) When $c_n > c_r$ and k is small

(c) When $c_n \leq c_r$

Figure 3.6: Comparison of Recycled Content under the Two Labels
Note: In (a): $c_n = 4, c_r = 1, v = 8, v_r = 7, k = 8$; In (b): $c_n = 4, c_r = 1, v = 8, v_r = 7, k = 2$; In (c): $c_n = 1, c_r = 4, v = 8, v_r = 7, k = 3$.

[3.14] Note that $R_B \doteq \begin{cases} P_{HH} \cap (B_{1H} \cup B_{MH}), & \text{if } c_n > c_r \\ P_{HH} \cap (B_{1H} \cup B'_{MH}), & \text{if } c_n \leq c_r \end{cases}$,
$R_I \doteq \begin{cases} P_{1L} \cup P_{LL} \cup (P_{1H} \cap B_{1H}), & \text{if } c_n > c_r \\ P_{1H} \cup P_{0L}, & \text{if } c_n \leq c_r \end{cases}$, and $R_P \doteq (P_{1H} \cup P_{HH}) \cap (B_{ML} \cup B_{HL})$.

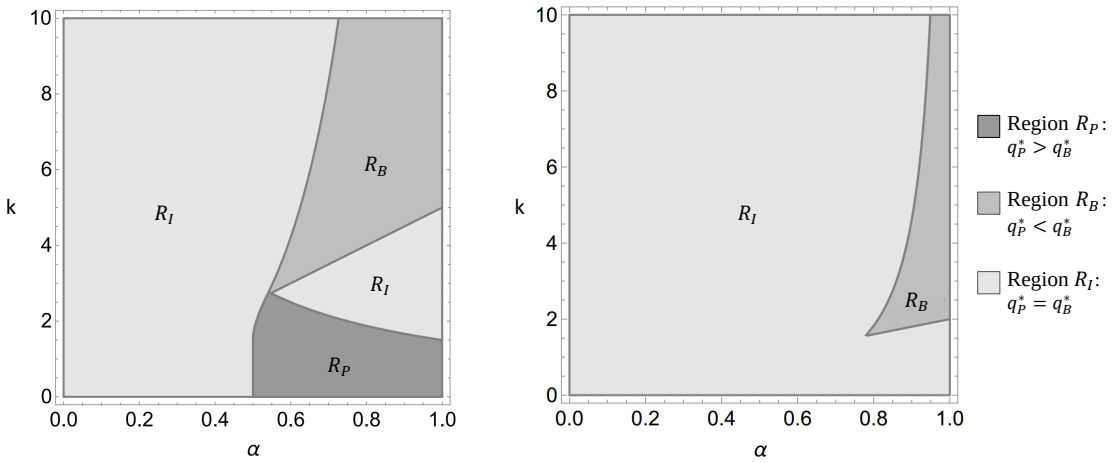

(a) When $c_n > c_r$ (b) When $c_n \leq c_r$

Figure 3.7: The Firm's and the NGO's Label Preferences.
Note: In (a): $c_n = 4, c_r = 1, v = 8, v_r = 7$; In (b): $c_n = 1, c_r = 4, v = 8, v_r = 7$. In R_P and R_B, the firm strictly prefers the percentage label while the NGO strictly prefers the binary label. Moreover, $q_P^* > q_B^*$ in R_P and $q_P^* < q_B^*$ in R_B. In R_I, both the firm and the NGO are indifferent between the two labels.

As shown in Proposition 3.4 and Figure 3.8, the firm's recycled content under the binary label is weakly higher than that under the percentage label when the virgin material is cheaper (i.e., $c_n \leq c_r$); while it could be higher or lower when the recycled material is cheaper (i.e., $c_n > c_r$). Under the percentage label, the firm can always choose his most preferred recycled content. By contrast, under the binary label, the firm's decision is influenced by the NGO's label standard. To induce higher total usage of recycled materials, the NGO may either set a high standard that encourages the firm to raise the recycled content that meets the standard (e.g., in region B_{1H}), or set a low standard that induces the firm to reduce recycled content but increase demand by setting a low price (e.g., in region B_{ML}). Thus, the firm's recycled content under the binary label can be higher (i.e., in region R_B) or lower (i.e., in region R_P).

Our results could provide some useful managerial insights for both NGOs and firms. Both binary labels (e.g., *PEFC* label) and percentage labels (e.g., *GreenCircle Certified* label) are commonly observed in practice. Our results may provide some possible explanations for the label choices. We find that the NGO and the firm often have different label preference. When the NGO has the negotiation power to design her most preferred label, a binary label might be selected, since the NGO

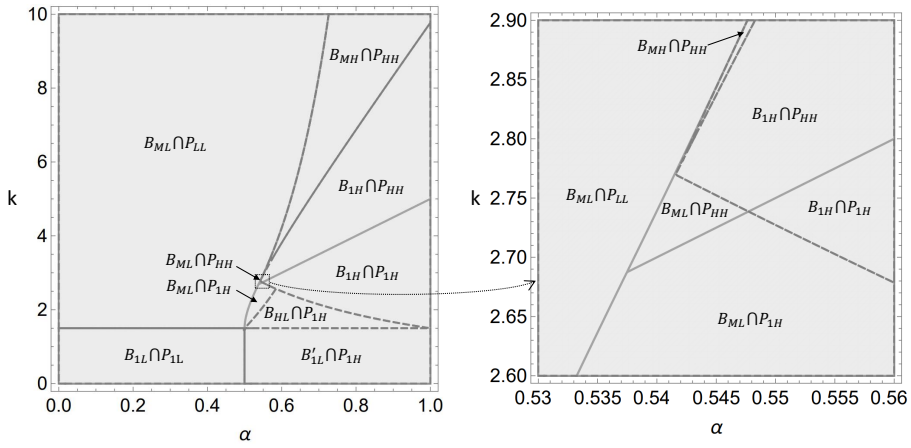

(a) When $c_n > c_r$

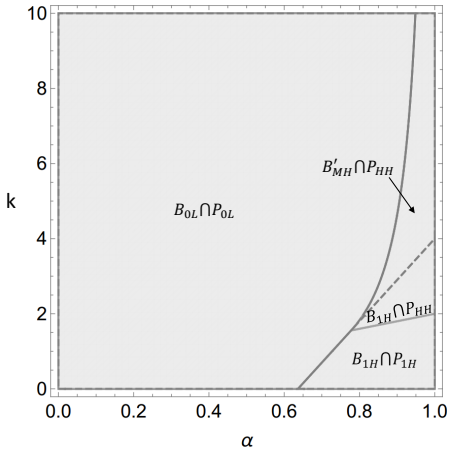

(b) When $c_n \leq c_r$

Figure 3.8: The Overlap of Decision Regions under the Labeling Schemes
Note: In (a): $c_n = 4, c_r = 1, v = 8, v_r = 7, k = 2$; In (b): $c_n = 1$,$c_r = 4$, $v = 8$, $v_r = 7$, $k = 2$.

is able to influence the firm's usage of recycled content through the appropriate choice of label standard. However, in some situations, the label design does not purely depend on the NGO's preference. For example, competition often exists among label providers in practice. In a competitive labeling market, firms may have stronger negotiation power, and NGOs may have to offer the firms' preferred percentage label in order to encourage their adoption. Moreover, sometimes there exists a third-party organization that can further coordinate the firms' and NGOs' preferences in working toward a sustainable development goal. For example, Ellen MacArthur Foundation (EMF), established in the UK, is one such advocate of the circular economy that partners with firms and label certifiers to promote the usage of recycled materials.

3.4.4 Consumer Surplus

In this section, we further examine consumers' total surplus (aggregate utility) under each type of labels and study which type of label most benefits consumers. Let CS_P and CS_B denote consumers' total surplus under the percentage and binary labels, respectively. Recall that if the firm adopts the high price $p = v + v_r q$ under the percentage label or $p = v + v_r \bar{q}$ under the binary label, only C-type consumers purchase the product and their utility is zero. Thus, $CS_B(p, \bar{q}) = CS_P(p, q) = 0$ when the firm adopts the high-price strategy. If the firm adopts the low price $p = v$, all consumers will purchase the product but only C-type consumers have positive utilities. Thus, $CS_B(p, \bar{q}) = \alpha v_r \bar{q}$ under the binary label and $CS_P(p, q) = \alpha v_r q$ under the percentage label in the case of low-price strategy. In short, the consumer surplus under each label is, respectively, given by

$$CS_P(p, q) = \begin{cases} \alpha v_r q, & \text{if } p = v \\ 0, & \text{if } p = v + v_r q \end{cases}, \quad CS_B(p, \bar{q}) = \begin{cases} \alpha v_r \bar{q}, & \text{if } p = v \\ 0, & \text{if } p = v + v_r \bar{q} \end{cases}.$$

Let $CS_P^* \doteq CS_P^*(p_P^*, q_P^*)$ and $CS_B^* \doteq CS_B^*(p_B^*, \bar{q}^*)$ denote the consumer surplus in equilibrium under the two labels, respectively. We summarize the comparison between consumer surplus under the two labels in Proposition 3.5.

Proposition 3.5. *Consumers always weakly prefer the binary label: $CS_P^* < CS_B^*$ if $c_n > c_r$ and $(\alpha, k) \in (B_{ML} \cup B_{HL} \cup B_{1L} \cup B'_{1L}) \cap (P_{1H} \cup P_{HH})$; otherwise, $CS_P^* = CS_B^*$.*

We find that consumers weakly prefer the binary label over the percentage label. Specifically, when the virgin material is cheaper (i.e., $c_n \leq c_r$), consumers will have zero surplus under either labeling scheme, i.e., $CS_P^* = CS_B^* = 0$, since the firm would either set the high price or choose purely virgin material. While, when the recycled material is cheaper (i.e., $c_n > c_r$), consumers might be strictly better off under the binary label. This occurs when the firm prefers a high price under the percentage label but has to set a low price under the binary label because the NGO sets a low label standard to stimulate high demand. In addition, since the percentage label can convey more information than the binary label, when comparing Proposition 3.5 with Proposition 3.4, we can conclude that firms may prefer more market transparency (information) than consumers, which aligns with Stahl and Strausz (2017).

We can further study the impact of the fraction of C-type consumers (α) and the technology cost of recycling (k) on consumer surplus, the result of which is shown in the following corollary.

Corollary 3.3. *(1) When $c_n \leq c_r$, $CS_P^* = CS_B^* = 0$. (2) When $c_n > c_r$, both CS_P^* and CS_B^* are non-monotone in α or k.*

As previously mentioned, when the virgin material is cheaper (i.e., $c_n \leq c_r$), consumer surplus is independent of the fraction of C-type consumers and the technology cost of recycling, since all consumers have zero surplus. However, when the recycled material is cheaper (i.e., $c_n > c_r$), consumers may be either better off or worse off when either the fraction of C-type consumers or the technology cost of recycling increases (e.g., see region P_{LL} or B_{ML}). As α or k increases, the firm will adjust not only recycled content but also price strategy. Thus, consumer surplus is not continuous and non-monotone in α and k. More details are referred to Appendix B.3.3.

3.5 Conclusion

Green products with recycled materials have been successfully promoted by some leading firms and many others are following suit incorporating it into their manufacturing process. Nevertheless, these products face a potential crisis of trust from consumers and the question of how to convince consumers to pay for the firm's green efforts in using recycled materials. A recognized environmental label that independently certifies the usage of recycled content is one good solution, but the design of such a label has yet to mature. Against this backdrop, we study two forms of commonly observed recycling labels and analyze the impacts of these different labels on a firm's recycling and pricing decisions, as well as the NGO's payoff and consumers' total surplus. To that end, we build a game-theoretical model wherein an NGO offers a certain type of label and a monopoly firm sells a product and decides the fraction of its recycled materials and price. The market is filled with both environmentally conscious and unconscious consumers. Then, we derive rich managerial insights about the firm's recycling decision and NGO's labelling scheme.

In summary, we find that the firm prefers the percentage label, while NGO and consumers prefer the binary label. In addition, as more consumers become environmentally conscious or as the technology cost of recycling decreases: 1) The firm's optimal recycled content increases under the percentage label but may decrease or increase under the binary label; 2) The firm is always better off; 3) The NGO is better off under the binary label and might be worse off under the percentage label. Some of these counterintuitive findings should attract the attention of label administrators. As the calls of governments, non-profit organizations, and industries are intensifying for a mature recycling label scheme that facilitates communication between the growing number of recycled products and consumers, our results provide useful insights for the development of an effective label design.

Our analysis also provides possible explanations for some observations of the recycling labels. Different types of labels could be prevalent in different markets, due to the frequently differing preferences of firms and NGOs. In some markets, the label design mainly depends on the NGOs' preference; while in others, it may also depend on the firms' preference (such as in a competitive label market). Therefore, different label designs may need to be adopted. Finally, we want to point out that our analytical results on the label preference of the firm and NGO are robust with respect to the following modifications. First, we change the linear form of marginal cost of materials to a quadratic form. Second, we consider consumers' environmental awareness is continuously distributed instead of the existing two types of consumers. Then, the demand can linearly depend on the price. Both of the two scenarios quantitatively change the firm's profit and NGO's payoff, however, they do not qualitatively change the information disclosure of the two labels. The firm can always choose his most preferred recycled content and fully reveal it by the percentage label while NGO can influence the firm's decision by the binary label.

Chapter 4

Summary and Future Research

This thesis explores two aspects of sustainable operations, in which our main theme is to make full use of the limited resource. The first part concerns the sustainable micromobility service in last-mile transportation. The service provider faces a limited number of vehicles to be allocated in the urban area, and he also wants to serve as many as customers. Hence, the deployment and efficient use of the vehicles are investigated. The second part concerns the label design for a sustainable consumer product. The use of recycled materials can save the limited resource on earth and reduce waste. Recycling labels can disclose information about recycled materials of products to consumers. Hence, an effective label design may incentivize firms to use a higher proportion of recycled materials or sell more products to increase the total usage of recycled materials. Thus, the second part of this thesis focuses on the impacts of recycling labels on firms' recycling and pricing decisions.

In our first study, we note that a sustainable urban transportation system should utilize mobility tools to avoid congestion. Recently, as the shared micromobility service was expanding rapidly with pending operational challenges yet to be overcome, we study the vehicle allocation and relocation in a shared micromobility system to help the shared micromobility firm operate a sustainable business. Particularly, we address the important role of rider crowdsourcing and the 3PL relocation in matching the supply with demand as well as increasing the utilization of vehicles.

Admittedly, there are limitations in our study. Based on them, we can extend the current research in several relevant directions. We then discuss the possible extensions in our first study as follows. First, we used the information from Citi

Bike's Angel Program to simplify the cost parameters for the relationship between the crowdsourcing cost and the number of crowdsourced riders. When more data for rider crowdsourcing behavior is available, this relationship can be modelled more accurately. Besides, we offer a reward for a specific trip with given origin and destination. There are alternative reward strategies, such as reward only at the origin to alleviate overburdened supply, reward only at the destination to prevent depleted supply. The reward size can also depend on the supply or be fixed. We are currently not clear under what conditions will one of the above reward strategies or a mixed of them performs the best. In view of the above, the crowdsourcing operations can be further refined and the total cost of our model can be further optimized. Second, we did not consider the vehicle routing for 3PL relocation, which was another tough optimization problem. In practice, the truck drivers hired by 3PL may have work shifts and the trucks may be prohibited for some roads. Hence, we can further consider the truck routing with time window constraints and/or spatial constraints. Besides, the truck can pick up and drop off micromobility vehicles at any point along the route, which poses new challenge on the design of 3PL relocation. In the future, we can take into consideration the dynamic pick-up and delivery. We may further investigate how rider crowdourcing interacts with the vehicle route. Third, we note that the rider crowdsourcing is a carbon neutral way for the micromobility vehicle rebalancing. By contrast, 3PL relocation with fossil fuel trucks increases the carbon emission. When we take the cost of carbon emission into the objective, or restrict the carbon emission under uncertain demand by a chance constraint, we can derive new insights about how different relocation strategies contribute to the carbon neutral goal.

In our second study, our focus is on the usage of recycling materials. We have studied the impact of two types of recycling labels, i.e., percentage label and binary label. Interestingly, we find that when more consumers are environmentally conscious or the technology cost of recycling decreases, the firm may decrease the recycled content when a binary label is applied. We also find that an NGO may be worse off when a percentage label is applied. Therefore, the labelling scheme should be carefully designed to better serve our sustainable goal.

In the following, we discuss a possible direction related to our second study for future research. We only consider two types of labelling schemes in our study. Indeed, there are other types of labels in practice. For example, the *FSCRecycled* label for paper or wood products has three tiers of recycled content; the *GRS* label for fashion industry has a mixed typed standard, which shows the percentage of recycled content only if it is above a threshold. Our study serves as a first step to understand the basic impacts of two simple labelling schemes, and investigating those other types of labels may generate additional results and interesting insights.

Appendix A

Supplements for Chapter 2

A.1 Table of Notation

Table A1: Summary of Notation

Notation	Description
Sets:	
$\mathcal{V}$	set of service regions $\mathcal{V} = \{1, 2, \ldots, V\}$
$\mathcal{T}$	operational horizon $\mathcal{T} = \{0, 1, \ldots, T-1\}$
$\mathcal{T}(l, s, e)$	$\{s, s+1, \ldots, e-l-1\}$
$\mathcal{G}$	time-space network $\mathcal{G} = (\mathcal{N}, \mathcal{A})$
$\mathcal{N}$	set of nodes on the network $\mathcal{G}$
$\mathcal{A}$	set of directed arcs on the network $\mathcal{G}$
$\mathcal{A}^{\mathrm{t}}, \mathcal{A}^{\mathrm{i}}, \mathcal{A}^{\mathrm{r}}$	trip arcs, idle arcs, 3PL relocation arcs
$\mathcal{K}$	set of scenarios of uncertain demands in all the service regions across all the periods.
$\mathcal{H}$	set of segments on the interval $[0, \bar{\phi}]$ used to approximate the incentive function $g(\cdot)$, $\mathcal{H} = \{1, 2, \ldots, H\}$
Parameters:	
l_{ij}	duration for a rider trip from region $i \in \mathcal{V}$ to region $j \in \mathcal{V}$
l_{r}	duration for the 3PL to relocate vehicles from region $i \in \mathcal{V}$ to region $j \in \mathcal{V}$
N	upper bound for the total number of allocated vehicles
B_j	upper bound for the number of vehicles allocated to region $j \in \mathcal{V}$
c_j	cost incurred for allocating a micromobility vehicle to region $j \in \mathcal{V}$
λ_a	customer demand (the number of customers) from region i in period t to region j with travel time l_{ij} for each arc $a = (n_{it}, n_{j,t+l_{ij}}) \in \mathcal{A}^{\mathrm{t}}$
R	revenue for serving a customer per period
C_{p}	penalty cost per customer lost
$\bar{\Lambda}_{ij}$	maximum number of riders that can be crowdsourced from region i to conduct trips to region j
β_{ij}	the rate of diminishing return on rewards in the incentive function $g(\cdot)$
B_{c}	upper bound for the total incentive used by the operator to crowdsource riders
C_{r}	fixed fee paid to the 3PL for relocating vehicles per request
$\bar{z}$	maximum number of times that the 3PL can relocate vehicles per day
$\bar{\bar{z}}$	maximum number of periods that the 3PL operates during any time interval of l_{f} periods
$\bar{q}$	upper bound for the total number of relocated vehicles by the 3PL in each period
$\underline{q}$	lower bound for the total number of relocated vehicles by the 3PL in each period
p^k	probability of each scenario $k \in \mathcal{K}$
$\bar{\phi}$	Given an arbitrarily small number $\epsilon > 0$, $\bar{\phi} = g^{-1}\left(\bar{\Lambda} - \epsilon\right)$
$\bar{k}_h$	slope of a linear function passing through points $((h-1)\delta, g((h-1)\delta))$ and $(h\delta, g(h\delta))$, $\bar{k}_h = (g(h\delta) - g((h-1)\delta))/\delta$ with $\delta = \bar{\phi}/H$
M	number of sub-networks for temporal decomposition
T_{sub}	number of periods in each sub-network $m \in \{1, 2, \ldots, M\}$
$\mathcal{D}_m$	dictionary to record the pair of initial vehicle allocation and the corresponding objective value of the two-stage problem over sub-network m
$\bar{N}_1, \bar{N}_2$	step sizes for heuristic search
Variables:	
x_i	number of vehicle allocated to region $i \in \mathcal{V}$
$\tilde{x}_i$	number of vehicles in the ending period $T-1$ in region $i \in \mathcal{V}$
η_a	unsatisfied demand on arc $a = (n_{it}, n_{j,t+l_{ij}}) \in \mathcal{A}^{\mathrm{t}}$

Table A1 Summary of Notation (Continued)

Notation	Description
Λ_a	number of crowdsourced riders from region i in period t to region j for a given arc $a = (n_{it}, n_{j,t+l_{ij}}) \in \mathcal{A}^{\mathrm{t}}$
ϕ_a	incentive used to motivate the riders to relocate the vehicles along arc $a = (n_{it}, n_{j,t+l_{ij}}) \in \mathcal{A}^{\mathrm{t}}$
y_a	realized flow on arc $a = (n_{it}, n_{j,t+l_{ij}}) \in \mathcal{A}^{\mathrm{i}} \cup \mathcal{A}^{\mathrm{t}}$
γ_a	number of vehicles relocated by the 3PL from region i in period t to region j for each arc $a = (n_{it}, n_{j,t+l_{\mathrm{r}}}) \in \mathcal{A}^{\mathrm{r}}$
z_t	$z_t = 1$ if the 3PL is requested by the operator in period t to relocate vehicles and $z_t = 0$ otherwise
$\widetilde{z}_t$	the status of the 3PL such that $\widetilde{z}_t = 1$ if the 3PL provides service in period t and $\widetilde{z}_t = 0$ otherwise
u_h	$u_h = 1$ if the optimal reward ϕ falls in the hth segment for each $h \in \mathcal{H}$, and $u_h = 0$ otherwise
$\widetilde{\phi}_h$	$\widetilde{\phi}_h \in [0, \delta]$ such that the optimal reward $\phi = (h-1)\delta + \widetilde{\phi}_h$ for each $h \in \mathcal{H}$
ω_h	variable to approximate $u_h \widetilde{\phi}_h$ for each segment $h \in \mathcal{H}$

A.2 Supplement to Section 2.3

A.2.1 Undefined Arcs

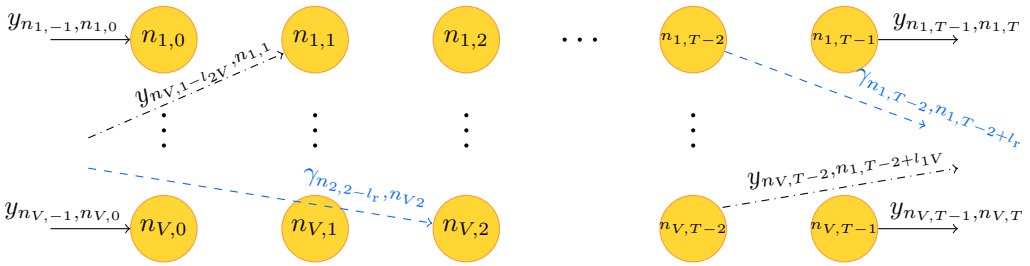

Figure A.1: The Example of Undefined Arcs

A.2.2 Vector Definition

For each $k \in \mathcal{K}$, we let $\boldsymbol{\lambda}^k$ denote the demand vector and define $\widetilde{\mathbf{x}}^k = (\widetilde{x}^k_j,\ j \in \mathcal{V})^\top$ as the idle vehicle flows after period $T-1$. Similarly, for each $k \in \mathcal{K}$, we let $\boldsymbol{\eta}^k = (\eta^k_{n_{it},n_{j,t+l_{ij}}},\ (n_{it}, n_{j,t+l_{ij}}) \in \mathcal{A}^{\mathrm{t}})^\top$ represent the vector of unsatisfied demands, $\mathbf{y}^k = (y^k_{n_{it},n_{j,t+l_{ij}}},\ (n_{it}, n_{j,t+l_{ij}}) \in \mathcal{A}^{\mathrm{t}})^\top$ the vector of realized flows, $\boldsymbol{\gamma}^k = (\gamma^k_{n_{it},n_{j,t+l_{ij}}},\ (n_{it}, n_{j,t+l_{ij}}) \in \mathcal{A}^{\mathrm{r}})^\top$ the vector of 3PL relocation flows, $\boldsymbol{\Lambda}^k = (\Lambda^k_{n_{it},n_{j,t+l_{ij}}},\ (n_{it}, n_{j,t+l_{ij}}) \in \mathcal{A}^{\mathrm{t}})^\top$ the vector of rider crowdsourcing relocation flows, $\boldsymbol{\phi}^k = (\phi^k_{n_{it},n_{j,t+l_{ij}}},\ (n_{it}, n_{j,t+l_{ij}}) \in \mathcal{A}^{\mathrm{t}})^\top$ the vector of rewards to crowdsource riders, $\mathbf{z}^k = (z^k_t,\ t \in \mathcal{T}(l_{\mathrm{r}}))^\top$ the vector of 3PL relocation requests, and $\widetilde{\mathbf{z}}^k = (\widetilde{z}^k_t,\ t \in \mathcal{T}(l_{\mathrm{r}}))^\top$ the vector of the 3PL relocation operation status (i.e., whether or not it is active).

A.3 Supplement to Section 2.4

A.3.1 Constraints

The constraint set $\mathcal{Y}(x_1, x_2, \boldsymbol{\lambda})$ is defined by the following constraints:

$$y_{n_{it},n_{i,t+1}} + y_{n_{it},n_{3-i,t+L}} + \gamma_{n_{it},n_{3-i,t+L}} =$$
$$\begin{cases} x_i, \ t = 0, \\ y_{n_{i,t-1},n_{it}}, \ t = 1, 2, \ldots, L-1, \\ y_{n_{i,t-1},n_{it}} + y_{n_{3-i,t-L},n_{it}} + \gamma_{n_{3-i,t-L},n_{it}}, \ t = L, \ldots, T-1, \end{cases} \quad i \in \{1,2\}, \tag{A.1a}$$

$$y_{n_{it},n_{3-i,t+L}} = \begin{cases} \lambda_{n_{it},n_{3-i,t+L}} + \Lambda_{n_{it},n_{3-i,t+L}} - \eta_{n_{it},n_{3-i,t+L}}, \ t = 0, 1, \ldots, T-L-1, \\ 0, \ t = T-L, \ldots, T-1, \end{cases}$$
$$i \in \{1,2\}, \tag{A.1b}$$

$$\gamma_{n_{it},n_{3-i,t+L}} \le \bar{q} z_t, \ i \in \{1,2\}, \ t \in \{0, 1, \ldots, T-L-1\}, \tag{A.1c}$$

$$\Lambda_{n_{it},n_{3-i,t+L}}, \ y_{n_{it},n_{3-i,t+L}}, \ \eta_{n_{it},n_{3-i,t+L}}, \gamma_{n_{it},n_{3-i,t+L}} \ge 0, \ i \in \{1,2\}, \ t \in \{0, 1, \ldots, T-L-1\},$$
$$z_t \in \{0,1\}, \ t \in \{0, 1, \ldots, T-L-1\},$$
$$y_{n_{it},n_{i,t+1}} \ge 0, \ i \in \{1,2\}, \ t \in \mathcal{T} \setminus \{T-1\}. \tag{A.1d}$$

A.3.2 Proof of Proposition 2.1

Proof. By substituting constraints (A.1b) to the objective for all $t \in \{0, 1, \ldots, T-L-1\}$ and removing the constant term, we can equivalently replace the objective in (2.4) by the following one:

$$\sum_{t=0}^{T-L-1} \left(\sum_{i=1}^{2} \Big((C_{\mathrm{p}} + RL)\, \eta_{n_{it},n_{3-i,t+L}} + \alpha \Lambda_{n_{it},n_{3-i,t+L}} \Big) + C_{\mathrm{r}} z_t \right). \tag{A.2}$$

We denote the optimal solution of problem (2.4) by $\mathbf{Y}^* = (\Lambda^*_{n_{it},n_{3-i,t+L}}, y^*_{n_{it},n_{3-i,t+L}}, \eta^*_{n_{it},n_{3-i,t+L}}, \gamma^*_{n_{it},n_{3-i,t+L}}, \ i \in \{1,2\}, \ t \in \{0, 1, \ldots, T-L-1\}, y^*_{n_{it},n_{i,t+1}}, \ i \in \{1,2\}, \ t \in \{0, 1, \ldots, T-1\}, \ z^*_t, \ t \in \{0, 1, \ldots, T-L-1\})$. In the following, we prove the proposition by contradiction and we first focus on part (b) and part (c) and then part (a).

For part (b), suppose, on the contrary, that there exists some $\tilde{i} \in \{1,2\}$ or $\tilde{t} \in \{0, 1, \ldots, T-L-1\}$ such that one of the following three cases happen: (i) $\alpha \Lambda^*_{n_{\tilde{i}\tilde{t}},n_{3-\tilde{i},\tilde{t}+L}} > C_{\mathrm{r}}$, (ii) $\alpha \Lambda^*_{n_{\tilde{i}t},n_{3-\tilde{i},t+L}} > C_{\mathrm{r}}$ for any $t \in \{0, 1, \ldots, T-L-1\}$, and (iii) $\alpha \Lambda^*_{n_{i\tilde{t}},n_{3-i,\tilde{t}+L}} > C_{\mathrm{r}}$ for any $i \in \{1,2\}$. For case (i), we construct a new solution $\mathbf{Y}^{**} = (\Lambda^{**}_{n_{it},n_{3-i,t+L}}, y^{**}_{n_{it},n_{3-i,t+L}}, \eta^{**}_{n_{it},n_{3-i,t+L}}, \gamma^{**}_{n_{it},n_{3-i,t+L}}, \ i \in \{1,2\}, \ t \in \{0, 1, \ldots, T-L-1\}, y^{**}_{n_{it},n_{i,t+1}}, \ i \in \{1,2\}, \ t \in \{0, 1, \ldots, T-1\}, \ z^{**}_t, \ t \in \{0, 1, \ldots, T-L-1\})$ such that

$$\Lambda^{**}_{n_{\tilde{i},\tilde{t}},n_{3-\tilde{i},\tilde{t}+L}} = 0,\ \gamma^{**}_{n_{\tilde{i}\tilde{t}},n_{3-\tilde{i},\tilde{t}+L}} = \gamma^{*}_{n_{\tilde{i}\tilde{t}},n_{3-\tilde{i},\tilde{t}+L}} + \Lambda^{*}_{n_{\tilde{i}\tilde{t}},n_{3-\tilde{i},\tilde{t}+L}},\ z^{**}_{\tilde{t}} = 1, \tag{A.3a}$$

$$y^{**}_{n_{\tilde{i}\tilde{t}},n_{3-\tilde{i},\tilde{t}+L}} = y^{*}_{n_{\tilde{i}\tilde{t}},n_{3-\tilde{i},\tilde{t}+L}} - \Lambda^{*}_{n_{\tilde{i},\tilde{t}},n_{3-\tilde{i},\tilde{t}+L}}, \tag{A.3b}$$

$$\Lambda^{**}_{n_{i\tilde{t}},n_{3-i,\tilde{t}+L}} = \Lambda^{*}_{n_{i\tilde{t}},n_{3-i,\tilde{t}+L}},\ y^{**}_{n_{i\tilde{t}},n_{3-i,\tilde{t}+L}} = y^{*}_{n_{i\tilde{t}},n_{3-i,\tilde{t}+L}},$$
$$\gamma^{**}_{n_{i\tilde{t}},n_{3-i,\tilde{t}+L}} = \gamma^{*}_{n_{i\tilde{t}},n_{3-i,\tilde{t}+L}},\ i \in \{1,2\}\backslash\{\tilde{i}\}, \tag{A.3c}$$

$$\Lambda^{**}_{n_{it},n_{3-i,t+L}} = \Lambda^{*}_{n_{it},n_{3-i,t+L}},\ y^{**}_{n_{it},n_{3-i,t+L}} = y^{*}_{n_{it},n_{3-i,t+L}},$$
$$\gamma^{**}_{n_{it},n_{3-i,t+L}} = \gamma^{*}_{n_{it},n_{3-i,t+L}},\ i \in \{1,2\}, t \in \{0,1,\ldots,T-L-1\}\backslash\{\tilde{t}\}, \tag{A.3d}$$

$$z^{**}_{t} = z^{*}_{t},\ t \in \{0,1,\ldots,T-L-1\}\backslash\{\tilde{t}\}, \tag{A.3e}$$

$$\eta^{**}_{n_{it},n_{3-i,t+L}} = \eta^{*}_{n_{it},n_{3-i,t+L}},\ i \in \{1,2\}, t \in \{0,1,\ldots,T-L-1\}, \tag{A.3f}$$

$$y^{**}_{n_{it},n_{i,t+1}} = y^{*}_{n_{it},n_{i,t+1}},\ i \in \{1,2\}, t \in \mathcal{T}. \tag{A.3g}$$

It is easy to verify that $\mathbf{Y}^{**}$ is feasible for problem (2.4). It follows that the objective (A.2) with respect to $\mathbf{Y}^{**}$ minus that with respect to $\mathbf{Y}^{*}$ equals $-\alpha\Lambda^{*}_{n_{\tilde{i}\tilde{t}},n_{3-\tilde{i},\tilde{t}+L}} + C_{\mathrm{r}}(1-z^{*}_{\tilde{t}}) \leq -\alpha\Lambda^{*}_{n_{\tilde{i}\tilde{t}},n_{3-\tilde{i},\tilde{t}+L}} + C_{\mathrm{r}} < 0$, where the first inequality holds because $C_{\mathrm{r}} \geq 0$ and $z^{*}_{\tilde{t}} \geq 0$ and the second inequality holds because of the case (i) assumption. Thus, a lower objective is achieved with respect to the solution $\mathbf{Y}^{**}$, which contradicts that $\mathbf{Y}^{*}$ is the optimal solution of problem (2.4). For both cases (ii) and (iii), we can similarly construct such a new solution $\mathbf{Y}^{**}$ and lead to the contradiction. We omit the details for brevity. Therefore, $\alpha\Lambda^{*}_{n_{it},n_{3-i,t+L}} \leq C_{\mathrm{r}}$ holds for any $i \in \{1,2\}$ and $t \in \{0,1,\ldots,T-L-1\}$.

For part (c), suppose, on the contrary, that there exists some $\tilde{i} \in \{1,2\}$ or $\tilde{t} \in \{0,1,\ldots,T-L-1\}$ such that one of the following cases happen: (i) $C_{\mathrm{r}} > \alpha\gamma^{*}_{n_{\tilde{i}\tilde{t}},n_{3-\tilde{i},\tilde{t}+L}}$ if $z^{*}_{\tilde{t}} = 1$ and $\gamma^{*}_{n_{\tilde{i}\tilde{t}},n_{3-\tilde{i},\tilde{t}+L}} > 0$, (ii) $C_{\mathrm{r}} > \alpha\gamma^{*}_{n_{\tilde{i}t},n_{3-\tilde{i},t+L}}$ if $z^{*}_{t} = 1$ and $\gamma^{*}_{n_{\tilde{i}t},n_{3-\tilde{i},t+L}} > 0$ for any $t \in \{0,1,\ldots,T-L-1\}$, and (iii) $C_{\mathrm{r}} > \alpha\gamma^{*}_{n_{i\tilde{t}},n_{3-i,\tilde{t}+L}}$ if $z^{*}_{\tilde{t}} = 1$ and $\gamma^{*}_{n_{i\tilde{t}},n_{3-i,\tilde{t}+L}} > 0$ for any $i \in \{1,2\}$. For case (i), we construct a new solution $\mathbf{Y}^{**} = (\Lambda^{**}_{n_{it},n_{3-i,t+L}}, y^{**}_{n_{it},n_{3-i,t+L}}, \eta^{**}_{n_{it},n_{3-i,t+L}}, \gamma^{**}_{n_{it},n_{3-i,t+L}},\ i \in \{1,2\},\ t \in \{0,1,\ldots,T-L-1\},\ y^{**}_{n_{it},n_{i,t+1}},\ i \in \{1,2\},\ t \in \{0,1,\ldots,T-1\},\ z^{**}_{t},\ t \in \{0,1,\ldots,T-L-1\})$ such that

$$\Lambda^{**}_{n_{\tilde{i},\tilde{t}},n_{3-\tilde{i},\tilde{t}+L}} = \gamma^{*}_{n_{\tilde{i}\tilde{t}},n_{3-\tilde{i},\tilde{t}+L}}, \tag{A.4a}$$

$$\gamma^{**}_{n_{\tilde{i}\tilde{t}},n_{3-\tilde{i},\tilde{t}+L}} = 0,\ z^{**}_{\tilde{t}} = 0, \tag{A.4b}$$

$$y^{**}_{n_{\tilde{i}\tilde{t}},n_{3-\tilde{i},\tilde{t}+L}} = y^{*}_{n_{\tilde{i}\tilde{t}},n_{3-\tilde{i},\tilde{t}+L}} + \gamma^{*}_{n_{\tilde{i}\tilde{t}},n_{3-\tilde{i},\tilde{t}+L}}, \tag{A.4c}$$

$$\Lambda^{**}_{n_{i\tilde{t}},n_{3-i,\tilde{t}+L}} = \Lambda^{*}_{n_{i\tilde{t}},n_{3-i,\tilde{t}+L}},\ y^{**}_{n_{i\tilde{t}},n_{3-i,\tilde{t}+L}} = y^{*}_{n_{i\tilde{t}},n_{3-i,\tilde{t}+L}},$$
$$\gamma^{**}_{n_{i\tilde{t}},n_{3-i,\tilde{t}+L}} = \gamma^{*}_{n_{i\tilde{t}},n_{3-i,\tilde{t}+L}},\ i \in \{1,2\}\backslash\{\tilde{i}\}, \tag{A.4d}$$

$$\Lambda^{**}_{n_{it},n_{3-i,t+L}} = \Lambda^{*}_{n_{it},n_{3-i,t+L}},\ y^{**}_{n_{it},n_{3-i,t+L}} = y^{*}_{n_{it},n_{3-i,t+L}},$$
$$\gamma^{**}_{n_{it},n_{3-i,t+L}} = \gamma^{*}_{n_{it},n_{3-i,t+L}},\ i \in \{1,2\}, t \in \{0,1,\ldots,T-L-1\}\backslash\{\tilde{t}\}, \quad \text{(A.4e)}$$
$$z^{**}_t = z^{*}_t,\ t \in \{0,1,\ldots,T-L-1\}\backslash\{\tilde{t}\}, \quad \text{(A.4f)}$$
$$\eta^{**}_{n_{it},n_{3-i,t+L}} = \eta^{*}_{n_{it},n_{3-i,t+L}},\ i \in \{1,2\}, t \in \{0,1,\ldots,T-L-1\}, \quad \text{(A.4g)}$$
$$y^{**}_{n_{it},n_{i,t+1}} = y^{*}_{n_{it},n_{i,t+1}},\ i \in \{1,2\}, t \in \mathcal{T}. \quad \text{(A.4h)}$$

It is easy to verify that $\mathbf{Y}^{**}$ is feasible for problem (2.4). It follows that the objective (A.2) with respect to $\mathbf{Y}^{**}$ minus that with respect to $\mathbf{Y}^{*}$ equals $\alpha\gamma^{*}_{n_{\tilde{i}\tilde{t}},n_{3-\tilde{i},\tilde{t}+L}} - C_{\mathrm{r}} < 0$ due to the case (i) assumption. Thus, a lower objective is achieved with respect to $\mathbf{Y}^{**}$, which contradicts that $\mathbf{Y}^{*}$ is the optimal solution of problem (2.4). For both cases (ii) and (iii), we can similarly construct such a new solution $\mathbf{Y}^{**}$ and lead to the contradiction. We omit the details for brevity. Therefore, $C_{\mathrm{r}} \leq \alpha\gamma^{*}_{n_{it},n_{3-i,t+L}}$ holds for any $i \in \{1,2\}$ and $t \in \{0,1,\ldots,T-L-1\}$ if $z^{*}_t = 1$ and $\gamma^{*}_{n_{it},n_{3-i,t+L}} > 0$.

For part (a), suppose, on the contrary, that there exists some $\tilde{i} \in \{1,2\}$ or $\tilde{t} \in \{0,1,\ldots,T-L-1\}$ such that one of the following cases happen: (i) $\Lambda^{*}_{n_{\tilde{i}\tilde{t}},n_{3-\tilde{i},\tilde{t}+L}} > 0$ and $\gamma^{*}_{n_{\tilde{i}\tilde{t}},n_{3-\tilde{i},\tilde{t}+L}} > 0$, (ii) $\Lambda^{*}_{n_{\tilde{i}t},n_{3-\tilde{i},t+L}} > 0$ and $\gamma^{*}_{n_{\tilde{i}t},n_{3-\tilde{i},t+L}} > 0$ for any $t \in \{0,1,\ldots,T-L-1\}$, and (iii) $\Lambda^{*}_{n_{i\tilde{t}},n_{3-i,\tilde{t}+L}} > 0$ and $\gamma^{*}_{n_{i\tilde{t}},n_{3-i,\tilde{t}+L}} > 0$ for any $i \in \{1,2\}$. For case (i), we further consider two subcases. Subcase 1): $\Lambda^{*}_{n_{\tilde{i}\tilde{t}},n_{3-\tilde{i},\tilde{t}+L}} + \gamma^{*}_{n_{\tilde{i}\tilde{t}},n_{3-\tilde{i},\tilde{t}+L}} \leq C_{\mathrm{r}}/\alpha$. We construct a new solution $\mathbf{Y}^{**} = (\Lambda^{**}_{n_{it},n_{3-i,t+L}}, y^{**}_{n_{it},n_{3-i,t+L}}, \eta^{**}_{n_{it},n_{3-i,t+L}}, \gamma^{**}_{n_{it},n_{3-i,t+L}}, i \in \{1,2\}, t \in \{0,1,\ldots,T-L-1\}, y^{**}_{n_{it},n_{i,t+1}}, i \in \{1,2\}, t \in \{0,1,\ldots,T-1\}, z^{**}_t, t \in \{0,1,\ldots,T-L-1\})$ such that $\Lambda^{**}_{n_{\tilde{i},\tilde{t}},n_{3-\tilde{i},\tilde{t}+L}} = \Lambda^{*}_{n_{\tilde{i}\tilde{t}},n_{3-\tilde{i},\tilde{t}+L}} + \gamma^{*}_{n_{\tilde{i}\tilde{t}},n_{3-\tilde{i},\tilde{t}+L}}$ and (A.4b) – (A.4h) hold. Subcase 2): $\Lambda^{*}_{n_{\tilde{i}\tilde{t}},n_{3-\tilde{i},\tilde{t}+L}} + \gamma^{*}_{n_{\tilde{i}\tilde{t}},n_{3-\tilde{i},\tilde{t}+L}} > C_{\mathrm{r}}/\alpha$. We construct a new solution $\mathbf{Y}^{**}$ such that (A.3a) – (A.3g) hold. The objective (A.2) with respect to $\mathbf{Y}^{**}$ in either subcase is strictly lower as shown before, which contradicts that $\mathbf{Y}^{*}$ is the optimal solution of problem (2.4). For both cases (ii) and (iii), we can similarly construct such a new solution $\mathbf{Y}^{**}$ and lead to the contradiction. We omit the details for brevity. Therefore, $\Lambda^{*}_{n_{it},n_{3-i,t+L}}\gamma^{*}_{n_{it},n_{3-i,t+L}} = 0$ holds for any $i \in \{1,2\}$ and $t \in \{0,1,\ldots,T-L-1\}$. □

A.4 Supplement to Section 2.5

A.4.1 Proof of Proposition 2.2

Proof. Note that given the allocation solution $\mathbf{x}$, the solution to the second-stage problem $(\mathcal{Q}_0)$ (or $(\mathcal{Q})$) with respect to any scenario $k \in \mathcal{K}$ is independent from that with respect to any other scenario $k' \in \mathcal{K}$. Thus, it suffices to consider only one scenario in $\mathcal{K}$ for both problems $(\mathcal{Q}_0)$ and $(\mathcal{Q})$. To that end, we omit the superscript k in both problems $(\mathcal{Q}_0)$ and $(\mathcal{Q})$ and denote by $\widetilde{\mathbf{Y}} = (\widetilde{\mathbf{x}}, \boldsymbol{\eta}, \mathbf{y}, \boldsymbol{\gamma}, \mathbf{z}, \widetilde{\mathbf{z}}, \boldsymbol{\Lambda}, \boldsymbol{\phi}, \mathbf{u}, \widetilde{\boldsymbol{\phi}}, \boldsymbol{\omega})$ the second-stage variables of problem $(\mathcal{Q}_0)$ or $(\mathcal{Q})$ with respect to any scenario in $\mathcal{K}$. For ease of notation, we also split $\widetilde{\mathbf{Y}}$ into three parts: $\widetilde{\mathbf{Y}}_1 = (\widetilde{\mathbf{x}}, \boldsymbol{\eta}, \mathbf{y}, \boldsymbol{\gamma}, \mathbf{z}, \widetilde{\mathbf{z}})$, $\widetilde{\mathbf{Y}}_2 = (\boldsymbol{\Lambda}, \boldsymbol{\phi})$ and $\widetilde{\mathbf{Y}}_3 = (\mathbf{u}, \widetilde{\boldsymbol{\phi}}, \boldsymbol{\omega})$. Moreover, to differentiate the notation in problems $(\mathcal{Q}_0)$ and $(\mathcal{Q})$, we denote the variables of problem $(\mathcal{Q}_0)$ by $\widetilde{\mathbf{Y}}^{\mathrm{b}}$ and the corresponding feasible region by $\mathcal{Y}^{\mathrm{b}} = \{\widetilde{\mathbf{Y}}^{\mathrm{b}} \mid (2.2a) - (2.2h), (2.1b), (2.1c), (2.3), ((2.5c) - (2.5e), (2.6),\ a \in \mathcal{A}^{\mathrm{t}})\}$. Similarly, we denote the variables of problem $(\mathcal{Q})$ by $\widetilde{\mathbf{Y}}^{\mathrm{r}}$ and the corresponding feasible region by $\mathcal{Y}^{\mathrm{r}} = \{\widetilde{\mathbf{Y}}^{\mathrm{r}} \mid (2.2a) - (2.2h), (2.1b), (2.1c), (2.3), ((2.5c) - (2.5d), (2.6), (u_{h,a} \in [0,1],\ h \in \mathcal{H}),\ a \in \mathcal{A}^{\mathrm{t}})\}$. The optimal solutions of both $(\mathcal{Q}_0)$ and $(\mathcal{Q})$ are specified with superscript $\cdot^*$. The optimal objective values of both problems are denoted by $\Theta'(\mathbf{x}) = \Psi(\widetilde{\mathbf{Y}}^{\mathrm{b}*})$ and $\Theta''(\mathbf{x}) = \Psi(\widetilde{\mathbf{Y}}^{\mathrm{r}*})$. Because $\mathcal{Y}^{\mathrm{b}} \subseteq \mathcal{Y}^{\mathrm{r}}$ and both problems $(\mathcal{Q}_0)$ and $(\mathcal{Q})$ are minimization problems sharing the same objective function (2.7), we have

$$\Theta'(\mathbf{x}) \geq \Theta''(\mathbf{x}). \tag{A.5}$$

In the following, we will show that $\Theta'(\mathbf{x}) \leq \Theta''(\mathbf{x})$.

We claim that

$$\begin{aligned}
&\left(\widetilde{\mathbf{Y}}_1^{\mathrm{r}*}, \widetilde{\mathbf{Y}}_2^{\mathrm{r}*}\right) \in \mathrm{Proj}_{\left(\widetilde{\mathbf{Y}}_1^{\mathrm{b}}, \widetilde{\mathbf{Y}}_2^{\mathrm{b}}\right)}\left(\mathcal{Y}^{\mathrm{b}}\right) \\
&= \left\{\left(\widetilde{\mathbf{Y}}_1^{\mathrm{b}}, \widetilde{\mathbf{Y}}_2^{\mathrm{b}}\right) \in \mathbb{R}_+^{(|\mathcal{V}|+4|\mathcal{A}^{\mathrm{t}}|+|\mathcal{A}^{\mathrm{r}}|+2|\mathcal{T}(l_{\mathrm{r}})|)} \;\middle|\; \exists \widetilde{\mathbf{Y}}_3^{\mathrm{b}} \in \mathbb{R}_+^{3H|\mathcal{A}^{\mathrm{t}}|} \text{ such that } \widetilde{\mathbf{Y}}^{\mathrm{b}} \in \mathcal{Y}^{\mathrm{b}}\right\}.
\end{aligned} \tag{A.6}$$

Note that $(\widetilde{\mathbf{Y}}_1^{\mathrm{r}*}, \widetilde{\mathbf{Y}}_2^{\mathrm{r}*})$ satisfies constraints (2.2a) – (2.2h), (2.1b), (2.1c), and (2.3) because these constraints are shared by $\mathcal{Y}^{\mathrm{b}}$ and $\mathcal{Y}^{\mathrm{r}}$ and $\widetilde{\mathbf{Y}}_3$ is involved in none of these constraints. Thus, to show that our claim holds, it suffices to show that there exists $\widetilde{\mathbf{Y}}_3^{\mathrm{r}'} \in \mathbb{R}_+^{3H|\mathcal{A}^{\mathrm{t}}|}$ such that $(\widetilde{\mathbf{Y}}_2^{\mathrm{r}*}, \widetilde{\mathbf{Y}}_3^{\mathrm{r}'})$ satisfies (2.5c) – (2.5e) and (2.6) for any $a \in \mathcal{A}^{\mathrm{t}}$, thereby leading to $(\widetilde{\mathbf{Y}}_1^{\mathrm{r}*}, \widetilde{\mathbf{Y}}_2^{\mathrm{r}*}, \widetilde{\mathbf{Y}}_3^{\mathrm{r}'}) \in \mathcal{Y}^{\mathrm{b}}$. We will prove this by contradiction.

Note that for any given $a \in \mathcal{A}^{\mathrm{t}}$, if $(\widetilde{\mathbf{Y}}_2^{\mathrm{r}*}, \widetilde{\mathbf{Y}}_3^{\mathrm{r}'})$ satisfies (2.5c) – (2.5e) and (2.6), then $\widetilde{\mathbf{Y}}_{2,a}^{\mathrm{r}*} = (\phi^{\mathrm{r}*}, \Lambda^{\mathrm{r}*})$ amounts to a point in the projection space $\mathrm{Proj}_{\widetilde{\mathbf{Y}}_{2,a}^{\mathrm{b}}}(\mathcal{Y}^{\mathrm{b}}) = \{\widetilde{\mathbf{Y}}_{2,a}^{\mathrm{b}} \in \mathbb{R}_+^2 \mid \exists(\widetilde{\mathbf{Y}}_1^{\mathrm{b}}, \widetilde{\mathbf{Y}}_3^{\mathrm{b}})$ and $(\widetilde{\mathbf{Y}}_{2,e}^{\mathrm{b}}, e \in \mathcal{A}^{\mathrm{t}}, e \neq a)$ such that $\widetilde{\mathbf{Y}}^{\mathrm{b}} \in \mathcal{Y}^{\mathrm{b}}\}$. This projection space can be represented by a piece-wise linear curve with H segment and ϕ runs in $[0, \bar{\phi}]$, as illustrated in Figure A.2, and such a point can be illustrated by point B in this figure. Now, for the contradiction, we suppose that there exists some $a' \in \mathcal{A}^{\mathrm{t}}$ such that $\widetilde{\mathbf{Y}}_{2,a'}^{\mathrm{r}*} = (\phi_{a'}^{\mathrm{r}*}, \Lambda_{a'}^{\mathrm{r}*})$ does not amount to a point in the projection space $\mathrm{Proj}_{\widetilde{\mathbf{Y}}_{2,a}^{\mathrm{b}}}(\mathcal{Y}^{\mathrm{b}})$. More specifically, by the feasibility of $\widetilde{\mathbf{Y}}_{2,a'}^{\mathrm{r}*}$ from ($\mathcal{Q}$), it will amount to a point in the projection space $\mathrm{Proj}_{\widetilde{\mathbf{Y}}_{2,a}^{\mathrm{r}}}(\mathcal{Y}^{\mathrm{r}}) = \{\widetilde{\mathbf{Y}}_{2,a}^{\mathrm{r}} \in \mathbb{R}_+^2 \mid \exists(\widetilde{\mathbf{Y}}_1^{\mathrm{r}}, \widetilde{\mathbf{Y}}_3^{\mathrm{r}})$ and $(\widetilde{\mathbf{Y}}_{2,e}^{\mathrm{r}}, e \in \mathcal{A}^{\mathrm{t}}, e \neq a)$ such that $\widetilde{\mathbf{Y}}^{\mathrm{r}} \in \mathcal{Y}^{\mathrm{r}}\}$, which is the convex hull of $\mathrm{Proj}_{\widetilde{\mathbf{Y}}_{2,a}^{\mathrm{b}}}(\mathcal{Y}^{\mathrm{b}})$ and can be illustrated by the gray region Ω in Figure A.2. Also, $\widetilde{\mathbf{Y}}_{2,a'}^{\mathrm{r}*}$ can be illustrated by point P.

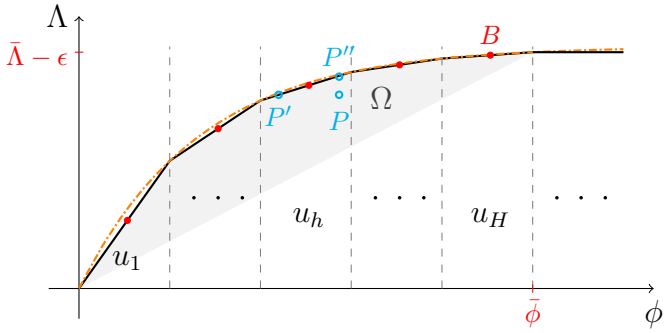

Figure A.2: A Geometric Illustration of (ϕ, Λ)

Now, we construct a solution $(\widetilde{\mathbf{Y}}_1^{\mathrm{b}\prime}, \widetilde{\mathbf{Y}}_2^{\mathrm{b}\prime}, \widetilde{\mathbf{Y}}_3^{\mathrm{b}\prime})$. We let $\widetilde{\mathbf{Y}}_1^{\mathrm{b}\prime} = \widetilde{\mathbf{Y}}_1^{\mathrm{r}*}$. For $\widetilde{\mathbf{Y}}_2^{\mathrm{b}\prime} = (\phi^{\mathrm{b}\prime}, \Lambda^{\mathrm{b}\prime})$, we let $(\phi_e^{\mathrm{b}\prime}, \Lambda_e^{\mathrm{b}\prime}) = (\phi_e^{\mathrm{r}*}, \Lambda_e^{\mathrm{r}*})$ for any $e \in \mathcal{A}^{\mathrm{t}}$ and $e \neq a'$, $\Lambda_{a'}^{\mathrm{b}\prime} = \Lambda_{a'}^{r*}$, and $\phi_{a'}^{\mathrm{b}\prime} = (h'-1)\delta + (\Lambda^{\mathrm{r}*} - \sum_{m=1}^{h'-1} \bar{k}_m \delta)/\bar{k}_{h'}$, where $h' = argmin\{h \in \{1, 2, \ldots, H\} | \sum_{m=1}^{h-1} \bar{k}_m \delta \leq \Lambda_{a'}^{\mathrm{r}*} < \sum_{m=1}^{h} \bar{k}_m \delta\}$. For $\widetilde{\mathbf{Y}}_3^{\mathrm{b}\prime} = (\mathbf{u}^{\mathrm{b}\prime}, \widetilde{\boldsymbol{\phi}}^{\mathrm{b}\prime}, \boldsymbol{\omega}^{\mathrm{b}\prime})$, we let $(\mathbf{u}_e^{\mathrm{b}\prime}, \widetilde{\boldsymbol{\phi}}_e^{\mathrm{b}\prime}, \boldsymbol{\omega}_e^{\mathrm{b}\prime}) = (\mathbf{u}_e^{\mathrm{r}*}, \widetilde{\boldsymbol{\phi}}_e^{\mathrm{r}*}, \boldsymbol{\omega}_e^{\mathrm{r}*})$ for any $e \in \mathcal{A}^{\mathrm{t}}$ and $e \neq a'$. For $(\mathbf{u}_{a'}^{\mathrm{b}\prime}, \widetilde{\boldsymbol{\phi}}_{a'}^{\mathrm{b}\prime}, \boldsymbol{\omega}_{a'}^{\mathrm{b}\prime})$, we let $u_{a',h'}^{\mathrm{b}\prime} = 1$ and $u_{a',h}^{\mathrm{b}\prime} = 0$ for any $h \in \{1, 2, \ldots, H\}$ and $h \neq h'$, and $\omega_{a',h} = \widetilde{\phi}_{a',h} = (\Lambda^{\mathrm{r}*} - \sum_{m=1}^{h'-1} \bar{k}_m \delta)/\bar{k}_{h'}$ and $\omega_{a',h'} = 0$ for any $h \in \{1, 2, \ldots, H\}$ and $h \neq h'$. Based on the construction, we have $(\widetilde{\mathbf{Y}}_1^{\mathrm{b}\prime}, \widetilde{\mathbf{Y}}_2^{\mathrm{b}\prime}, \widetilde{\mathbf{Y}}_3^{\mathrm{b}\prime}) \in \mathcal{Y}^{\mathrm{b}}$ and the corresponding objective value is $\Theta''(\mathbf{x}) + (\phi_{a'}^{\mathrm{b}\prime} - \phi_{a'}^{\mathrm{r}*})$ by the formulation of (2.7). Because $(\widetilde{\mathbf{Y}}_1^{\mathrm{b}\prime}, \widetilde{\mathbf{Y}}_2^{\mathrm{b}\prime}, \widetilde{\mathbf{Y}}_3^{\mathrm{b}\prime}) \in \mathcal{Y}^{\mathrm{b}}$, we also have

$$\Theta''(\mathbf{x}) + (\phi_{a'}^{\mathrm{b}\prime} - \phi_{a'}^{\mathrm{r}*}) \geq \Theta'(\mathbf{x}). \tag{A.7}$$

because the objective value with respect to a feasible solution for a minimization problem is no greater than the optimal objective value.

Note that $(\phi_{a'}^{\mathrm{b}\prime}, \Lambda_{a'}^{\mathrm{b}\prime})$ amounts to a point in the projection space $\mathrm{Proj}_{\widetilde{\mathbf{Y}}_{2,a}^{\mathrm{b}}}(\mathcal{Y}^{\mathrm{b}})$ and can be illustrated by point P' in Figure A.2. For simplicity, we denote the projection space $\mathrm{Proj}_{\widetilde{\mathbf{Y}}_{2,a}^{\mathrm{b}}}(\mathcal{Y}^{\mathrm{b}})$, i.e., a piece-wise linear function, by $\Lambda = \Xi(\phi)$, which is also an increasing and concave function. Thus, we have $\Lambda_{a'}^{\mathrm{b}\prime} = \Lambda_{a'}^{r*} = \Xi(\phi_{a'}^{\mathrm{b}\prime})$. Also, there exists $\Lambda^{\mathrm{b}\prime\prime} \in [0, \bar{\Lambda} - \epsilon]$ such that $\Lambda_{a'}^{\mathrm{b}\prime\prime} = \Xi(\phi_{a'}^{r*})$, as illustrated by point P'' in Figure A.2. Because the function $\Lambda = \Xi(\phi)$ is concave and $(\phi_{a'}^{\mathrm{r}*}, \Lambda_{a'}^{\mathrm{r}*})$ is an interior point of $\mathrm{Proj}_{\widetilde{\mathbf{Y}}_{2,a}^{\mathrm{r}}}(\mathcal{Y}^{\mathrm{r}})$, we have $\Lambda_{a'}^{\mathrm{r}*} < \Lambda_{a'}^{\mathrm{b}\prime\prime} = \Xi(\phi_{a'}^{r*})$. It follows that $\Xi(\phi_{a'}^{\mathrm{b}\prime}) < \Xi(\phi_{a'}^{r*})$. Because the function $\Lambda = \Xi(\phi)$ is increasing, we have $\phi_{a'}^{\mathrm{b}\prime} < \phi_{a'}^{r*}$. It further indicates that

$$\Theta''(\mathbf{x}) + (\phi_{a'}^{\mathrm{b}\prime} - \phi_{a'}^{\mathrm{r}*}) < \Theta''(\mathbf{x}). \tag{A.8}$$

From (A.7) and (A.8), we obtain $\Theta''(\mathbf{x}) > \Theta'(\mathbf{x})$, which contradicts with (A.5). Therefore, we have (A.6) holds and $(\widetilde{\mathbf{Y}}_1^{\mathrm{r}*}, \widetilde{\mathbf{Y}}_2^{\mathrm{r}*}, \widetilde{\mathbf{Y}}_3^{\mathrm{r}'}) \in \mathcal{Y}^{\mathrm{b}}$. It follows that $\Psi(\widetilde{\mathbf{Y}}_1^{\mathrm{r}*}, \widetilde{\mathbf{Y}}_2^{\mathrm{r}*}, \widetilde{\mathbf{Y}}_3^{\mathrm{r}'}) \geq \Theta'(\mathbf{x})$ because of the same reason for (A.7) to hold. In addition, by the formulation of (2.7), where $\widetilde{\mathbf{Y}}_3$ is not involved, we have $\Psi(\widetilde{\mathbf{Y}}_1^{\mathrm{r}*}, \widetilde{\mathbf{Y}}_2^{\mathrm{r}*}, \widetilde{\mathbf{Y}}_3^{\mathrm{r}'}) = \Psi(\widetilde{\mathbf{Y}}^{\mathrm{r}*}) = \Theta''(\mathbf{x})$. Therefore, we have $\Theta''(\mathbf{x}) \geq \Theta'(\mathbf{x})$, which together with (A.5) imply that $\Theta''(\mathbf{x}) = \Theta'(\mathbf{x})$. This completes the proof. □

A.4.2 The Refined Model

Given a starting period $s \in \mathcal{T}$ and ending period $e \in \mathcal{T} \cup \{T\}$, we define $\mathcal{A}^{\mathrm{t}}(s,e)$ as the subset of $\mathcal{A}^{\mathrm{t}}$ in period $t \in \mathcal{T}(l_{ij}, s, e)$ and denote the second-stage variables between the time range $[s,e)$ in each scenario $k \in \mathcal{K}$ by vector $\widetilde{\mathbf{Y}}_{(s,e)}^k = (\widetilde{\mathbf{x}}^k, \boldsymbol{\eta}^k, \mathbf{y}^k, \boldsymbol{\gamma}^k, \boldsymbol{\Lambda}^k, \mathbf{u}^k, \boldsymbol{\phi}^k, \widetilde{\boldsymbol{\phi}}^k, \mathbf{z}^k, \widetilde{\mathbf{z}}^k, \boldsymbol{\omega}^k)_{(s,e)}$. Then, we can write $\mathcal{Q}(s,e)$ as follows:

$$\Theta''_{(s,e)}(\mathbf{x}) = \min_{\mathbf{Y}_{(s,e)}^k,\ k\in\mathcal{K}} \sum_{k\in\mathcal{K}} p^k \left(\sum_{a\in\mathcal{A}^{\mathrm{t}}(s,e)} (C_{\mathrm{p}}\eta_a^k + \phi_a^k - Rl_a(y_a^k - \Lambda_a^k)) + \sum_{t\in\mathcal{T}(l_{\mathrm{r}},s,e)} C_{\mathrm{r}} z_t^k \right) \tag{$\mathcal{Q}(s,e)$}$$

$$\text{s.t.} \quad \mathbf{Y}_{(s,e)}^k \in \mathcal{Y}_{(s,e)}(\mathbf{x}, \boldsymbol{\lambda}^k),\ k \in \mathcal{K}.$$

For ease of notation, we omit superscript k for variables and parameters in $\mathcal{Y}_{(s,e)}(\mathbf{x}, \boldsymbol{\lambda}^k)$ for any $k \in \mathcal{K}$. Then, the feasible region $\mathcal{Y}_{(s,e)}(\mathbf{x}, \boldsymbol{\lambda})$ with respect to each scenario is given by

$$\mathcal{Y}_{(s,e)}(\mathbf{x},\boldsymbol{\lambda}) := \Big\{\widetilde{\mathbf{Y}}_{(s,e)} \geq \mathbf{0} \;\Big|\; \tag{A.9a}$$

$$\left(y_{n_{it},n_{i,t+1}} + \sum_{j\in\mathcal{V},j\neq i}\left(y_{n_{it},n_{j,t+l_{ij}}} + \gamma_{n_{it},n_{j,t+l_{\mathrm{r}}}}\right)\right) - \left(y_{n_{i,t-1},n_{i,t}}\right.$$

$$\left. + \sum_{j\in\mathcal{V},j\neq i}\left(y_{n_{j,t-l_{ij}},n_{i,t}} + \gamma_{n_{j,t-l_{\mathrm{r}}},n_{i,t}}\right)\right) = \begin{cases} x_i, & \text{if } t = s, \\ 0, & \text{if } t = s+1,\ldots,e-2, \quad i\in\mathcal{V}, \\ -\widetilde{x}_i, & \text{if } t = e-1, \end{cases} \tag{A.9b}$$

$$\lambda_{n_{it},n_{j,t+l_{ij}}} + \Lambda_{n_{it},n_{j,t+l_{ij}}} - \eta_{n_{it},n_{j,t+l_{ij}}} = y_{n_{it},n_{j,t+l_{ij}}},\ t\in\mathcal{T}(l_{ij},s,e), j\neq i, i,j\in\mathcal{V}, \tag{A.9c}$$

$$\phi_{n_{it},n_{j,t+l_{ij}}} = \sum_{h=1}^{H}(h-1)u_{h,n_{it},n_{j,t+l_{ij}}}\delta_{ij} + \omega_{h,n_{it},n_{j,t+l_{ij}}},\ t\in\mathcal{T}(l_{ij},s,e), j\neq i, i,j\in\mathcal{V}, \tag{A.9d}$$

$$\Lambda_{n_{it},n_{j,t+l_{ij}}} = \sum_{h=1}^{H} u_{h,n_{it},n_{j,t+l_{ij}}} \sum_{m=1}^{h-1}\bar{k}_{mij}\delta_{ij} + \sum_{h=1}^{H}\bar{k}_{h,n_{it},n_{j,t+l_{ij}}}\omega_{h,n_{it},n_{j,t+l_{ij}}},$$
$$t\in\mathcal{T}(l_{ij},s,e), j\neq i, i,j\in\mathcal{V}, \tag{A.9e}$$

$$u_{h,n_{it},n_{j,t+l_{ij}}}\delta_{ij} - \omega_{h,n_{it},n_{j,t+l_{ij}}} \geq 0,\ t\in\mathcal{T}(l_{ij},s,e), j\neq i, i,j\in\mathcal{V}, \tag{A.9f}$$

$$\widetilde{\phi}_{h,n_{it},n_{j,t+l_{ij}}} - \omega_{h,n_{it},n_{j,t+l_{ij}}} \geq 0,\ t\in\mathcal{T}(l_{ij},s,e), j\neq i, i,j\in\mathcal{V}, \tag{A.9g}$$

$$\delta_{ij} - u_{h,n_{it},n_{j,t+l_{ij}}}\delta_{ij} - \widetilde{\phi}_{h,n_{it},n_{j,t+l_{ij}}} + \omega_{h,n_{it},n_{j,t+l_{ij}}} \geq 0,\ t\in\mathcal{T}(l_{ij},s,e), j\neq i, i,j\in\mathcal{V}, \tag{A.9h}$$

$$\sum_{h=1}^{H} u_{h,n_{it},n_{j,t+l_{ij}}} = 1,\ t\in\mathcal{T}(l_{ij},s,e), j\neq i, i,j\in\mathcal{V}, \tag{A.9i}$$

$$\widetilde{\phi}_{h,n_{it},n_{j,t+l_{ij}}} \leq \delta_{ij},\ h\in\mathcal{H}, t\in\mathcal{T}(l_{ij},s,e), j\neq i, i,j\in\mathcal{V}, \tag{A.9j}$$

$$u_{h,n_{it},n_{j,t+l_{ij}}} \leq 1,\ h\in\mathcal{H}, t\in\mathcal{T}(l_{ij},s,e), j\neq i, i,j\in\mathcal{V}, \tag{A.9k}$$

$$\sum_{i=t}^{t+l_{\mathrm{f}}-1}\widetilde{z}_i \leq \bar{\bar{z}},\ t\in\{s,\ldots,e-l_{\mathrm{r}}-l_{\mathrm{f}}-1\}, \tag{A.9l}$$

$$\sum_{t\in\mathcal{T}(l_{\mathrm{r}},s,e)} z_t \leq \bar{z}, \tag{A.9m}$$

$$\underline{q}\widetilde{z}_t \leq \sum_{i\in\mathcal{V}}\sum_{j\in\mathcal{V},j\neq i}\gamma_{n_{it},n_{j,t+1}} \leq \bar{q}\widetilde{z}_t,\ t\in\mathcal{T}(l_{\mathrm{r}},s,e), \tag{A.9n}$$

$$z_t - \widetilde{z}_t \geq 0,\ t = s, \tag{A.9o}$$

$$z_t - \widetilde{z}_t + \widetilde{z}_{t-1} \geq 0,\ t\in\mathcal{T}(l_{\mathrm{r}},s+1,e), \tag{A.9p}$$

$$z_t + \widetilde{z}_{t-1} - 1 \leq 0,\ t\in\mathcal{T}(l_{\mathrm{r}},s+1,e), \tag{A.9q}$$

$$z_t - \widetilde{z}_t \leq 0,\ t\in\mathcal{T}(l_{\mathrm{r}},s,e), \tag{A.9r}$$

$$\widetilde{z}_t \in \{0,1\},\ t\in\mathcal{T}(l_{\mathrm{r}},s,e)\Big\}. \tag{A.9s}$$

Note that $\widetilde{\mathbf{Y}}_{(s,e)} \geq \mathbf{0}$ indicates every variable in the vector $\widetilde{\mathbf{Y}}_{(s,e)}$ is non-negative. Finally, the two-stage stochastic program $\mathcal{M}(s,e)$ is given by

$$\min_{\mathbf{x}} \sum_{j\in\mathcal{V}} c_j x_j + \Theta''(\mathbf{x}) \;\text{ s.t. }\; \mathbf{x}\in\mathcal{X} = \left\{\mathbf{x}\in\mathbb{Z}_+^{|\mathcal{V}|} \;\middle|\; x_j - B_j \leq 0,\ j\in\mathcal{V},\ \sum_{j\in\mathcal{V}} x_j \leq N\right\}. \tag{$\mathcal{M}(s,e)$}$$

A.4.3 Algorithm 1 Details

For any $s\in\mathcal{T}$ and $e\in\mathcal{T}\cup\{T\}$ such that $e-s\geq 3$, we fix some binary variables in problem $\mathcal{M}(s,e)$ to be 0 by making use of its LP relaxation solution. Specifically, in Algorithm 1, we apply the following procedure for each scenario $k\in\mathcal{K}$. First, we construct two sets (i.e., $\mathcal{T}^{\mathrm{r1}}$ and $\mathcal{T}^{\mathrm{r2}}$) by, respectively, collecting the following

two sets of values: (i) $\gamma^{ks}_{sum,t} = \sum_{i\in\mathcal{V}}\sum_{j\in\mathcal{V},j\neq i}\gamma_{n_{it},n_{j,t+1}},\ t \in \mathcal{T}(l_{\rm r},s,e)$ and (ii) $\hat{\gamma}^{ks}_{sum,t} = \gamma^{ks}_{sum,t} + \gamma^{ks}_{sum,t+1},\ t \in \mathcal{T}(l_{\rm r},s,e-1)$, while each of these two sets of values are sorted in decreasing order in sets $\mathcal{T}^{\rm r1}$ and $\mathcal{T}^{\rm r2}$. Next, we collect the time indices (i.e., t) of the first $n_I \leq e-s-1$ elements of the ordered set $\mathcal{T}^{\rm r1}$ in $\hat{\mathcal{T}}^{\rm r1}$ and those of $\mathcal{T}^{\rm r2}$ in $\hat{\mathcal{T}}^{\rm r2}$. In addition, by increasing the value of each element in $\hat{\mathcal{T}}^{\rm r2}$ by 1, we collect these indices in $\hat{\mathcal{T}}^{\rm r3}$. It is noted that for each scenario $k \in \mathcal{K}$, the subset of variables $\{\widetilde{z}^k_t,\ t \in \hat{\mathcal{T}}^{\rm r1}\cup\hat{\mathcal{T}}^{\rm r2}\cup\hat{\mathcal{T}}^{\rm r3}\}$ are most likely to take value 1. Thus, we reduce the binary variables $\widetilde{z}^k_t$ in the operational problem $\mathcal{Q}_{\rm LP}(s,e)$ and $\mathcal{Q}(s,e)$ by restricting $\widetilde{z}^k_t = 0$ if $t \in \mathcal{T}(l_{\rm r},s,e)\backslash(\hat{\mathcal{T}}^{\rm r1}\cup\hat{\mathcal{T}}^{\rm r2}\cup\hat{\mathcal{T}}^{\rm r3})$ for any scenario $k \in \mathcal{K}$. By constraints (2.2f), when $\widetilde{z}^k_t = 0$, the number of vehicles relocated by the 3PL $\gamma_{n_{it},n_{j,t+l_{\rm r}}} = 0$ from region i in period to region j. Thus, the solution space is reduced and the solution process can be accelerated.

Algorithm 1 Reduction of the Binary Variables for 3PL Relocation (s,e)

1: Initialize: $\mathcal{T}^{\rm r1} = \hat{\mathcal{T}}^{\rm r1} = \mathcal{T}^{\rm r2} = \hat{\mathcal{T}}^{\rm r2} = \hat{\mathcal{T}}^{\rm r3} := \emptyset$
2: Solve $\mathcal{M}_{\rm LP}(s,e)$ to obtain $\gamma^{ks}_{sum,t},\ t \in \mathcal{T}(l_{\rm r},s,e),\ k \in \mathcal{K}$
3: **for** $k \in \mathcal{K}$ **do**
4: $\quad\mathcal{T}^{\rm r1} \leftarrow \{\gamma^{ks}_{sum,t} \mid t \in \mathcal{T}(l_{\rm r},s,e)\}$ such that $\gamma^{ks}_{sum,(1)} \geq \cdots \geq \gamma^{ks}_{sum,(e-s-l_{\rm r}-1)}$ and $\mathcal{T}^{\rm r1} = \{\gamma^{ks}_{sum,t} \mid t \in \mathcal{T}(l_{\rm r},1,e-s)\}$
5: $\quad\hat{\gamma}^{ks}_{sum,t} \leftarrow \{\gamma^{ks}_{sum,t} + \{\gamma^{ks}_{sum,t+1},\ t \in \mathcal{T}(l_{\rm r},s,e-1)$
6: $\quad\mathcal{T}^{\rm r2} \leftarrow \{\hat{\gamma}^{ks}_{sum,t} \mid t \in \mathcal{T}(l_{\rm r},s,e)\}$ such that $\hat{\gamma}^{ks}_{sum,(1)} \geq \cdots \geq \hat{\gamma}^{k*}_{sum,(e-s-l_{\rm r}-2)}$ and $\mathcal{T}^{\rm r2} = \hat{\gamma}^{ks}_{sum,t} \mid t \in \mathcal{T}(l_{\rm r},1,e-s-1)\}$
7: $\quad\hat{\mathcal{T}}^{\rm r1} \leftarrow \{t \in \mathcal{T}(l_{\rm r},s,e) \mid \gamma^{ks}_{sum,t} \geq \gamma^{ks}_{sum,(n_I)}\}$, $\hat{\mathcal{T}}^{\rm r2} \leftarrow \{t \in \mathcal{T}(l_{\rm r},s,e-1) \mid \hat{\gamma}^{ks}_{sum,t} \geq \hat{\gamma}^{ks}_{sum,(n_I)}\}$, $\hat{\mathcal{T}}^{\rm r3} \leftarrow \{t+1 \mid t \in \hat{\mathcal{T}}^{\rm r2}\}$
8: $\quad$Set $\widetilde{z}^k_t = 0,\ t \in \mathcal{T}(l_{\rm r},s,e)\backslash(\hat{\mathcal{T}}^{\rm r1}\cup\hat{\mathcal{T}}^{\rm r2}\cup\hat{\mathcal{T}}^{\rm r3})$ in $\mathcal{Q}_{\rm LP}(s,e)$ and $\mathcal{Q}(s,e)$
9: $\quad\mathcal{T}^{\rm r1},\hat{\mathcal{T}}^{\rm r1},\mathcal{T}^{\rm r2},\hat{\mathcal{T}}^{\rm r2},\hat{\mathcal{T}}^{\rm r3} \leftarrow \emptyset$

A.4.4 Algorithm 2 Details

In Algorithm 2, we solve smaller and thus simpler two-stage stochastic programs over each sub-network $m \in \{1,2,\ldots,M\}$ in a backward sequence, from the last sub-network $m = M$ to the first $m = 1$. For each sub-network, we follow a four-step solution procedure, with the first step to reduce the number of second-stage binary variables by applying Algorithm 1. In the following, we detail the remaining three steps for solving the two-stage stochastic programs (i.e., $\mathcal{M}((m-1)T_{\rm sub}, mT_{\rm sub})$) over the sub-networks $m \geq 2$ and $m = 1$ separately.

For any $m \geq 2$, we have the following detailed Steps 2 - 4:

Algorithm 2 Temporal Decomposition

Initialize: $\underline{\mathbf{x}} := \mathbf{0}$, $x_{\text{sum}} := 0$, $\mathcal{D}_m := \emptyset,\ m \in \{1, 2, \ldots, M\}$
for $m = M, \ldots, 1$ **do**
  $s \leftarrow (m-1)T_{\text{sub}}$, $e \leftarrow mT_{\text{sub}}$
  Update problem $\mathcal{Q}_{\text{LP}}(s, e)$ and $\mathcal{Q}(s, e)$ to reduce binary variables by Algorithm 1
  Solve $\mathcal{M}_{\text{LP}}(s, e)$ with $\widetilde{\mathbf{Y}}_{(s,e)} \in \mathcal{Y}_{\text{LP}(s,e)}(\mathbf{x}, \boldsymbol{\lambda}) \cap \{\widetilde{\mathbf{Y}}_{(s,e)} \mid \widetilde{x}_i \geq \underline{x}_i,\ i \in \mathcal{V}\}$ to obtain solution $\mathbf{x}^s$ and objective v^s
  $\mathcal{D}_m \leftarrow \mathcal{D}_m \cup \{(\mathbf{x}^s, v^s)\}$, $\underline{x}_i \leftarrow x_i^s$, $x_{\text{sum}} \leftarrow \sum_{i \in \mathcal{V}} x_i^s$
  for $\sigma_{\text{sum}} = \underline{\sigma}, \ldots, \bar{\sigma}$ **do**
    $\mathcal{X}' \leftarrow \mathcal{X} \cap \{\mathbf{x} \in \mathbb{Z}_+^{|\mathcal{V}|} \mid \sum_{i \in \mathcal{V}} x_i = x_{\text{sum}} + \sigma_{\text{sum}},\ \underline{x}_i - \sigma_i \leq x_i \leq \underline{x}_i + \sigma_i,\ i \in \mathcal{V}\}$
    Resolve $\mathcal{M}_{\text{LP}}(s, e)$ where $\mathbf{x} \in \mathcal{X}'$ by Bender's decomposition
    Obtain solution $\mathbf{x}^s$ and objective v^s
    $\mathcal{D}_m \leftarrow \mathcal{D}_m \cup \{(\mathbf{x}^s, v^s)\}$, $\mathcal{X} \leftarrow \emptyset$
  if $m \neq 1$ **then**
    $\mathcal{D}_m \leftarrow \{(\mathbf{x}_\ell, v_\ell) \in \mathcal{D}_m,\ \ell \in \{1, 2, \ldots, |\mathcal{D}_m|\} | v_1 \leq \cdots \leq v_{|\mathcal{D}_m|}\}$
    $\mathbf{x}^s \leftarrow \mathcal{D}_m[0].key$, $\underline{\mathbf{x}} \leftarrow \mathbf{x}^s$
  else
    for all $(\mathbf{x}^s, v^s) \in \mathcal{D}_1$ **do**
      $\hat{\mathcal{T}} \leftarrow \{(t, k) \in \mathcal{T}(l_{\text{r}}, 0, T) \times \mathcal{K} \mid \widetilde{z}_t^k = 0$ in $\mathcal{Q}(s, e)$ with $t \in \mathcal{T}(l_{\text{r}}, s, e)$ where $s = (m-1)T_{\text{sub}},\ e = mT_{\text{sub}},\ m \in \{1, 2, \ldots, M\}\}$
      Resolve $\mathcal{M}(0, T)$ where $\mathbf{x} \in \mathcal{X} \cap \{\mathbf{x} \in \mathbb{Z}_+^{|\mathcal{V}|} \mid \mathbf{x} = \mathbf{x}^s\}$ and $\widetilde{\mathbf{Y}} \in \mathcal{Y}(\mathbf{x}, \boldsymbol{\lambda}) \cap \{\widetilde{\mathbf{Y}} \mid \widetilde{z}_t^k = 0, (t, k) \in \hat{\mathcal{T}}\}$ to obtain v'
      $v^s \leftarrow v'$, update $(\mathbf{x}^s, v^s)$ in $\mathcal{D}_1$
Return $\mathcal{D}_1$

- Step 2. When solving the two-stage problem $\mathcal{M}_{\text{LP}}(s, e)$ over the sub-network m (i.e., $s = (m-1)T_{\text{sub}},\ e = mT_{\text{sub}}$), we add the constraints $\widetilde{x}_i \geq \underline{x}_i,\ i \in \mathcal{V}$, in the second-stage problem. That is, for each region $i \in \mathcal{V}$, we denote the outflow of the sub-network m by $\widetilde{x}_i$ and the lower bound for the outflow by $\underline{x}_i$. This lower bound takes the value of the first-stage solution $x_i^s,\ i \in \mathcal{V}$, of the two-stage problem $\mathcal{M}_{\text{LP}}(s, e)$ over the sub-network $m+1$ if $m < M$ (i.e., $s = mT_{\text{sub}},\ e = (m+1)T_{\text{sub}}$) and takes the value of 0 if $m = M$. These lower-bound constraints follow the intuition that, by splitting the entire network, the vehicle allocation solution of the two-stage problem over the sub-network m approximates that over the sub-networks from m to M. Intuitively, the demand of the two-stage problem over sub-networks from m to M is no less than that over the sub-networks from $m+1$ to M and the higher demand often leads to more allocated vehicles. Thus, the number of vehicles leaving sub-network m in each region should be no less than the number of vehicles allocating to each region over sub-network $m+1$. Then, we derive the first-stage allocation solution to the problem $\mathcal{M}_{\text{LP}}(s, e)$ over the sub-network m.

- Step 3. We refine and re-solve the problem $\mathcal{M}_{\text{LP}}(s, e)$ several more times, where for each time, two types of constraints are added, yielding several candidate allocations. One type of constraints are to perturb the total number of allocated vehicles to take a different value. Particularly, we set the total number of allocated vehicles $\sum_{i\in\mathcal{V}} x_i = x_{\text{sum}} + \sigma_{\text{sum}}$ for each $\sigma_{\text{sum}} \in \{\underline{\sigma}, \ldots, \bar{\sigma}\}$, where σ_{sum} denotes the perturbed value. The others are box constraints $x_i \in [\underline{x}_i - \sigma_i, \underline{x}_i + \sigma_i],\ i \in \mathcal{V}$, where σ_i (with $\sum_{i\in\mathcal{V}} \sigma_i \leq \sigma_{\text{sum}}$) is the maximum purterbed value for the regional vehicle allocation. Slightly perturbing the total number of allocated vehicles to different potential values has two advantages. First, it can reduce the feasible region of the vehicle allocation variables. Second, we observe that, when the total number of allocated vehicles is fixed, a small perturbation of the total number of vehicles allocated to one or more regions has a minor impact on the objective value of the integrated allocation and relocation problem. The reason is intuitive. That is, though regional vehicle allocation is perturbed, the vehicles can be relocated to proper places at a low cost. However, when the total number of allocated vehicles takes different values, the resulting objective values of the two-stage problem changes significantly. This is because the allocation cost of one vehicle is often higher than the relocation cost of multiple vehicles. Thus, perturbing the total allocation has a larger impact on the objective value than perturbing the regional allocation with a fixed total allocation.

- Step 4. With several candidate solutions for allocating vehicles in sub-network m, we store each solution $\mathbf{x}^s$ as the *key* and the objective value v^s as the *value* in dictionary $\mathcal{D}_m$, which stores data by the key-value pairs and the subscript m represents the sub-network index. Then, the solution $\mathbf{x}^s$ with the smallest objective v^s in $\mathcal{D}_m$ is chosen and for each $i \in \mathcal{V}$, x_i^s is taken as the lower bound $\underline{x}_i$ for the two-stage problem over sub-network $m-1$.

When $m = 1$, a similar four-step solution procedure is applied as above except that in the final step, we do not choose the x_i^s with the smallest objective value in $\mathcal{D}_1$. Instead, for each candidate solution $\mathbf{x}^s$ in $\mathcal{D}_1$, a two-stage problem $\mathcal{M}(0, T)$

over the entire network is solved with the first-stage decisions fixed as $\mathbf{x}^s$ and the number of second-stage binary variables reduced. The resulting objective value is denoted by v' and used to update v^s with respect to $\mathbf{x}^s$. We thus obtain several candidate solutions $\mathbf{x}^s$ and the corresponding objectives value v^s in $\mathcal{D}_1$ for the two-stage problem $\mathcal{M}(0,T)$ over the original time-space network.

We note that the network split in Algorithm 2 will break some original arcs connecting the sub-networks. However, there are periods when the shared micro-mobility system has a relatively low demand and thus a low volume of traffic on the broken arcs. Thus, the temporal decomposition shall cause a minor error when splitting the network in those low-demand periods.

Whenever solving a two-stage problem, we apply Bender's decomposition such that the second-stage problem can be further decomposed into independent scenario-based subproblems, which can be solved in parallel. Our temporal decomposition algorithm can efficiently solve large-scale problems because (i) the problem size at each iteration is reduced, so is the number of binary variables; (ii) the solution space of $\mathcal{M}_{\text{LP}}(s,e)$ is reduced by fixing $\sum_{i\in\mathcal{V}} x_i$ to different values, thereby enabling a quick search of better solutions; and (iii) by employing Bender's decomposition, we can leverage the parallel capacity to solve the second-stage problem $\mathcal{P}^k$ for each separate scenario $k \in \mathcal{K}$ in parallel, further enhancing the computational efficiency.

Furthermore, we formulate the Bender's cuts used in the above Algorithm 2. We note that our two-stage problem $\mathcal{M}_{\text{LP}}(s,e)$ over any sub-network has a complete recourse, and hence we only need to derive the Bender's optimality cuts. Given the operational horizon $[s,e)$, denote the arc set $\mathcal{A}^{\text{t}}$ with $t \in \mathcal{T}(l_{ij},s,e)$ by $\mathcal{A}^{\text{t}}(s,e)$. Also, given the first-stage solution $\mathbf{x}$, denote the multipliers for the first case of constraints (A.9b) (with right-hand-side x_i) by $\pi_i^1 \in \mathbb{R},\ i \in \mathcal{V}$, those for constraints (A.9c) by $\pi_a^2 \in \mathbb{R}, a \in \mathcal{A}^{\text{t}}(s,e)$, those for constraints (A.9l) by $\pi_t^3 \geq 0,\ t \in \{s,\dots,e-l_{\text{r}}-l_{\text{f}}\}$, that for constraint (A.9m) by $\pi^4 \geq 0$, those for constraints (A.9i) by $\pi_a^5 \in \mathbb{R},\ a \in \mathcal{A}^{\text{t}}(s,e)$, those for constraints (A.9j) by $\pi_{h,a}^6 \geq 0,\ h \in \mathcal{H},\ a \in \mathcal{A}^{\text{t}}(s,e)$, those for constraints (A.9h) by $\pi_{h,a}^7 \geq 0,\ h \in \mathcal{H},\ a \in \mathcal{A}^{\text{t}}(s,e)$, those for (A.9k) by $\pi_{h,a}^8 \geq 0,\ h \in \mathcal{H},\ a \in \mathcal{A}^{\text{t}}(s,e)$, those for constraints (A.9q) by $\pi_t^9 \geq 0, t \in \mathcal{T}(l_{\text{r}},s,e)$, and those for continuous relaxation of constraints (A.9s) by $\pi_t^0 \geq 0, t \in \mathcal{T}(l_{\text{r}},s,e)$.

We omit the dual variables for other constraints because they do not appear in the optimality cuts. At a given iteration, a Bender's optimality cut takes the following form:

$$\theta - \sum_{k \in \mathcal{K}} p^k q^k(\mathbf{x}) \geq 0,$$

where θ denotes the lower bound approximation of the second-stage value function $\Theta''_{(s,e)}(\mathbf{x})$ and

$$\begin{aligned} q^k(\mathbf{x}) = \sum_{i \in \mathcal{V}} \pi_i^1 x_i + \sum_{a \in \mathcal{A}^{\mathrm{t}}(s,e)} \pi_a^2 \lambda_a - \sum_{t=0}^{e-l_{\mathrm{r}}-l_{\mathrm{f}}-1} \pi_t^3 \bar{\bar{z}} - \pi^4 \bar{z} + \sum_{a \in \mathcal{A}^{\mathrm{t}}(s,e)} \pi_a^5 \\ - \sum_{h \in \mathcal{H}, a \in \mathcal{A}^{\mathrm{t}}(s,e)} \left(\left(\pi_{h,a}^6 + \pi_{h,a}^6 \right) \delta_{ij} + \pi_{h,a}^8 \right) - \sum_{t \in \mathcal{T}(l_{\mathrm{r}},s,e)} (\pi_t^9 + \pi_t^0). \end{aligned}$$

Note that only one cut is generated at each iteration. One can also use a multi-cut version, by which $|\mathcal{K}|$ Bender's optimality cuts are generated at each iteration (Birge and Louveaux 2011).

In the numerical experiments, we set the perturbation for regional allocation $\sigma_i = 1$ for $i \in \mathcal{V}$, $\underline{\sigma} = \bar{\sigma} = 1$ for the total allocation, and the step sizes $\bar{N}_1 = |\mathcal{V}|$ and $\bar{N}_2 = \lfloor |\mathcal{V}|/3 \rfloor$.

A.4.5 Algorithm 3 Details

Algorithm 3 mainly consists of two steps. First, we set the search step of the total number of allocated vehicles x_{sum} as a positive value $\bar{N}_1 \leq N$. If the solution $\mathbf{x}^0$ in $\mathcal{D}_1$ with the smallest objective value (denoted by $v_{\min}$) has the largest (resp. smallest) total number of allocated vehicles x_{sum}, we then generate a new candidate solution by increasing (resp. decreasing) x_{sum} by $\bar{N}_1$. This is done by randomly choosing x_i, $i \in \mathcal{V}$, for $\bar{N}_1$ times, where for each time the value of the chosen x_i is increased (resp. decreased) by 1. Then, we append this new solution and the corresponding objective value of the two-stage problem $\mathcal{M}(0,T)$ to $\mathcal{D}_1$. If the newly added objective is the smallest in $\mathcal{D}_1$, then we similarly generate another new candidate solution. Otherwise, the search in the first step terminates, and we denote by $\bar{x}_{\mathrm{sum}}$ (resp. $\underline{x}_{\mathrm{sum}}$) the current largest (resp. smallest) total number of allocated vehicles. The intuition of this step is as follows. Suppose we observe the objective

Algorithm 3 Heuristic Search ($\mathcal{D}_1$)

Initialize $v_{\min} := \infty$, $x_{\text{sum}} := \infty$, $\underline{x}_{\text{sum}} := -\infty$, $\bar{x}_{\text{sum}} := \infty$, $\mathcal{V}' \leftarrow \emptyset$
$\hat{\mathcal{D}}_1 \leftarrow \{(q, v) \mid (\mathbf{x}, v) \in \mathcal{D}_1,\ q = \sum_{i \in \mathcal{V}} x_i\}$
$\hat{\mathcal{D}}_1 \leftarrow \{(x_l, v_l) \in \hat{\mathcal{D}}_1 \mid x_1 \leq \cdots \leq x_{|\hat{\mathcal{D}}_1|}\}$, $\bar{x}_{\text{sum}} \leftarrow \hat{\mathcal{D}}_1[|\hat{\mathcal{D}}_1| - 1].key$, $\underline{x}_{\text{sum}} \leftarrow \hat{\mathcal{D}}_1[0].key$
$\mathcal{D}_1 \leftarrow \{(\mathbf{x}_l, v_l) \in \mathcal{D}_1 \mid v_1 \leq \cdots \leq v_{|\mathcal{D}_1|}\}$, $v^0 \leftarrow \mathcal{D}_1[0].value$, $\mathbf{x}^0 \leftarrow \mathcal{D}_1[0].key$, $x_{\text{sum}} \leftarrow \sum_{i \in \mathcal{V}} x_i^0$
$I \leftarrow 0$
if $x_{\text{sum}} \geq \bar{x}_{\text{sum}}$ **then**
    while $v^0 < v_{\min}$ and $I \leq 20$ **do**
        Randomly pick $\mathcal{V}' \subseteq \mathcal{V}$ such that $|\mathcal{V}'| = \bar{N}_1$
        $x_i^0 \leftarrow x_i^0 + 1,\ i \in \mathcal{V}'$, $\bar{x}_{\text{sum}} \leftarrow \sum_{i \in \mathcal{V}} x_i^0$, $v_{\min} \leftarrow v^0$
        Resolve $\mathcal{M}(0, T)$ where $\mathbf{x} \in \mathcal{X} \cap \{\mathbf{x} \in \mathbb{Z}_+^{|\mathcal{V}|} \mid \mathbf{x} = \mathbf{x}^0\}$ to obtain v^0
        $\mathcal{D}_1 \leftarrow \mathcal{D}_1 \cup \{(\mathbf{x}^0, v^0)\}$, $I \leftarrow I + 1$
    if $I \leq 20$ **then** $x_i^0 \leftarrow x_i^0 - 1,\ i \in \mathcal{V}'$, $x_{\text{sum}} \leftarrow \sum_{i \in \mathcal{V}} x_i^0$, $v^0 \leftarrow v_{\min}$, $v_{\min} \leftarrow \infty$
        while $v^0 < v_{\min}$ and $x_{\text{sum}} + \bar{N}_2 < \bar{x}_{\text{sum}}$ **do**
            Randomly pick $\mathcal{V}' \subseteq \mathcal{V}$ such that $|\mathcal{V}'| = \bar{N}_2$
            $x_i^0 \leftarrow x_i^0 + 1,\ i \in \mathcal{V}'$, $x_{\text{sum}} \leftarrow \sum_{i \in \mathcal{V}} x_i^0$, $v_{\min} \leftarrow v^0$
            Resolve $\mathcal{M}(0, T)$ where $\mathbf{x} \in \mathcal{X} \cap \{\mathbf{x} \in \mathbb{Z}_+^{|\mathcal{V}|} \mid \mathbf{x} = \mathbf{x}^0\}$ to obtain v^0
            $\mathcal{D}_1 \leftarrow \mathcal{D}_1 \cup \{(\mathbf{x}^0, v^0)\}$
        if $x_{\text{sum}} + \bar{N}_2 < \bar{x}_{\text{sum}}$ **then** $x_i^0 \leftarrow x_i^0 - 1,\ i \in \mathcal{V}', v^0 \leftarrow v_{\min}$
else
    if $x_{\text{sum}} \leq \underline{x}_{\text{sum}}$ **then**
        while $v^0 < v_{\min}$ and $I \leq 20$ and $x_i^0 > 0,\ i \in \mathcal{V}$ **do**
            Randomly pick $\mathcal{V}' \subseteq \mathcal{V}$ such that $|\mathcal{V}'| = \bar{N}_1$
            $x_i^0 \leftarrow x_i^0 - 1,\ i \in \mathcal{V}'$, $\underline{x}_{\text{sum}} \leftarrow \sum_{i \in \mathcal{V}} x_i^0$, $v_{\min} \leftarrow v^0$
            Resolve $\mathcal{M}(0, T)$ where $\mathbf{x} \in \mathcal{X} \cap \{\mathbf{x} \in \mathbb{Z}_+^{|\mathcal{V}|} \mid \mathbf{x} = \mathbf{x}^0\}$ to obtain v^0
            $\mathcal{D}_1 \leftarrow \mathcal{D}_1 \cup \{(\mathbf{x}^0, v^0)\}$, $I \leftarrow I + 1$
        if $I \leq 20$ **then** $x_i^0 \leftarrow x_i^0 + 1,\ i \in \mathcal{V}'$, $x_{\text{sum}} \leftarrow \sum_{i \in \mathcal{V}} x_i^0$, $v^0 \leftarrow v_{\min}$, $v_{\min} \leftarrow \infty$
            while $v^0 < v_{\min}$ and $x_{\text{sum}} - \bar{N}_2 > \underline{x}_{\text{sum}}$ and $x_i^0 > 0,\ i \in \mathcal{V}$ **do**
                Randomly pick $\mathcal{V}' \subseteq \mathcal{V}$ such that $|\mathcal{V}'| = \bar{N}_2$
                $x_i^0 \leftarrow x_i^0 - 1,\ i \in \mathcal{V}'$, $x_{\text{sum}} \leftarrow \sum_{i \in \mathcal{V}} x_i^0$, $v_{\min} \leftarrow v^0$
                Resolve $\mathcal{M}(0, T)$ where $\mathbf{x} \in \mathcal{X} \cap \{\mathbf{x} \in \mathbb{Z}_+^{|\mathcal{V}|} \mid \mathbf{x} = \mathbf{x}^0\}$ to obtain v^0
                $\mathcal{D}_1 \leftarrow \mathcal{D}_1 \cup \{(\mathbf{x}^0, v^0)\}$
            if $x_{\text{sum}} - \bar{N}_2 > \underline{x}_{\text{sum}}$ **then** $x_i^0 \leftarrow x_i^0 + 1,\ i \in \mathcal{V}', v^0 \leftarrow v_{\min}$
Return $\mathbf{x}^0$ and v^0

values in $\mathcal{D}_1$ monotonically decrease as the corresponding total number of allocated vehicles increases (resp. decreases), then a smaller objective can be found highly possibly by further increasing (resp. decreasing) total number of allocated vehicles (note that we do observe this phenomenon in our numerical experiments, see Section 2.6). If such observation is not found, we immediately output the solution with the smallest objective value in $\mathcal{D}_1$.

Second, we set the search step of x_{sum} as a positive value $\bar{N}_2 \leq \bar{N}_1/2$ and search within the range between $\bar{x}_{\text{sum}} - |\bar{N}_1|$ and $\bar{x}_{\text{sum}}$ (resp. between $\underline{x}_{\text{sum}}$ and $\underline{x}_{\text{sum}} + |\bar{N}_1|$). That is, we generate a new candidate solution by increasing x_{sum} starting from $\bar{x}_{\text{sum}} - |\bar{N}_1|$ (resp. decreasing x_{sum} starting from $\underline{x}_{\text{sum}} + |\bar{N}_1|$) with a step size $\bar{N}_2$. We append the new solution and the corresponding objective value of the two-stage problem $\mathcal{M}(0, T)$ to $\mathcal{D}_1$. If the sequence of objective values derived in this step stops decreasing during the search, then we end up with a locally optimal solution $\mathbf{x}^0$ with the smallest objective in $\mathcal{D}_1$. We can also obtain the corresponding second-stage solution. This second step is to refine the search with a smaller step size hoping that a smaller objective can be found.

A.5 Supplement to Section 2.6

A.5.1 Performance of Solution Approaches

We compare the CPLEX approach with our solution approach, and report the results in Table A2. The CPLEX approach cannot find any feasible solution in weekday instances (can find low-quality solution with low profit in weekend instances) within the time limit of three hours. In contrast, our approach can produce good-quality solution with high profit and computational time around 1 hour. Hence, our solution approach perform better in both solution quality and time.

Then, we show the convergence performance of our solution approach in Tables A3 and A4. Variant instances are tested with different sizes of demand scenarios (denoted by $|\mathcal{K}|$) and time horizons (denoted by Range). In Table A3, taking weekday instances for example, CPLEX can derive a feasible solution with optimality gap (denoted by Opt Gap) 5.8% on average upon termination in 24 hours. Our

Table A2: Performance of Solution Approaches

Cases			Weekdays				Weekends			
			The CPLEX Approach		Our Solution Approach		The CPLEX Approach		Our Solution Approach	
c_j	C_r	C_p	Profit ($)	Time(s)	Profit ($)	Time(s)	Profit ($)	Time(s)	Profit ($)	Time(s)
0.5	13	0.1	–	10,800	2,126.9	3,216	-255.8	10,800	877.6	3,563
		0.3	–	10,800	2,127.8	3,356	-767.4	10,800	878.6	3,248
		0.5	–	10,800	2,124.7	2,845	-1,279.1	10,800	879.7	3,319
		0.7	–	10,800	2,124.3	2,121	-1,790.7	10,800	879.2	3,282
	15	0.1	–	10,800	2,125.0	3,037	-255.8	10,800	875.8	3,503
		0.3	–	10,800	2,126.7	2,964	-767.4	10,800	876.6	2,581
		0.5	–	10,800	2,123.2	2,885	-1,279.1	10,800	877.5	3,366
		0.7	–	10,800	2,122.7	2,920	-1,790.7	10,800	877.9	2,322
	17	0.1	–	10,800	2,122.7	3,039	-255.8	10,800	875.2	3,186
		0.3	–	10,800	2,111.7	2,106	-767.4	10,800	875.8	2,977
		0.5	–	10,800	2,117.8	2,229	-1,279.1	10,800	876.6	3,012
		0.7	–	10,800	2,118.4	2,901	-1,790.7	10,800	876.8	2,113
0.8	13	0.1	–	10,800	2,041.3	2,172	-255.8	10,800	848.9	2,822
		0.3	–	10,800	2,041.8	2,816	-767.4	10,800	849.6	2,063
		0.5	–	10,800	2,037.9	1,639	-1,279.1	10,800	849.7	2,820
		0.7	–	10,800	2,028.6	2,464	-1,790.7	10,800	849.7	2,089
	15	0.1	–	10,800	2,036.8	2,065	-255.8	10,800	847.7	2,763
		0.3	–	10,800	2,033.6	2,110	-767.4	10,800	848.0	2,804
		0.5	–	10,800	2,031.9	2,348	-1,279.1	10,800	848.1	2,852
		0.7	–	10,800	2,030.3	2,315	-1,790.7	10,800	848.0	2,485
	17	0.1	–	10,800	2,032.3	2,136	-255.8	10,800	847.2	2,775
		0.3	–	10,800	2,032.1	1,486	-767.4	10,800	847.4	2,854
		0.5	–	10,800	2,028.2	2,467	-1,279.1	10,800	847.9	2,778
		0.7	–	10,800	2,031.4	1,615	-1,790.7	10,800	848.0	2,603
1.0	13	0.1	–	10,800	1,999.2	1,489	-255.8	10,800	831.4	2,425
		0.3	–	10,800	1,985.2	2,051	-767.4	10,800	830.9	2,616
		0.5	–	10,800	1.985.9	2,027	-1,279.1	10,800	830.6	2,598
		0.7	–	10,800	1,980.4	2,196	-1,790.7	10,800	831.2	2,610
	15	0.1	–	10,800	1,991.5	2,156	-255.8	10,800	830.3	2,616
		0.3	–	10,800	1,984.2	2,134	-767.4	10,800	829.5	2,626
		0.5	–	10,800	1,978.4	2,190	-1,279.1	10,800	830.1	2,570
		0.7	–	10,800	1,976.4	1,493	-1,790.7	10,800	829.6	1,804
	17	0.1	–	10,800	1,988.6	2,185	-255.8	10,800	830.1	2,578
		0.3	–	10,800	1,979.2	2,121	-767.4	10,800	828.9	2,572
		0.5	–	10,800	1,975.8	1,470	-1,279.1	10,800	829.6	2,550
		0.7	–	10,800	1,976.8	1,442	-1,790.7	10,800	828.9	2,648

Table A3: Performance of Convergence for Our Solution Approach($|\mathcal{K}| > 1$)

Cases		Weekdays						Weekends					
		The CPLEX Approach			Our Approach			The CPLEX Approach			Our Approach		
$\|K\|$	Range	Profit ($)	Opt Gap(%)	Time(s)	Profit($)	Time(s)	Profit Gap(%)	Profit($)	Opt Gap(%)	Time(s)	Profit($)	Time(s)	Profit Gap(%)
40	[40,140]	1053.98	5.35	86,400	1033.04	1044.39	1.99	371.76	9.38	86,400	366.35	592.08	1.45
	[30,150]	1157.92	5.38	86,400	1123.60	683.44	2.96	446.49	11.02	86,400	434.44	416.35	2.70
	[140,240]	1137.47	4.64	86,400	1100.23	843.57	3.27	576.74	7.66	86,400	557.18	655.75	3.39
	[120,240]	1339.22	4.96	86,400	1289.28	647.04	3.73	727.61	8.51	86,400	703.10	706.39	3.37
	[50,210]	2094.89	5.66	86,400	2028.59	950.63	3.16	849.83	11.40	86,400	833.55	1066.79	1.92
	[40,220]	2119.43	6.76	86,400	2085.27	1165.65	1.61	890.03	10.87	86,400	866.96	1139.95	2.59
60	[40,140]	1047.85	5.71	86,400	1029.17	1537.17	1.78	372.41	9.79	86,400	367.82	958.78	1.23
	[30,150]	1149.76	5.74	86,400	1121.47	1124.32	2.46	450.28	10.43	86,400	440.19	1037.25	2.24
	[140,240]	1090.06	5.10	86,400	1056.69	1355.32	3.06	572.75	8.88	86,400	559.59	1238.03	2.30
	[120,240]	1289.42	5.46	86,400	1250.08	903.61	3.05	716.45	10.65	86,400	709.56	1310.85	0.96
	[50,210]	2038.98	6.33	86,400	1996.06	1954.31	2.10	841.80	12.87	86,400	838.45	1670.96	0.40
	[40,220]	2074.42	6.84	86,400	2040.21	1816.97	1.65	876.33	13.00	86,400	872.81	1884.92	0.40
80	[40,140]	1046.26	5.83	86,400	1027.93	2128.56	1.75	346.76	10.66	86,400	345.08	1342.17	0.48
	[30,150]	1147.68	5.89	86,400	1120.14	1494.76	2.40	418.84	11.86	86,400	413.63	1510.07	1.24
	[140,240]	1107.77	5.09	86,400	1072.53	1607.27	3.18	542.36	8.95	86,400	528.87	1462.90	2.49
	[120,240]	1308.71	5.29	86,400	1262.03	1279.33	3.57	680.90	10.31	86,400	673.11	1820.05	1.14
	[50,210]	2016.48	8.41	86,400	2004.17	2674.13	0.61	787.54	13.87	86,400	789.36	2272.17	-0.23
	[40,220]	2076.55	7.63	86,400	2052.47	2607.70	1.16	820.02	13.99	86,400	821.06	2363.86	-0.13

approach can derive the result in 23 minutes on average. The relative gap of profits by two approaches is 2.4% on average. Hence, our approach shows an numerically reasonable convergence performance. Furthermore, since CPLEX approach has difficulty to solve the instances and terminates with relatively large optimality gap, we further test some instances of single scenario (scenario 0, 55, 172, respectively) in different sizes of time range, where CPLEX can terminate with tiny optimality gap. The results are shown in Table A4. By comparing the profits, our approach has gap 3.7% with CPLEX results on average. It further strengthens the convergence

Table A4: Performance of Convergence for Our Solution Approach($|\mathcal{K}| = 1$)

Cases		Weekdays					
		The CPLEX Approach			Our Approach		
Scenario	Range	Profit ($)	Opt Gap(%)	Time(s)	Profit($)	Time(s)	Profit Gap(%)
0	[40,140]	480.97	0.01	27.86	474.11	93.12	1.43
	[140,240]	569.15	0.01	24.24	556.63	70.97	2.20
	[50,210]	1014.07	0.50	9624.85	990.11	65.78	2.36
	[40,220]	1030.21	0.50	8928.45	992.53	73.90	3.66
55	[40,140]	953.94	0.01	139.68	929.55	88.16	2.56
	[140,240]	1014.38	0.01	42.25	966.51	90.38	4.72
	[50,210]	1903.93	0.50	38122.5	1859.37	188.32	2.34
	[40,220]	1942.64	0.50	96833.50	1849.99	64.83	4.77
172	[40,140]	1322.18	0.01	33.81	1262.25	46.56	4.53
	[140,240]	1407.56	0.01	32.14	1327.00	52.21	5.72
	[50,210]	2611.32	0.50	18808.20	2468.59	26.35	5.47
	[40,220]	2673.52	0.50	47991.00	2529.64	39.22	5.38

Table A5: Comparison of Approximation with Different Sample Sizes

Cases			Weekday Profits($)		
c_j	C_r	C_p	Averaged 250 scenarios	80 scenarios	Gap(%)
0.5	13	0.1	2,126.9	2,104.3	1.06
		0.3	2,127.8	2,129.4	0.07
		0.5	2,124.7	2,103.4	1.00
		0.7	2,124.3	2,092.8	1,48
	15	0.1	2,125.0	2,103.4	1.01
		0.3	2,126.7	2,114.7	0.56
		0.5	2,123.2	2,101.9	1.00
		0.7	2,122.7	2,092.1	1.44
	17	0.1	2,122.7	2,104.1	0.88
		0.3	2,111.7	2,082.1	1.40
		0.5	2,117.8	2,105.9	0.56
		0.7	2,118.4	2,111.5	0.33
0.8	13	0.1	2,041.3	2,030.3	0.54
		0.3	2,041.8	2,044.5	0.13
		0.5	2,037.9	2,041.5	0.18
		0.7	2,028.6	2,043.7	0.74
	15	0.1	2,036.8	2,027.1	0.48
		0.3	2,033.6	2,032.1	0.08
		0.5	2,031.9	2,031.2	0.04
		0.7	2,030.3	2,031.8	0.07
	17	0.1	2,032.3	2,026.4	0.28
		0.3	2,032.1	2,028.1	0.19
		0.5	2,028.2	2,028.6	0.02
		0.7	2,031.4	2,021.6	0.48
1.0	13	0.1	1,999.2	1,988.7	0.52
		0.3	1,985.2	1,994.0	0.44
		0.5	1.985.9	1,992.4	0.32
		0.7	1,980.4	1,993.8	0.67
	15	0.1	1,991.5	1,988.7	0.14
		0.3	1,984.2	1,990.6	0.32
		0.5	1,978.4	1,990.4	0.61
		0.7	1,976.4	1,990.2	0.70
	17	0.1	1,988.6	1,988.7	0.01
		0.3	1,979.2	1,988.7	0.47
		0.5	1,975.8	1,988.4	0.63
		0.7	1,976.8	1,988.2	0.57

performance of our solution approach.

In addition, we show our solution approach with 80 scenarios for weekday instances does not lead to significant approximation error with the practical case of uncertain demand by two steps. First, we note Citi Bike has applied predictive methods to estimate the demand and then use a deterministic model to derive relocation decisions (O'Mahony and Shmoys 2015). Second, we average the weekday demand of 250 scenarios in a year to a single scenario and use it to replace the predictive supply in practical case. Then, we compare our results with those by

the deterministic model in Table A5. It shows the gap of profits between two cases is less than 1.5% for various instances. Hence, the sample size of 80 scenarios for weekday instances is suitable to approximate the reality.

A.5.2 Data Processing via ARIMA Models

In contrast to the previous experiments, we re-generate the training and testing samples separately, with each having 120 samples of scenarios for both the weekday and weekend demands. To that end, the data in 2018 is fitted in seasonal ARIMA models. We use 20 weekdays (resp. 8 weekend days) of trip records in each month to fit a time series model of the bimodal (resp. unimodal) pattern. Thus, we have 12 fitted time series models for weekdays (resp. weekend days) in 12 months. Then, each model generates 20 new samples for the corresponding month by forecasting: 10 for training and 10 for testing, leading to 120 scenarios of demand for training and 120 scenarios of demand for testing. To keep the mean values of the weekday and weekend samples the same in each given month, we follow the following three steps: (i) first, scale the sample values; (ii) then, randomly select an arc in the network $\mathcal{G}$ and add one more demand to the sample with a lower mean value; and (iii) do the above step until the mean values are the same.

Appendix B

Proofs for Chapter 3

B.1 Proofs Under the Percentage Label

B.1.1 Proof of Lemma 1

In the case of percentage label, the firm can always obtain a label. In Stage 2, the firm chooses a price and the percentage of the recycled material to maximize profit, i.e., max $\pi(p, q)$. As shown in Equation (3.1), the firm can set either a low price to serve all consumers or a high price to serve only the environmentally conscious consumers. Besides, one can verify that the firm's profit increases in p (i.e., $\frac{\partial \pi}{\partial p} > 0$) in both scenarios. Thus, the firm's optimal price is either $p_P^* = v + v_r q$ or $p_P^* = v$.

Next, we compare the firm's optimal profit in the high price scenario (i.e., $\pi(v + v_r q, q)$) with that in the low price scenario (i.e., $\pi(v, q)$). Solving $\pi(v, q) - \pi(v + v_r q, q) = q(\alpha(c_r - v_r - c_n) + c_n - c_r) - (1-\alpha)(v - c_n) = 0$ leads to $q = \frac{(\alpha-1)(v-c_n)}{(\alpha-1)(c_r-c_n)-\alpha v_r}$. Define $\tilde{q} = \frac{(\alpha-1)(v-c_n)}{(\alpha-1)(c_r-c_n)-\alpha v_r}$ and $\tilde{\alpha} = \frac{v-c_r}{v+v_r-c_r}$. By algebraic analysis, we finally have $\pi(v, q) - \pi(v+v_r q, q) \geq 0$ if $\alpha \leq \tilde{\alpha}$ or if $\alpha > \tilde{\alpha}$ and $q \leq \tilde{q}$, and $\pi(v, q) - \pi(v+v_r q, q) < 0$ if $\alpha > \tilde{\alpha}$ and $q > \tilde{q}$, as shown in Lemma 1.

B.1.2 Proof of Proposition 3.1

We prove proposition 1 by first solving the firm's optimal recycled content q_P^* in the second stage given the pricing strategy in Lemma 1. Then we compare the resulting firm's profits in all possible cases. To simplify the discussion, we only consider strict inequalities during the analysis and incorporate the equality conditions in the final results.

Table B1: Summary of q_P^* by Cases

Case	q_P^*	$\pi(p_P^*, q_P^*)$	Conditions	Condition Set
$H1$	$\tilde{q}$	$\frac{(v-c_n)(\alpha v_r(c_r-c_n+\alpha(v_r+c_n-c_r))-k(v-c_n)(1-\alpha)^2)}{(c_r-c_n+\alpha(v_r+c_n-c_r))^2}$	$\alpha > \tilde{\alpha}$, $q_H^* < \tilde{q}$	Q_{H1}
$H2$	q_H^*	$\frac{\alpha(\alpha(v_r+c_n-c_r)^2+4k(v-c_n)))}{4k}$	$\alpha > \tilde{\alpha}$, $\tilde{q} < q_H^* < 1$	Q_{H2}
$H3$	1	$\alpha(v+v_r-c_r)-k$	$\alpha > \tilde{\alpha}$, $q_H^* > 1$	Q_{H3}
$L1$	0	$v-c_n$	$\alpha > \tilde{\alpha}$, $q_l^* < 0$	Q_{L1}
$L2$	q_l^*	$\frac{(c_n-c_r)^2+4k(v-c_n))}{4k}$	$\alpha > \tilde{\alpha}$, $0 < q_l^* < \tilde{q}$	Q_{L2}
$L3$	$\tilde{q}$	$\frac{(v-c_n)(\alpha v_r(c_r-c_n+\alpha(v_r+c_n-c_r))-k(v-c_n)(1-\alpha)^2)}{(c_r-c_n+\alpha(v_r+c_n-c_r))^2}$	$\alpha > \tilde{\alpha}$, $q_l^* > \tilde{q}$	Q_{L3}
$L4$	0	$v-c_n$	$\alpha < \tilde{\alpha}$, $q_l^* < 0$	Q_{L4}
$L5$	q_l^*	$\frac{(c_n-c_r)^2+4k(v-c_n))}{4k}$	$\alpha < \tilde{\alpha}$, $0 < q_l^* < 1$	Q_{L5}
$L6$	1	$v-c_r-k$	$\alpha < \tilde{\alpha}$, $q_l^* > 1$	Q_{L6}

Optimal Recycled Content in High and Low Prices

When the price is high, i.e., $p_P^* = v + v_r q$, the profit $\pi(v+v_r q, q) = -kq^2 + \alpha q(v_r + c_n - c_r) + \alpha(v - c_n)$ is concave in q. Solving the first-order condition $\frac{\partial \pi(v+v_r q, q)}{\partial q} = 0$ yields the maximizer $q_H^* = \frac{\alpha(v_r+c_n-c_r)}{2k}$. Recall $\tilde{\alpha} < \alpha \leq 1$ and $\tilde{q} < q \leq 1$ for the high price as shown in B.1.1, then the optimal recycled content q_P^* is discussed in three cases $H1 \sim H3$, see Table B1. When the price is low, i.e., $p_P^* = v$, the profit $\pi(v, q) = -kq^2 + q(c_n - c_r) + v - c_n$ is also concave in q. Solving the first-order condition $\frac{\partial \pi(v,q)}{\partial q} = 0$ yields the maximizer $q_l^* = \frac{c_n - c_r}{2k}$. Recall the conditions for the low price: 1) $\alpha > \tilde{\alpha}$ and $q \leq \tilde{q}$ where we discuss three cases $L1 \sim L3$; 2) $\alpha \leq \tilde{\alpha}$ where we discuss three cases $L4 \sim L6$. Then the corresponding q_P^* is given in Table B1 and the conditions are collected in $Q_t, \forall t \in \{H1, ..., H3, L1, ..., L6\}$.

By Lemma 3.1 and simple algebraic calculations, the conditions (the fourth column in Table B1) in each case are collected in the sets (the last column in Table B1) as follows with equality sign included. Due to the focus of our study, all sets are described with focus on (α, k). $Q_{H1} \doteq \{(\alpha, k) : \alpha > \tilde{\alpha}, k > \max\{0, \bar{k}_H\}\}$ where $\bar{k}_H = \frac{\alpha(v_r+c_n-c)(c_r-c_n+\alpha(v_r+c_n-c))}{2(v-c_n)(1-\alpha)}$, $Q_{H2} \doteq \{(\alpha, k) : \alpha > \tilde{\alpha}, v_r > c_r - c_n, \frac{1}{2}\alpha(v_r + c_n - c_r) < k \leq \bar{k}_H\}$, $Q_{H3} \doteq \{(\alpha, k) : \alpha > \tilde{\alpha}, v_r > c_r - c_n, k \leq \frac{1}{2}\alpha(v_r + c_n - c_r)\}$, $Q_{L1} \doteq \{(\alpha, k) : c_r > c_n, \alpha > \tilde{\alpha}\}$, $Q_{L2} \doteq \{(\alpha, k) : c_n > c_r, \alpha > \tilde{\alpha}, k > \max\{0, \bar{k}_L\}\}$ where $\bar{k}_L = \frac{(c_n-c_r)(\alpha(v_r+c_n-c_r)-(c_n-c_r))}{2(v-c_n)(1-\alpha)}$, $Q_{L3} \doteq \{(\alpha, k) : c_n > c_r, \alpha > \tilde{\alpha}, k \leq \bar{k}_L\}$, $Q_{L4} \doteq \{(\alpha, k) : c_r > c_n, \alpha \leq \tilde{\alpha}\}$, $Q_{L5} \doteq \{(\alpha, k) : c_n > c_r, \alpha \leq \tilde{\alpha}, k > \frac{c_n - c_r}{2}\}$, $Q_{L6} \doteq \{(\alpha, k) : c_n > c_r, \alpha \leq \tilde{\alpha}, k \leq \frac{c_n - c_r}{2}\}$.

Comparison of the Cases in High and Low Prices

Next, we derive the firm's optimal q_P^* by comparing the resulting profits in cases $H1 \sim H3$ with those in $L1 \sim L6$. A trivial case is that, when $\alpha \leq \tilde{\alpha}$, only the cases $L4 \sim L6$ exist and no comparison is needed. Then, we consider $\alpha > \tilde{\alpha}$ and compare cases $H1 \sim H3$ with $L1 \sim L3$. There are 9 comparisons in total and the results are given in Table B2, where $\bar{k}_3 = \frac{(c_r-c_n)^2-\alpha^2(-c_r+v_r+c_n)^2}{4(\alpha-1)(v-c_n)}$,

$\bar{k}_4 = \frac{(c_n-c_r)((\alpha-1)(c_n-c_r)+\alpha v_r)}{(1-\alpha)(v-c_n)}$, $\bar{k}_1 = \frac{1}{2}(\alpha(v+v_r-c_r)+c_n-v+\sqrt{(\alpha(c_r-v-v_r)+v-c_r)(\alpha(c_r-v-v_r)+v+c_r-2c_n)})$,

$\alpha_a = \sqrt{\frac{c_r^3-c_r^2(2v+v_r+c_n)+c_r(v^2+2c_n(v+v_r))-v^2(v_r+c_n)+2vv_rc_n-2v_rc_n^2}{(c_r-v_r-c_n)(c_r-2v-v_r+c_n)^2}} + \frac{c_n-v}{c_r-2v-v_r+c_n}$,

$\alpha_b = \frac{1}{2}\sqrt{\frac{-c_r^3+c_r^2(2v+v_r+c_n)-c_r(v^2+2v(c_n-v_r)+4v_rc_n)+v^2(v_r+c_n)-4vv_rc_n+4v_rc_n^2}{(v-c_n)^2(-c_r+v_r+c_n)}} + \frac{c_r+v-2c_n}{2(v-c_n)}$.

Next, we define five sets: P_{ij}, $\forall i \in \{1, H, L, 0\}$, $j \in \{H, L\}$ where i indexes the recycled content and j the high or low price. Specifically, P_{1H}, P_{HH}, P_{LL} and P_{0L} are derived from Q_{L4}, Q_{L5} and Table B2, the firm's corresponding optimal recycled contents (q_P^*) are 1 (with high price), q_H^*, q_l^* and 0, respectively. Note that for each row of Table B2, we combine the conditions in the third and forth columns. For the rows whose q_P^* are the same, we further collect the combined conditions into the corresponding set. The other set P_{1L} is derived from Q_{L6} where only the case $L6$ holds. The firm's corresponding recycled content is 1 (with low price). $P_{1H} \doteq \{(\alpha, k) : \alpha > \underline{\alpha}_{1H}, k \leq \bar{k}_{1H}\}$, $P_{HH} \doteq \{(\alpha, k) : \alpha > \underline{\alpha}_{HH}, \frac{1}{2}\alpha(c_n + v_r - c_r) < k \leq \bar{k}_{HH})\}$, $P_{LL} \doteq \{(\alpha, k) : c_n > c_r, k > \underline{k}_{LL}\}$, $P_{1L} \doteq \{(\alpha, k) : c_n > c_r, \alpha \leq \tilde{\alpha}, k \leq \frac{1}{2}(c_n - c_r)\}$, $P_{0L} \doteq \{(\alpha, k) : c_n \leq c_r, k > \underline{k}_{0L}\}$, where the boundaries for α and k are given by $\bar{k}_{1H} = \begin{cases} \min\{\bar{k}_1, \frac{1}{2}\alpha(c_n+v_r-c_r)\}, \text{ if } c_n > c_r \\ \min\{\alpha(v+v_r-c_r)+c_n-v, \frac{1}{2}\alpha(c_n+v_r-c_r)\}, \text{ otherwise} \end{cases}$, $\underline{\alpha}_{1H} = \begin{cases} \tilde{\alpha}, \text{ if } c_n > c_r \\ 0, \text{ otherwise} \end{cases}$, $\bar{k}_{HH} = \begin{cases} \bar{k}_3, \text{ if } c_n > c_r \\ \frac{\alpha^2(-c_r+c_n+v_r)^2}{4(1-\alpha)(v-c_n)}, \text{ otherwise} \end{cases}$, $\underline{\alpha}_{HH} = \begin{cases} \alpha_a, \text{ if } c_n > c_r \\ \frac{2(v-c_n)}{-c_r-c_n+v_r+2v}, \text{ otherwise} \end{cases}$, $\underline{k}_{LL} = \begin{cases} \frac{1}{2}(c_n-c_r), \text{ if } \alpha \leq \tilde{\alpha} \\ \bar{k}_1, \text{ if } \tilde{\alpha} < \alpha \leq \alpha_a \\ \bar{k}_3, \text{ if } \alpha > \alpha_a \end{cases}$, $\underline{k}_{0L} = \begin{cases} \alpha(v+v_r-c_r)+c_n-v), \text{ if } \alpha \leq \frac{2(v-c_n)}{-c_r-c_n+v_r+2v} \\ \frac{\alpha^2(-c_r+c_n+v_r)^2}{4(1-\alpha)(v-c_n)}, \text{ otherwise} \end{cases}$. A visualization example of the regions P_{ij}, $\forall\, i \in \{1,H,L,0\}$, $j \in \{H, L\}$ is shown in Figure 3.2.

B.1.3 Proof of Corollary 3.1

We first prove Corollary 1(1). For q_P^*: by Proposition 3.1, we can easily check that *i)* $\frac{\partial q_P^*}{\partial \alpha} > 0$, if $(\alpha, k) \in P_{HH}$; $\frac{\partial q_P^*}{\partial \alpha} = 0$, otherwise; *ii)* $\frac{\partial q_P^*}{\partial k} < 0$, if $(\alpha, k) \in$

Table B2: Comparison of the Firm's Profit in Percentage Label by Cases

Case1	Case2	$Q_{case1} \cap Q_{case2}$	$\pi_{case1} - \pi_{case2}$	q_P^*
$H1$	$L1$	$\{(\alpha,k) : c_n < c_r, \alpha > \tilde{\alpha}, k > \max\{0, \bar{k}_H\}\}$	< 0	0
$H1$	$L2$	$\{(\alpha,k) : c_n > c_r, \alpha > \tilde{\alpha}, k > \bar{k}_H\}$	< 0	q_l^*
$H1$	$L3$	$\emptyset$	NA	NA
$H2$	$L1$	$\{(\alpha,k) : c_n < c_r, v_r > c_r - c_n, \alpha > \tilde{\alpha}, \frac{1}{2}\alpha(v_r + c_n - c_r) < k < \bar{k}_H\}$	> 0 if $c_r > c_n$, $v_r > c_r - c_n$, $\alpha > \frac{2(v-c_n)}{-c_r-c_n+v_r+2v}$ and $\frac{1}{2}\alpha(c_n+v_r-c_r) < k < \frac{\alpha^2(-c_r+c_n+v_r)^2}{4(1-\alpha)(v-c_n)}$	q_H^*
			< 0 otherwise	0
$H2$	$L2$	$\{(\alpha,k) : c_n > c_r, \alpha > \tilde{\alpha}, \max\{\frac{1}{2}\alpha(v_r + c_n - c_r), \bar{k}_L\} < k < \bar{k}_H\}$	> 0 if $c_n > c_r$, $\alpha > \alpha_a$, $\max\{\frac{1}{2}\alpha(c_n + v_r - c_r), \frac{1}{2}\bar{k}_4\} < k < \bar{k}_3$	q_H^*
			< 0 otherwise	q_l^*
$H2$	$L3$	$\{(\alpha,k) : c_n > c_r, \alpha > \alpha_b, \bar{k}_3 < k < \frac{1}{2}\bar{k}_4\}$	> 0	q_H^*
$H3$	$L1$	$\{(\alpha,k) : c_n < c_r, v_r > c_r - c_n, \alpha > \tilde{\alpha}, k < \frac{1}{2}\alpha(v_r + c_n - c_r)\}$	> 0 if $c_r > c_n$, $v_r > c_r - c_n$, $\alpha > \frac{v-c_n}{v+v_r-c_r}$ and $k < \min\{\alpha(v+v_r-c_r)+c_n - v, \frac{1}{2}\alpha(c_n + v_r - c_r)\}$	1
			< 0 otherwise	0
$H3$	$L2$	$\{(\alpha,k) : c_n > c_r, \alpha > \tilde{\alpha}, \bar{k}_L < k < \frac{1}{2}\alpha(v_r + c_n - c_r)\}$	> 0 if $c_n > c_r$, $\tilde{\alpha} < \alpha < \alpha_b$ and $\frac{1}{2}\bar{k}_4 < k < \min\{\bar{k}_1, \frac{1}{2}\alpha(c_n + v_r - c_r)\}$	1
			< 0 otherwise	q_l^*
$H3$	$L3$	$\{(\alpha,k) : c_n > c_r, \alpha > \tilde{\alpha}, k < \min\{\bar{k}_L, \frac{1}{2}\alpha(v_r + c_n - c_r)\}\}$	> 0	1

Note: NA implies the corresponding case is not applicable and no result is given.

$P_{HH} \cup P_{LL}$; $\frac{\partial q_P^*}{\partial k} = 0$, otherwise. Hence, the firm's optimal recycled content weakly increases in α and weakly decreases in k. Note that from now on, we use "weakly" to indicate q_P^* is not continuous but monotone across regions. For π_P^*, by Equation (3.2), we can verify *i)* $\frac{\partial \pi_P^*}{\partial \alpha} > 0$ if $(\alpha, k) \in P_{1H} \cup P_{HH}$ and $\frac{\partial \pi_P^*}{\partial \alpha} = 0$ otherwise; *ii)* $\frac{\partial \pi_P^*}{\partial k} = 0$ if $(\alpha, k) \in P_{0L}$ and $\frac{\partial \pi_P^*}{\partial k} < 0$ otherwise. Hence, the firm's profit weakly increases in α and weakly decreases in k. Next, we prove Corollary 1(2). From Equation (3.2), we have *i)* $\frac{\partial \Pi_P^*}{\partial \alpha} > 0$ if $(\alpha, k) \in P_{1H} \cup P_{HH}$ and $\frac{\partial \Pi_P^*}{\partial \alpha} = 0$ otherwise; *ii)* $\frac{\partial \Pi_P^*}{\partial k} < 0$ if $(\alpha, k) \in P_{HH} \cup P_{LL}$ and $\frac{\partial \Pi_P^*}{\partial k} = 0$ otherwise. However, NGO's payoff may drop as α increases and may rise as k increases across boundary $(\alpha, k) \in (P_{1H} \cup P_{HH}) \cap (P_{LL} \cup P_{1L} \cup P_{0L})$. For example, $\Pi_{P_{1L}}^* = 1 > \Pi_{P_{1H}}^* = \alpha$, then NGO's payoff drops at the boundary $P_{1H} \cap P_{1L}$ as α grows (e.g., from P_{1L} to P_{1H}). Hence, NGO's payoff is non-monotone in α and in k.

B.2 Proofs Under the Binary Label

B.2.1 Proof of Lemma 2

This lemma shows the firm's optimal price in the case of the binary label. Given the label standard $\bar{q}$ and the firm's recycled content q, the firm can set a price $p \in [0, v]$ to serve all consumers or set $p \in (v, v + v_r\bar{q}]$ to serve the environmentally conscious consumers. We obtain the optimal price $p_B^* = v$ or $p_B^* = v + v_r\bar{q}$ by observing the firm's profit is increasing in p (i.e., $\frac{\partial \pi(p,q)}{\partial p} > 0$) in either case. Moreover, the firm can set the high price $p_B^* = v + v_r\bar{q}$ only if he obtains the label, i.e., $q \geq \bar{q}$. Solving $\pi(v + v_r\bar{q}, q) - \pi(v, q) = \alpha v_r\bar{q} + (1 - \alpha)[c_r q + c_n(1 - q) - v] > 0$ yields $\bar{q} > \frac{(\alpha-1)[c_r q + c_n(1-q) - v]}{\alpha v_r}$ (denoted as $\bar{\bar{q}}$). Then, the firm prefers the high price if $\bar{\bar{q}} < \bar{q} \leq q$ and the low price otherwise.

B.2.2 Proof of Lemma 3.3

The proof logic is similar to that for Proposition 1. Given the binary label standard $\bar{q}$ and the optimal price in Lemma 2, we solve for the firm's optimal recycled content q_B^*, which leads to a few different cases. Then, we compare the resulting firm's profits in these cases. Note that we only consider strict inequalities during the analysis and incorporate the equality conditions in the final results.

The Optimal Recycled Content in High and Low Prices

When $p_B^* = v + v_r\bar{q}$, the firm needs to obtain the label, i.e., $q \geq \bar{q}$. Since the profit $\pi(v+v_r\bar{q}, q) = \alpha\bar{q}v_r - kq^2 + \alpha q(c_n - c_r) + \alpha(v - c_n)$ is concave in q, solving $\frac{\partial \pi(v+v_r\bar{q},q)}{\partial q} = 0$ yields the maximizer $q_h^* = \frac{\alpha(c_n - c_r)}{2k}$. Recall Lemma 3.2, solving $\bar{q} > \bar{\bar{q}}$ with respect to q yields $q > \hat{q}(\bar{q})$ if $c_r > c_n$ and $q < \hat{q}(\bar{q})$ if $c_r < c_n$ where $\hat{q}(\bar{q}) = \frac{v - c_n - \alpha(v + \bar{q}v_r - c_n)}{(1-\alpha)(c_r - c_n)}$. Then, we need to compare whether q_h^* is greater or smaller than $\hat{q}(\bar{q})$, $\bar{q}$ and 1, respectively, under the high price conditions. The resulting values of q_B^* are summarized in Cases $h1 \sim h4$ in Table B3. For example, if $q_h^* > 1$ (Case $h4$), then $q_B^* = 1$ is optimal. When $p_B^* = v$, the profit $\pi(v, q) = -kq^2 + q(c_n - c_r) + v - c_n$ is concave in q. Solving $\frac{\partial \pi(v,q)}{\partial q} = 0$ yields the maximizer $q_l^* = \frac{c_n - c_r}{2k}$ as in the percentage label case. There are also four cases for q_B^*, summarized in Cases $l1 \sim l4$ in Table B3, where the firm sets a low price and may get the label (as in Cases $l3$, $l4$) or not (as in Cases $l1$, $l2$).

Table B3: Summary of q_B^* by Cases

Case	q_B^*	$\pi(p_B^*, q_B^*)$	Conditions
$h1$	$\hat{q}(\bar{q})$	$-\frac{(\alpha-1)\alpha\bar{q}v_r(c_r-c_n)^2+k(\alpha\bar{q}v_r+(\alpha-1)v-\alpha c_n+c_n)^2}{(\alpha-1)^2(c_r-c_n)^2}$	$\bar{\bar{q}} < \bar{q} < q < \hat{q}(\bar{q}) < 1,\ q_h^* > \hat{q}(\bar{q})$
			$\bar{\bar{q}} < \bar{q} < \hat{q}(\bar{q}) < q < 1,\ q_h^* < \hat{q}(\bar{q})$
$h2$	$\bar{q}$	$\alpha(\bar{q}(-c+v_r+c_n)+v-c_n)-k\bar{q}^2$	$\hat{q}(\bar{q}) < \bar{q},\ q_h^* < \bar{q},\ \bar{\bar{q}} < \bar{q} < q < 1$
$h3$	q_h^*	$\frac{\alpha^2(c_r-c_n)^2}{4k}+\alpha(\bar{q}v_r+v-c_n)$	$\bar{q} < q < \hat{q}(\bar{q}) < 1,\ \bar{\bar{q}} < \bar{q} < q_h^* < \hat{q}(\bar{q})$
$h4$	1	$\alpha(\bar{q}v_r+v-c_r)-k$	$\hat{q}(\bar{q}) > 1,\ \bar{\bar{q}} < \bar{q} < q < 1 < q_h^*$
$l1$	0	$v-c_n$	$q_l^* < 0 < q$
$l2$	q_l^*	$\frac{(c_n-c_r)^2+4k(v-c_n)}{4k}$	$0 < q_l^* < \bar{q}$
$l3$	q_l^*	$\frac{(c_n-c_r)^2+4k(v-c_n)}{4k}$	$\bar{q} < q_l^* < 1,\ \bar{q} \le \bar{\bar{q}}$
$l4$	1	$v-c_r-k$	$q_l^* > 1,\ \bar{q} \le \bar{\bar{q}}$

Note: The conditions (in the forth column) include those for the firm's pricing strategy and recycled content decision. Cases $h1 \sim h4$ always have $q > \bar{q} > \bar{\bar{q}}$ such that the high price and the label can be applied. In Case $h3$, only the subcase when $c_n > c_r$ is feasible. Since $c_n < c_r$ leads to $q_h^* < 0 \le \bar{q}$ that contradicts the condition for the high price. Cases $l1 \sim l4$ are under the low price scenario. In Cases $l1$ and $l2$, the firm cannot obtain the label. Otherwise, he can obtain the label but has higher profit with the low price (i.e., $\bar{q} < \bar{\bar{q}}$). Moreover, Case $l1$ implies only the subcase with $c_n < c_r$ holds. Cases $l2 \sim l4$ imply $c_n > c_r$ holds because $c_n < c_r$ leads to $q_l^* < 0$ that contradicts $q_l^* > 0$ in these cases.

By simple algebraic calculations, the conditions in the last column of each row in Table B3 are solved, and according to q_B^*, the conditions in different rows are combined into sets Q_x, where x represents the case's name. $Q_{h1} \doteq \{(\alpha, k, \bar{q}) : \alpha > \tilde{\alpha}, k < \bar{k}_{h1}, \underline{q}_{h1} < \bar{q} < \bar{q}_{h1}\}$, $Q_{h2} \doteq \{(\alpha, k, \bar{q}) : \alpha > \tilde{\alpha}, k > \underline{k}_{h2}, \bar{q} > \bar{q}_{h2}\}$, $Q_{h3} \doteq \{(\alpha, k, \bar{q}) : c_n > c_r, \alpha > \tilde{\alpha}, \frac{\alpha(c_n-c_r)}{2} < k < \tilde{k}_{h1}, \bar{q}_{h1}^2 < \bar{q} < q_h^*\}$, $Q_{h4} \doteq \{(\alpha, k, \bar{q}) : c_n > c_r, \alpha > \tilde{\alpha}, k < \frac{\alpha(c_n-c_r)}{2}, \bar{q}_{h1}^1 < \bar{q}\}$, $Q_{l1} \doteq \{(\alpha, k, \bar{q}) : c_n < c_r\}$, $Q_{l2} \doteq \{(\alpha, k, \bar{q}) : c_n > c_r, k > \frac{c_n-c_r}{2}, q_l^* < \bar{q}\}$, $Q_{l3} \doteq \{(\alpha, k, \bar{q}) : c_n > c_r, k > \frac{c_n-c_r}{2}, \bar{q} < \bar{q}_{l3}\}$, $Q_{l4} \doteq \{(\alpha, k, \bar{q}) : c_n > c_r,\ k < \frac{c_n-c_r}{2}, \bar{q} < \bar{q}_{l4}\}$. The boundaries are: $\underline{q}_{h1} = \begin{cases} \tilde{q}, & \text{if } c_n > c_r \\ \bar{q}_{h1}^1, & \text{otherwise} \end{cases}$, $\bar{q}_{h1} = \begin{cases} \min\{\bar{q}_{h1}^1, \bar{q}_{h1}^2\}, & \text{if } c_n > c_r \\ \tilde{q}, & \text{otherwise} \end{cases}$, $\bar{k}_{h1} = \begin{cases} \tilde{k}_{h1}, & \text{if } c_n > c_r \\ \infty, & \text{otherwise} \end{cases}$, $\bar{q}_{h2} = \begin{cases} \max\{\tilde{q}, q_h^*\}, & \text{if } c_n > c_r \\ \tilde{q}, & \text{otherwise} \end{cases}$, $\underline{k}_{h2} = \begin{cases} \frac{\alpha(c_n-c_r)}{2}, & \text{if } c_n > c_r \\ 0, & \text{otherwise} \end{cases}$, $\bar{q}_{l3} = \begin{cases} q_l^*, & \text{if } \alpha < \tilde{\alpha} \\ \min\{\bar{q}_{l1}, q_l^*\}, & \text{otherwise} \end{cases}$, $\bar{q}_{l4} = \begin{cases} 1, & \text{if } \alpha < \tilde{\alpha} \\ \bar{q}_{h1}^1, & \text{otherwise} \end{cases}$. In the above, $\tilde{\alpha}$, $\tilde{q}$ are defined in Lemma 1. $\tilde{k}_{h1} = \frac{\alpha(c_r-c_n)(\alpha(c-v_r-c_n)+c_n-c_r)}{2(1-\alpha)(v-c_n)}$, $\bar{q}_{h1}^1 = \frac{(1-\alpha)(v-c_r)}{v_r\alpha}$, $\bar{q}_{h1}^2 = \frac{(1-\alpha)\big(\alpha(c_r-c_n)^2+2k(v-c_n)\big)}{2\alpha k v_r}$, $\bar{q}_{l1} = \frac{(1-\alpha)\big((c_r-c_n)^2+2k(v-c_n)\big)}{2\alpha k v_r}$.

Firm's Optimal Decision

Next, we derive the optimal solutions by comparing the resulting profits in Cases $h1 \sim h4$ and $l1 \sim l4$, the results are summarized in Table B4, where

$\underline{q}'_{MH} = \frac{\alpha(v_r-c_r+c_n)-\sqrt{\alpha^2(v_r-c_r+c_n)^2+4k(v-c_n)(\alpha-1)}}{2k}$, $\bar{q}'_{MH} = \frac{\alpha(v_r-c_r+c_n)+\sqrt{\alpha^2(v_r-c_r+c_n)^2+4k(v-c_n)(\alpha-1)}}{2k}$,

$\underline{q}_{MH} = \frac{\alpha(v_r-c_r+c_n)-\sqrt{\alpha^2(v_r-c_r+c_n)^2+4k(v-c_n)(\alpha-1)-(c_n-c_r)^2}}{2k}$,

$\bar{q}_{MH} = \frac{\alpha(v_r-c_r+c_n)+\sqrt{\alpha^2(v_r-c_r+c_n)^2+4k(v-c_n)(\alpha-1)-(c_n-c_r)^2}}{2k}$.

For a clearer display of the firm's decisions, we combine the conditions in the third and fourth columns of each row in Table B4. According to the value of q_B^*, we combine those conditions in different rows into six regions Q_{ij} where $i \in \{1, H, M, L, 0\}$ indexes the recycled content and $j \in \{H, L\}$ the high or low price: $Q_{MH} \doteq \{(\alpha,k,\bar{q})$: $\alpha > \alpha_{LH}$, $\underline{Q}_{MH} < \bar{q} \le \bar{Q}_{MH}\}$, $Q_{HH} \doteq \{(\alpha,k,\bar{q})$: $c_n > c_r$, $\alpha > \tilde{\alpha}$, $k > \frac{\alpha(c_n-c_r)}{2}$, $\underline{Q}_{HH} < \bar{q} \le q_h^*\}$, $Q_{1H} \doteq \{(\alpha,k,\bar{q})$: $c_n > c_r$, $\alpha > \tilde{\alpha}$, $k < \frac{\alpha(c_n-c_r)}{2}$, $\bar{q}_{h1}^1 < \bar{q} \le 1\}$, $Q_{0L} \doteq \{(\alpha,k,\bar{q})$: $c_n \le c_r$, $(v_r \le c_r - c_n \;||\; v_r > c_r - c_n \;\&\; (\bar{q} \le \underline{q}'_{MH} \;||\; \bar{q}'_{MH} < \bar{q} \le 1))\}$, $Q_{HL} \doteq \{(\alpha,k,\bar{q})$: $c_n > c_r$, $k > \bar{k}_{HL}$, $\bar{q} < \frac{c_n-c_r}{2k}$, $\bar{q} < \tilde{q}_{HL}\}$, $Q_{LL} \doteq \{(\alpha,k,\bar{q})$: $c_n > c_r, k > \bar{k}_{HL}$, $\bar{q} > \frac{c_n-c_r}{2k}$, $\bar{q} < \tilde{q}_{HL}\}$, $Q_{1L} \doteq \{(\alpha,k,\bar{q})$: $k \le \frac{c_n-c_r}{2}$, $\bar{q} \le \bar{q}_{1L}\}$. Each of these sets corresponds to q_B^* in cases $h2(\bar{q})$, $h3(q_h^*)$, $h4(1)$, $l1(0)$, $l2(q_l^*)$, $l3(q_l^*)$, $l4(1)$, respectively. An example of the regions in $(k, \bar{q})$ space is shown in Figure 3.3. The boundaries are: $\underline{Q}_{HH} = \begin{cases} \bar{Q}_{1L}, \text{ if } \frac{\alpha(c_n-c_r)}{2} < k < \frac{c_n-c_r}{2} \\ \bar{Q}_{HL}, \text{ if } \frac{c_n-c_r}{2} < k < \frac{(c_r-c_n)\left(\alpha^2(-c_r+2v_r+c_n)+c_r-c_n\right)}{4(\alpha-1)(v-c_n)} \end{cases}$, $\underline{\alpha}_{LH} = \begin{cases} \tilde{\alpha}, \text{ if } c_n > c_r \\ 0, \text{ otherwise} \end{cases}$,

$\underline{Q}_{MH} = \begin{cases} \max\{q_l^*, \underline{q}_{MH}\}, \text{ if } c_n > c_r \\ \underline{q}'_{MH}, \text{ if } c_n \le c_r, v_r > c_r - c_n \\ \infty, \text{ otherwise} \end{cases}$, $\bar{Q}_{MH} = \begin{cases} \min\{1, \bar{q}_{MH}\}, \text{ if } c_n > c_r \\ \min\{1, \bar{q}'_{MH}\}, \text{ if } c_n \le c_r, v_r > c_r - c_n \\ -\infty, \text{ otherwise} \end{cases}$, $\bar{k}_{HL} = \begin{cases} \frac{c_n-c_r}{2}, \text{ if } \alpha \le \tilde{\alpha} \\ 0, \text{ otherwise} \end{cases}$,

$\tilde{q}_{HL} = \begin{cases} 1, \text{ if } \alpha \le \tilde{\alpha} \\ \bar{Q}_{HL}, \text{ otherwise} \end{cases}$, $\bar{q}_{1L} = \begin{cases} 1, \text{ if } \alpha \le \tilde{\alpha} \\ \bar{Q}_{1L}, \text{ otherwise} \end{cases}$. In the above, $\bar{Q}_{HL}$ denotes the upper bound of $\bar{q}$ in region $Q_{HL} \cup Q_{LL}$ in $(k, \bar{q})$ space as shown in Figure 3.3. It can be derived from rows 3, 6, 7, 11 of Table B4 as

$$\bar{Q}_{HL} = \begin{cases} \frac{(1-\alpha)\left((1+\alpha)(c_r-c_n)^2+4k(v-c_n)\right)}{4\alpha k v_r}, \text{ if } \frac{c_n-c_r}{2} < k < \frac{(c_r-c_n)\left(\alpha^2(-c_r+2v_r+c_n)+c_r-c_n\right)}{4(\alpha-1)(v-c_n)} \\ \underline{q}_{MH}, \text{ if } \max\{\frac{c_n-c_r}{2}, \frac{(c_r-c_n)\left(\alpha^2(-c_r+2v_r+c_n)+c_r-c_n\right)}{4(\alpha-1)(v-c_n)}\} < k < \bar{k}_3 \\ 1, \text{ if } k > \bar{k}_3 \end{cases}.$$

$\bar{Q}_{1L}$ denotes the upper bound of $\bar{q}$ in region Q_{1L}. It can be derived from rows 4, 8, 12 of Table B4 as

$$\bar{Q}_{1L} = \begin{cases} \frac{(1-\alpha)(v-c_r)}{v_r \alpha}, \text{ if } k < \frac{\alpha(c_n-c_r)}{2} \\ -\frac{4k(c_r+k-v)+\alpha^2(c_r-c_n)^2+4\alpha k(v-c_n)}{4\alpha k v_r}, \text{ if } \frac{\alpha(c_n-c_r)}{2} < k < \min\{\frac{c_n-c_r}{2}, \bar{k}_5\} \\ \frac{\alpha(-c_r+v_r+c_n)-\sqrt{4k(c_r+k-v)+\alpha^2(-c_r+v_r+c_n)^2+4\alpha k(v-c_n)}}{2k}, \text{ if } \bar{k}_5 < k < \frac{c_n-c_r}{2} \end{cases},$$

where $\bar{k}_5 = \frac{1}{2}(-\sqrt{\alpha^2(-c_r^2+2c_r(v_r+c_n)+v^2-2c_n(v+v_r))+2\alpha(c_r-v)(v-c_n)+(c_r-v)^2}+\alpha(c_n-v)+v-c_r)$. Note that for Q_{HH}, $\underline{Q}_{HH} < \bar{q} \le q_h^*$ contradicts $\bar{k}_5 < k < \frac{c_n-c_r}{2}$. Hence, only the first two cases of $\underline{Q}_{1L}$ apply to $\underline{Q}_{HH}$.

Finally, we can easily compare $\bar{q}$ and $q_B^*(\bar{q})$. First, consider $c_n > c_r$. In Q_{MH}, $\bar{q} = q_B^*(\bar{q})$. In Q_{HH}, by definition, $\bar{q} \le q_B^*(\bar{q}) = \frac{\alpha(c_n-c_r)}{2k}$. In Q_{1H} and Q_{1L}, $\bar{q} \le q_B^*(\bar{q}) = 1$. In Q_{HL}, $\bar{q} \le q_B^*(\bar{q}) = \frac{c_n-c_r}{2k}$. In Q_{LL}, $\bar{q} > q_B^*(\bar{q}) = \frac{c_n-c_r}{2k}$. Next, consider $c_n \le c_r$. In Q_{MH}, $\bar{q} = q_B^*(\bar{q})$ as before. In Q_{0L}, $\bar{q} > q_B^*(\bar{q}) = 0$. Hence, the firm cannot obtain

the label given Q_{LL} and Q_{0L}.

B.2.3 Proof of Proposition 3.2

This section solves NGO's optimal label standard $\bar{q}^*$ in the first stage. Given the firm's optimal decisions in the second stage, NGO chooses $\bar{q}$ to maximize her payoff, i.e.,

$$\max_{\bar{q}} \ \Pi(\bar{q})=\begin{cases}\alpha q_B^*(\bar{q}), & \text{if } p_B^*(q_B^*(\bar{q}),\bar{q})=v+v_r\bar{q}\\ q_B^*(\bar{q}), & \text{if } p_B^*(q_B^*(\bar{q}),\bar{q})=v\end{cases}.$$

For a clearer discussion, we first discuss the NGO's optimal label standard by cases in Table B5, where (α,k) space is divided into 11 components. Each component case may be related to multiple subcases where NGO's corresponding payoffs need to be further compared. Note in Table B5,

$$\bar{Q}^*=\begin{cases}1, \text{ if } \frac{c_n-c_r}{2\alpha}<k<\bar{k}_1\\ \min\{\bar{Q}_{HL},q_l^*\} \text{ if } k<\min\{\frac{c_n-c_r}{2\alpha},\bar{k}_1\} \text{ or } \min\{\bar{k}_{MH},\bar{k}_1\}<k<\bar{k}_3\\ \bar{q}_{MH} \text{ if } \bar{k}_1<k<\bar{k}_{MH}\end{cases}, \text{ where } \bar{k}_{MH}=\begin{cases}\bar{k}_2, \text{ if } \alpha<\sqrt{\frac{c_r-c_n}{c_r-c_n-v_r}}\\ \bar{k}_3, \text{ otherwise}\end{cases},$$

$$\bar{k}_1=\tfrac{1}{2}(\alpha(v+v_r-c_r)+c_n-v+\sqrt{(\alpha(c_r-v-v_r)+v-c_r)(\alpha(c_r-v-v_r)+v+c_r-2c_n)}),\ \bar{k}_2=\frac{(c_r-c_n)\left(\alpha^2(-c_r+2v_r+c_n)+c_r-c_n\right)}{4\alpha^2(\alpha-1)(v-c_n)}.$$

Note that $\bar{q}_{MH}$ and $\bar{q}=1$ intersects at $k=\bar{k}_1$, $\underline{q}_{MH}$ and q_h^* intersects at $\alpha^2\bar{k}_2$, $\underline{q}_{MH}$ and q_l^* intersects at $k=\frac{(c_n-c_r)(\alpha(v_r+c_n-c_r)-(c_n-c_r))}{2(v-c_n)(1-\alpha)}$. $\bar{k}_3$ is the right-most k bound for region Q_{MH}. For the fifth case in Table B5, NGO can obtain payoff q_l^* regardless of any $\bar{q}\le 1$, she will set $\bar{q}=q_l^*$ to let the firm obtain the label and benefit consumer surplus. Similar cases occur in the last two cases of Table B5.

Then, we summarize the equilibrium outcomes and combine the conditions in (α,k) space in sets B_{1H}, B_{MH}, B'_{MH}, B_{ML}, B_{HL}, B_{1L}, B'_{1L} and B_{0L} as follows.

$B_{1H}\doteq\{(\alpha,k)\text{: }\alpha>\underline{\alpha}_{1H},\ \underline{k}_{1H}<k\le\bar{k}'_{1H}\}$, where $\underline{k}_{1H}=\begin{cases}\frac{c_n-c_r}{2\alpha}, \text{ if } c_n>c_r\\ 0, \text{ otherwise}\end{cases}$, $\bar{k}'_{1H}=\begin{cases}\bar{k}_1, \text{ if } c_n>c_r\\ \alpha(v+v_r-c_r)-v+c_n, \text{ otherwise}\end{cases}$.

$B_{MH}\doteq\{(\alpha,k)\text{: }c_n>c_r,\ \alpha>\frac{\sqrt{(c_r-v)^2+2v_r(c_n-c_r)}+v-c_n}{-c_r+2(v+v_r)-c_n},\ \bar{k}_1<k\le\bar{k}_{MH}\}$.

$B'_{MH}\doteq\{(\alpha,k)\text{: }c_n\le c_r,\ \alpha>\frac{2(v-c_n)}{2v+v_r-c_r-c_n},\ \alpha(v+v_r-c_r)-v+c_n<k\le\frac{\alpha^2(-c_r+v_r+c_n)^2}{4(1-\alpha)(v-c_n)}\}$.

$B_{ML}\doteq\{(\alpha,k)\text{: }c_n>c_r,\ k>\frac{(c_n-c_r)(\alpha(v_r+c_n-c_r)-(c_n-c_r))}{2(v-c_n)(1-\alpha)},\ (\frac{c_n-c_r}{2}<k\le\frac{c_n-c_r}{2\alpha}\ ||\ k>\max\{\frac{c_n-c_r}{2\alpha},\bar{k}_1,\bar{k}_{MH}\})\}$.

$B_{HL}\doteq\{(\alpha,k)\text{: }c_n>c_r,\ k\le\frac{(c_n-c_r)(\alpha(v_r+c_n-c_r)-(c_n-c_r))}{2(v-c_n)(1-\alpha)},\ (\frac{c_n-c_r}{2}<k\le\frac{c_n-c_r}{2\alpha}\ ||\ k>\max\{\frac{c_n-c_r}{2\alpha},\bar{k}_1,\bar{k}_{MH}\})\}$.

$B_{1L}\doteq\{(\alpha,k)\text{: }c_n>c_r,\ \alpha\le\tilde{\alpha},\ k\le\frac{c_n-c_r}{2})\}$.

$B'_{1L}\doteq\{(\alpha,k)\text{: }c_n>c_r,\ \alpha>\tilde{\alpha},\ k\le\frac{c_n-c_r}{2})\}$.

$B_{0L}\doteq\{(\alpha,k)\text{: }c_n\le c_r,\ k>\underline{k}_{0L}\}$, where $\underline{k}_{0L}=\begin{cases}\alpha(v+v_r-c_r)-v+c_n), \text{ if } \alpha\le\frac{2(v-c_n)}{2v+v_r-c_r-c_n}\\ \frac{\alpha^2(-c_r+v_r+c_n)^2}{4(1-\alpha)(v-c_n)}, \text{ otherwise}\end{cases}$.

The corresponding label decisions $(\bar{q}^*)$ are 1, $\bar{q}_{MH}$, $\bar{q}'_{MH}$, q_l^*, $\bar{q}_{HL}$, 1, $\bar{q}_{1L}$, $(0,1]$,

respectively. In particular, $\bar{q}_{MH}$, $\bar{q}'_{MH}$ are referred to Section B.2.2 and

$$\bar{q}_{HL}=\begin{cases}\frac{(1-\alpha)\left((1+\alpha)(c_r-c_n)^2+4k(v-w)\right)}{4\alpha k v_r}, \text{ if } (\alpha,k)\in B_{HL} \text{ and } k\leq\frac{(c_r-c_n)\left(\alpha^2(-c_r+2v_r+c_n)+c_r-c_n\right)}{4(\alpha-1)(v-c_n)}\\ \underline{q}_{MH}, \text{ if } (\alpha,k)\in B_{HL} \text{ and } k>\frac{(c_r-c_n)\left(\alpha^2(-c_r+2v_r+c_n)+c_r-c_n\right)}{4(\alpha-1)(v-c_n)}\end{cases},$$

which includes the first two cases of $\bar{Q}_{HL}$.

$$\bar{q}_{1L}=\begin{cases}\frac{(1-\alpha)(v-c_r)}{v_r\alpha}, \text{ if } (\alpha,k)\in B'_{1L} \text{ and } k<\frac{(c_n-c_r)\alpha}{2}\\ -\frac{4k(c_r+k-v)+\alpha^2(c_r-c_n)^2+4\alpha k(v-c_n)}{4\alpha k v_r}, \text{ if } (\alpha,k)\in B'_{1L} \text{ and } \frac{(c_n-c_r)\alpha}{2}<k\leq\bar{k}_5\\ \frac{\alpha(-c_r+v_r+c_n)-\sqrt{4k(c_r+k-v)+\alpha^2(-c_r+v_r+c_n)^2+4\alpha k(v-c_n)}}{2k}, \text{ if } (\alpha,k)\in B'_{1L} \text{ and } k>\bar{k}_5\end{cases},$$

which coincides with $\bar{Q}_{1L}$. The results in proposition 2 then immediately follow.

B.2.4 Proof of Proposition 3.3

By Proposition 3.2, we can easily compare $\bar{q}^*$ and q_B^*. For Proposition 3.3(1): In B_{0L}, $\bar{q}^* > q_B^* = 0$ since here $\bar{q}^* \in (0, 1]$. For Proposition 3.3(2): In B_{HL}, by the analysis in Section B.2.3, $\bar{q}_{HL}(\subset \bar{Q}_{HL}) < q_B^*$. In B'_{1L}, by Section B.2.3, $\bar{q}_{1L}(\subset \bar{Q}_{1L}) < q_B^* = 1$. For Proposition 3.3(3): When $c_n > c_r$, in B_{1H}, B_{MH}, B_{ML}, B_{1L}, obviously $\bar{q}^* = q_B^*$. When $c_n \leq c_r$, in B_{1H} and B'_{MH}, $\bar{q}^* = q_B^*$.

B.2.5 Proof of Corollary 3.2

For Corollary 3.2(1): By Proposition 3.2, we can easily verify $\frac{\partial \bar{q}^*}{\partial \alpha} > 0$ if $(\alpha, k) \in B_{MH} \cup B'_{MH}$, $\frac{\partial \bar{q}^*}{\partial \alpha} < 0$ if $(\alpha, k) \in B_{HL} \cup B'_{1L}$ and $\frac{\partial \bar{q}^*}{\partial \alpha} = 0$ otherwise. Hence, the optimal label standard $\bar{q}^*$ may increase or decrease in α. We can also verify $\frac{\partial \bar{q}^*}{\partial k} < 0$ if $(\alpha, k) \in B_{MH} \cup B'_{MH} \cup B_{ML}$ or if $(\alpha, k) \in B'_{1L}$ and $k > \frac{(c_n-c_r)\alpha}{2}$, and $\frac{\partial \bar{q}^*}{\partial k} = 0$ otherwise. We see $\bar{q}^*$ weakly decreases in k in each individual region. In addition, $\bar{q}^* < \frac{c_n-c_r}{2k}$ when $(\alpha, k) \in B_{HL}$ and $\bar{q}^* = 1$ when $(\alpha, k) \in B_{1H}$. One can easily verify $\frac{c_n-c_r}{2k} < 1$ at the boundary $(\alpha, k) \in B_{1H} \cap B_{HL}$. Then, $\bar{q}^*$ increases as k increases from B_{HL} to B_{1H}. Hence, $\bar{q}^*$ may increase or decrease in k.

For Corollary 3.2(2): By Proposition 3.2, we can verify $\frac{\partial q_B^*}{\partial \alpha} > 0$ if $(\alpha, k) \in B_{MH} \cup B'_{MH}$ and $\frac{\partial q_B^*}{\partial \alpha} = 0$ otherwise. Hence, the firm's optimal recycled content q_B^* weakly increases in α. Moreover, $\frac{\partial q_B^*}{\partial k} < 0$ if $(\alpha, k) \in B_{MH} \cup B_{ML} \cup B_{HL} \cup B'_{MH}$ and $\frac{\partial q_B^*}{\partial k} = 0$ otherwise. However, similar to $\bar{q}^*$, $q_B^* = \frac{c_n-c_r}{2k}$ in region B_{HL}, which is smaller than $q_B^* = 1$ in region B_{1H}. Then, q_B^* increases as k increases from B_{HL} to B_{1H}. Hence, q_B^* may increase or decrease in k.

For Corollary 3.2(3): Let $\Pi_B^* \doteq \Pi_B^*(\bar{q}^*)$ denote the NGO's optimal payoff and $\pi_B^* \doteq \pi_B^*(p_B^*(\bar{q}^*), q_B^*(\bar{q}^*))$ the firm's optimal profit. By Proposition 3.2, we obtain

equation (B.1) below. Then, we can verify $i)$ $\frac{\partial \pi_B^*}{\partial \alpha} > 0$, if $(\alpha, k) \in B_{1H}$ and $\frac{\partial \pi_B^*}{\partial \alpha} = 0$ otherwise; $ii)$ $\frac{\partial \pi_B^*}{\partial k} < 0$ if $(\alpha, k) \notin B_{MH}^{'} \cup B_{0L}$ and $\frac{\partial \pi_B^*}{\partial k} = 0$ otherwise. Hence, the firm's optimal profit weakly increases in α and weakly decreases in k. Moreover, we can also verify $i)$ $\frac{\partial \Pi_B^*}{\partial \alpha} > 0$ if $(\alpha, k) \in B_{1H} \cup B_{MH} \cup B_{MH}^{'}$ and $\frac{\partial \Pi_B^*}{\partial \alpha} = 0$ otherwise; $ii)$ $\frac{\partial \Pi_B^*}{\partial k} < 0$, if $(\alpha, k) \in B_{MH} \cup B_{MH}^{'}$ and $\frac{\partial \Pi_B^*}{\partial k} = 0$ otherwise. Hence, NGO's optimal payoff weakly increases in α and weakly decreases in k.

$$(\pi_B^*,\Pi_B^*)=\begin{cases}(\alpha(v+v_r-c_r)-k,\alpha), & (\alpha,k)\in B_{1H}\\ (\frac{(c_n-c_r)^2+4k(v-c_n)}{4k}, \frac{\alpha^2(v_r-c_r+c_n)+\alpha\sqrt{\alpha^2(v_r-c_r+c_n)^2+4k(v-c_n)(\alpha-1)-(c_n-c_r)^2}}{2k}), & (\alpha,k)\in B_{MH}\\ (v-c_n, \frac{\alpha^2(v_r-c_r+c_n)+\alpha\sqrt{\alpha^2(v_r-c_r+c_n)^2+4k(v-c_n)(\alpha-1)}}{2k}), & (\alpha,k)\in B_{MH}^{'}\\ (\frac{(c_n-c_r)^2+4k(v-c_n)}{4k}, \frac{c_n-c_r}{2k}), & (\alpha,k)\in B_{ML}\cup B_{HL}\\ (v-c_r-k,1), & (\alpha,k)\in B_{1L}\cup B_{1L}^{'}\\ (v-c_n,0), & (\alpha,k)\in B_{0L}\end{cases}. \tag{B.1}$$

B.3 Comparison Under the Two Labels

B.3.1 Proof of Proposition 3.4

We present the proof in two parts. In the first part, we compare q_P^* and q_B^* following Propositions 3.1 and 3.2. The comparison is valid in the following non-empty regions: When $c_n > c_r$, there are $B_{1H} \cap P_{1H}$, $B_{1H} \cap P_{HH}$, $B_{MH} \cap P_{HH}$, $B_{ML} \cap P_{HH}$, $B_{ML} \cap P_{LL}$, $B_{ML} \cap P_{1H}$, $B_{HL} \cap P_{1H}$, $B_{1L}^{'} \cap P_{1H}$, $B_{1L} \cap P_{1L}$; When $c_n \leq c_r$, there are $B_{1H} \cap P_{1H}$, $B_{1H} \cap P_{HH}$, $B_{MH}^{'} \cap P_{HH}$, $B_{0L} \cap P_{0L}$. Otherwise, the intersection is empty. Then, the comparison is given below.

First, when $c_n > c_r$: (1) $B_{1H} \cap P_{1H}$, $q_P^* = q_B^* = 1$. (2) $B_{1H} \cap P_{HH}$, $q_P^* = \frac{\alpha(v_r+c_n-c_r)}{2k} < q_B^* = 1$ since $k > \frac{1}{2}\alpha(c_n + v_r - c_r)$ by the definition of P_{HH}. (3) $B_{MH} \cap P_{HH}$, $q_B^* - q_P^* = \frac{\sqrt{\alpha^2(v_r-c_r+c_n)^2+4k(v-c_n)(\alpha-1)-(c_n-c_r)^2}}{2k} > 0$, hence $q_P^* < q_B^*$. (4) $B_{ML} \cap P_{HH}$, $q_P^* - q_B^* = \frac{\alpha v_r}{2k} > 0$, hence $q_P^* > q_B^*$. (5) $B_{ML} \cap P_{LL}$, $q_P^* = q_B^* = \frac{c_n-c_r}{2k}$. (6) $(B_{ML} \cup B_{HL}) \cap P_{1H}$, $q_B^* = \frac{c_n-c_r}{2k} < q_P^* = 1$ since $k > \frac{c_n-c_r}{2}$ by the definition of B_{ML} and B_{HL}. (7) $B_{1L}^{'} \cap P_{1H}$, $q_B^* = q_P^* = 1$. (8) $B_{1L} \cap P_{1L}$, $q_B^* = q_P^* = 1$. Proposition 3.4(2) follows.

Then, when $c_n \leq c_r$: The first two cases are the same as above. For $B_{MH}^{'} \cap P_{HH}$, $q_B^* - q_P^* = \frac{\sqrt{\alpha^2(v_r-c_r+c_n)^2+4k(v-c_n)(\alpha-1)}}{2k} > 0$, hence $q_P^* < q_B^*$. For $B_{0L} \cap P_{0L}$, $q_B^* = q_P^* = 0$. Proposition 3.4(1) follows.

In the second part, we compare the firm's profits as well as the NGO's payoffs under the binary label and the percentage label. First, given equations (3.2) and (B.1), the profit comparison is shown in Table B6. We only show the results where the intersection of any pair of P_{ij} and $B_{i'j'}$ is non-empty. When the intersection is empty, the case is trivial that the firm only has one choice, either the percentage label or the binary label. Next, given equations (3.2) and (B.1), we compare the NGO's payoffs under the two labels and summarize the results in Table B7.

By the definition of the regions and the results shown in Table 10 and 11, we can easily find the firm prefers the percentage label while NGO prefers the binary label when $c_n \leq c_r$ and $(\alpha, k) \in P_{HH} = (B_{1H} \cup B'_{MH}) \cap P_{HH}$, or when $c_n > c_r$ and $(\alpha, k) \in (B_{MH} \cup B'_{1L} \cup B_{ML} \cup B_{HL}) \cap (P_{HH} \cup P_{1H})$. Otherwise, they are both indifferent in two labels. Hence, we conclude that the firm weakly prefers the percentage label while NGO weakly prefers the binary label.

B.3.2 Proof of Proposition 3.5

We first show the consumer surplus under each label given (α, k) and then compare them under the two labels. First and foremost, environmentally unconscious consumers exit the market if the product has a high price (i.e., $p = v + v_r q$ or $p = v + v_r \bar{q}$), or pay the same with their valuation for the product if the product has a low price (i.e., $p = v$). Hence, these consumers cannot obtain positive surplus. By contrast, the environmentally conscious consumers pay the same with their valuation for the product when the product is labeled and the price is high, where they have zero surplus. When the product has a low price, each of these consumers obtains surplus $v_r q$ if a percentage label is applied or $v_r \bar{q}$ if a binary label is applied. Hence, the aggregate consumer surplus is either $\alpha v_r q$ or $\alpha v_r \bar{q}$. In summary, given α and k, we have

$$CS_P^*(p_P^*, q_P^*) = \begin{cases} \alpha v_r \frac{c_n - c_r}{2k}, & \text{if } (\alpha, k) \in P_{LL} \\ \alpha v_r, & \text{if } (\alpha, k) \in P_{1L} \\ 0, & \text{otherwise} \end{cases}, \quad CS_B^*(p_B^*, \bar{q}_B^*) = \begin{cases} \alpha v_r \frac{c_n - c_r}{2k}, & \text{if } (\alpha, k) \in B_{ML} \\ \alpha v_r \bar{q}_{HL}, & \text{if } (\alpha, k) \in B_{HL} \\ \alpha v_r, & \text{if } (\alpha, k) \in B_{1L} \\ \alpha v_r \bar{q}_{1L}, & \text{if } (\alpha, k) \in B'_{1L} \\ 0, & \text{otherwise} \end{cases},$$

where $CS_P^*(p_P^*, q_P^*)$ and $CS_B^*(p_B^*, \bar{q}_B^*)$ describe the consumer surplus under the percentage label and the binary label, respectively.

We then check the consumer surplus in three components of (α, k) space: $(\alpha, k) \in (B_{1H} \cup B_{MH} \cup B'_{MH}) \cap (P_{1H} \cup P_{HH})$, wherein the firm sets a high price under both labels; $(\alpha, k) \in (B_{ML} \cup B_{HL} \cup B_{1L} \cup B'_{1L}) \cap (P_{1H} \cup P_{HH})$, wherein the firm sets a low price under the binary label and a high price under a percentage label; $(\alpha, k) \in (B_{ML} \cup B_{HL} \cup B_{1L}) \cap (P_{LL} \cup P_{1L})$, wherein the firm sets a low price under both labels. Then, one can easily verify that $CS_P^* = CS_B^*$ for the following cases: $(\alpha, k) \in (B_{1H} \cup B_{MH} \cup B'_{MH}) \cap (P_{1H} \cup P_{HH})$, $CS_P^* = CS_B^* = 0$; $(\alpha, k) \in (B_{ML} \cup B_{HL}) \cap P_{LL}$, $CS_P^* = CS_B^* = \alpha v_r \frac{c_n - c_r}{2k}$; $(\alpha, k) \in B_{1L} \cap P_{1L}$, $CS_P^* = CS_B^* = \alpha v_r$. The remaining component is $(\alpha, k) \in (B_{ML} \cup B_{HL} \cup B_{1L} \cup B'_{1L}) \cap (P_{1H} \cup P_{HH})$, one can check in this case $CS_P^* = 0$ while $CS_B^* > 0$.

B.3.3 Proof of Corollary 3.3

By Proposition 3.5, we can easily verify that *i)* $\frac{\partial CS_P^*}{\partial \alpha} > 0$, if $(\alpha, k) \in P_{LL} \cup P_{1L}$; $\frac{\partial CS_P^*}{\partial \alpha} = 0$ otherwise; *ii)* $\frac{\partial CS_P^*}{\partial k} < 0$, if $(\alpha, k) \in P_{LL}$; $\frac{\partial CS_P^*}{\partial k} = 0$ otherwise. Hence, when $c_n \leq c_r$, CS_P^* is not influenced by α and k, see Corollary 3.3(1). When $c_n > c_r$, a visualization is shown in Figure B.1. One can check $CS_P^* = 0$ when $(\alpha, k) \in P_{1H}$ and $CS_P^* = \alpha v_r \frac{c_n - c_r}{2k}$ when $(\alpha, k) \in P_{LL}$. Since $\alpha v_r \frac{c_n - c_r}{2k} > 0$, when α increases from P_{LL} to P_{1H}, CS_P^* decreases. Hence, CS_P^* increases in α when $(\alpha, k) \in P_{LL} \cup P_{1L}$ and weakly decreases otherwise; When k increases from P_{1H} to P_{LL}, CS_P^* increases. Hence, CS_P^* decreases in k when $(\alpha, k) \in P_{LL}$ and weakly increases otherwise, see Corollary 3.3(2).

Moreover, we can verify that *i)* $\frac{\partial CS_B^*}{\partial \alpha} > 0$, if $(\alpha, k) \in B_{ML} \cup B_{1L}$; $\frac{\partial CS_B^*}{\partial \alpha} < 0$, if $(\alpha, k) \in B_{HL} \cup B'_{1L}$; $\frac{\partial CS_B^*}{\partial \alpha} = 0$ otherwise; *ii)* $\frac{\partial CS_B^*}{\partial k} < 0$, if $(\alpha, k) \in (B_{ML} \cup B_{HL}) \cup (B_{1L}$ & $k > \frac{(c_n - c_r)\alpha}{2})$; $\frac{\partial CS_B^*}{\partial k} = 0$ otherwise. Hence, when $c_n \leq c_r$, CS_B^* is not influenced by α and k, see Corollary 3.3(1). When $c_n > c_r$, a visualization is shown in Figure B.2. One can check $CS_B^* = 0$ when $(\alpha, k) \in B_{1H} \cup B_{MH}$ and $CS_B^* > 0$ when $(\alpha, k) \in B_{ML} \cup B_{HL}$. By the similar reason discussed for CS_P^*, as α increases, CS_B^* increases when $(\alpha, k) \in B_{ML} \cup B_{1L}$ and weakly decreases otherwise; As k increases, CS_B^* weakly increases when $(\alpha, k) \in B_{1H} \cup B_{MH}$ and weakly decreases otherwise,

see Corollary 3.3(2). The above results are summarized in Corollary 3.3.

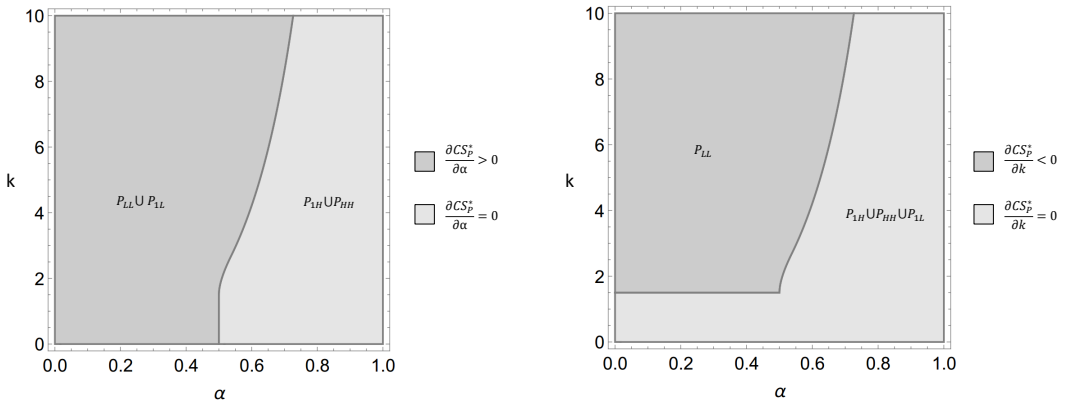

(a) The Sensitivity with Respect to α (b) The Sensitivity with Respect to k

Figure B.1: The Sensitivity of Consumer Surplus with Percentage Label.
Note: $c_n = 4, c_r = 1, v = 8, v_r = 7$

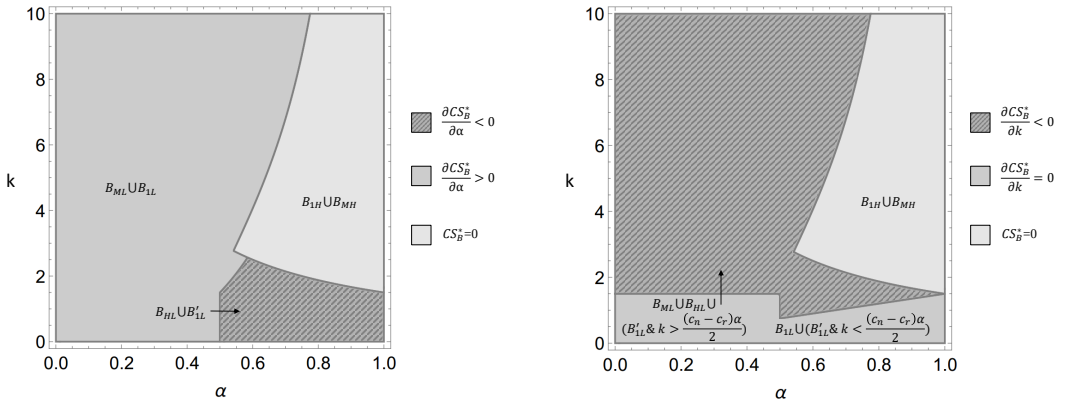

(a) The Sensitivity with Respect to α (b) The Sensitivity with Respect to k

Figure B.2: The Sensitivity of Consumer Surplus with Binary Label.
Note: $c_n = 4, c_r = 1, v = 8, v_r = 7$

Table B4: Comparison of the Firm's Profit by Cases Given Binary Label $\bar{q}$

Case1	Case2	$Q_{case1} \cap Q_{case2}$	$\pi_{case1} - \pi_{case2}$	q_B^*
$h1$	$l1$	$\{(\alpha, k, \bar{q}) : c_n < c_r, \alpha > \tilde{\alpha}, \bar{q}_{h1}^1 < \bar{q} < \tilde{q}\}$	< 0	0
$h1$	$l2$	$\emptyset$	NA	NA
$h1$	$l3$	$\{(\alpha, k, \bar{q}) : \alpha > \frac{\sqrt{(c_r-v)^2+4v_r(v-c_n)}+c_r+v-2c_n}{2(c_r-v_r-c_n)}, \frac{c_n-c_r}{2} < k < \tilde{k}_{h1}, \tilde{q} < \bar{q} < \bar{q}_{h1}^2\}$	< 0	q_l^*
$h1$	$l4$	$\{(\alpha, k, \bar{q}) : \alpha > \tilde{\alpha}, (k < \frac{\alpha(c_n-c_r)}{2}, \tilde{q} < \bar{q} < \bar{q}_{h1}^1) \ \|\| \ (\frac{\alpha(c_n-c_r)}{2} < k < \min\{\tilde{k}_{h1}, \frac{c_n-c_r}{2}\}, \tilde{q} < \bar{q} < \bar{q}_{h1}^2)\}$	< 0	1
$h2$	$l1$	$\{(\alpha, k, \bar{q}) : c_n < c_r, \alpha > \tilde{\alpha}, \bar{q} > \tilde{q}\}$	> 0 if $\underline{q}'_{MH} < \bar{q} < \min\{1, \bar{q}'_{MH}\}$ and $v_r > c_r - c_n$	$\bar{q}$
			< 0 otherwise	0
$h2$	$l2$	$\{(\alpha, k, \bar{q}) : c_n > c_r, \alpha > \tilde{\alpha}, \frac{\alpha(c_n-c_r)}{2} < k, \bar{q} > \max\{\tilde{q}, q_l^*\}\}$	> 0 if $\underline{q}_{MH} < \bar{q} < \min\{1, \bar{q}_{MH}\}$ and $k < \bar{k}_3$	$\bar{q}$
			< 0 otherwise	q_l^*
$h2$	$l3$	$\{(\alpha, k, \bar{q}) : c_n > c_r, \alpha > \tilde{\alpha}, \frac{\alpha(c_n-c_r)}{2} < k, \max\{\tilde{q}, q_h^*\} < \bar{q} < \min\{\bar{q}_{l1}, q_l^*\}\}$	> 0 if $\underline{q}_{MH} < \bar{q} < \min\{1, \bar{q}_{MH}\}$ and $k < \bar{k}_3$	$\bar{q}$
			< 0 otherwise	q_l^*
$h2$	$l4$	$\{(\alpha, k, \bar{q}) : c_n > c_r, \tilde{\alpha} < \alpha < \frac{\sqrt{(v-c_r)(-c_r+v+4v_r)}+c_r-v}{2v_r}, \frac{\alpha^2 v_r(c_n-c_r)}{2(\alpha-1)(c_r-v)} < k < \frac{c_n-c_r}{2}, \max\{\tilde{q}, q_h^*\} < \bar{q} < \bar{q}_{h1}^1\}$	> 0 if $\bar{q} > \frac{\alpha(-c_r+v_r+c_n)}{2k} - \frac{\sqrt{4k(c_r+k-v)+\alpha^2(-c_r+v_r+c_n)^2+4\alpha k(v-c_n)}}{2k}$	$\bar{q}$
			< 0 otherwise	1
$h3$	$l1$	$\emptyset$	NA	NA
$h3$	$l2$	$\emptyset$	NA	NA
$h3$	$l3$	$\{(\alpha, k, \bar{q}) : c_n > c_r, \alpha > \tilde{\alpha}, \frac{c_n-c_r}{2} < k < \tilde{k}_{h1}, \bar{q}_{h1}^2 < \bar{q} < \min\{q_h^*, \bar{q}_{l1}\}\}$	> 0 if $\bar{q} > \frac{(1-\alpha)\left((1+\alpha)(c_r-c_n)^2+4k(v-c_n)\right)}{4\alpha k v_r}$	q_h^*
			< 0 otherwise	q_l^*
$h3$	$l4$	$\{(\alpha, k, \bar{q}) : c_n > c_r, \alpha > \tilde{\alpha}, \frac{\alpha(c_n-c_r)}{2} < k < \min\{\frac{c_n-c_r}{2}, \tilde{k}_{h1}\}, \bar{q}_{h1}^2 < \bar{q} < \min\{q_h^*, \bar{q}_{h1}^1]\}$	> 0 if $\bar{q} > -\frac{4k(c_r+k-v)+\alpha^2(c_r-c_n)^2+4\alpha k(v-c_n)}{4\alpha k v_r}$	q_h^*
			< 0 otherwise	1
$h4$	$l1$	$\emptyset$	NA	NA
$h4$	$l2$	$\emptyset$	NA	NA
$h4$	$l3$	$\emptyset$	NA	NA
$h4$	$l4$	$\emptyset$	NA	NA

Table B5: Summary of the NGO's Decision by Cases

Cases	Subcases	$q_B^*(\bar{q})$	$\bar{q}$	Π^*	$\bar{q}^*$
$c_n < c_r$, $v_r < c_r - c_n$	Q_{0L}	0	≤ 1	0	$(0,1]$
$c_n < c_r$, $v_r > c_r - c_n$, $k < \alpha(v + v_r - c_r) - v + c_n$	Q_{MH}	$\bar{q}$	≤ 1	α	1
	Q_{0L}	0	≤ 1	0	
$c_n < c_r$, $v_r > c_r - c_n$, $\alpha > \frac{2(v-c_n)}{2v+v_r-c_r-c_n}$, $\alpha(v + v_r - c_r) - v + c_n < k < \frac{\alpha^2(-c_r+v_r+c_n)^2}{4(1-\alpha)(v-c_n)}$	Q_{MH}	$\bar{q}$	$\leq \bar{q}'_{MH}$	$\alpha\bar{q}'_{MH}$	$\bar{q}'_{MH}$
	Q_{0L}	0	≤ 1	0	
$c_n < c_r$, $v_r > c_r - c_n$, ($\alpha < \frac{2(v-c_n)}{2v+v_r-c_r-c_n}$, $k > \alpha(v + v_r - c_r) - v + c_n$) $\|\|$ ($\alpha > \frac{2(v-c_n)}{2v+v_r-c_r-c_n}$, $k > \frac{\alpha^2(-c_r+v_r+c_n)^2}{4(1-\alpha)(v-c_n)}$)	Q_{0L}	0	≤ 1	0	$(0,1]$
$c_n > c_r$, $\alpha < \tilde{\alpha}$, $k > \frac{c_n-c_r}{2}$	Q_{HL}	q_l^*	≤ 1	q_l^*	q_l^*
	Q_{LL}	q_l^*	≤ 1	q_l^*	
$c_n > c_r$, $\alpha < \tilde{\alpha}$, $k < \frac{c_n-c_r}{2}$	Q_{1L}	1	≤ 1	1	1
$c_n > c_r$, $\alpha > \tilde{\alpha}$, $k < \frac{\alpha(c_n-c_r)}{2}$	Q_{1H}	1	≤ 1	α	$\bar{Q}_{1L}$
	Q_{1L}	1	$\leq \bar{Q}_{1L}$	1	
$c_n > c_r$, $\alpha > \tilde{\alpha}$, $\frac{\alpha(c_n-c_r)}{2} < k < \min\{\frac{c_n-c_r}{2}, \bar{k}_5\}$	Q_{MH}	$\bar{q}$	$\leq \bar{Q}_{MH}$	$\alpha\bar{Q}_{MH}$	$\bar{Q}_{1L}$
	Q_{HH}	q_h^*	$\leq q_h^*$	αq_h^*	
	Q_{1L}	1	$\leq \bar{Q}_{1L}$	1	
$c_n > c_r$, $\alpha > \tilde{\alpha}$, $\bar{k}_5 < k < \frac{c_n-c_r}{2}$	Q_{MH}	$\bar{q}$	$\leq \bar{Q}_{MH}$	$\alpha\bar{Q}_{MH}$	$\bar{Q}_{1L}$
	Q_{1L}	1	$\leq \bar{Q}_{1L}$	1	
$c_n > c_r$, $\alpha > \tilde{\alpha}$, $\frac{c_n-c_r}{2} < k < \bar{k}_3$	Q_{MH}	$\bar{q}$	$\leq \bar{Q}_{MH}$	$\alpha\bar{Q}_{MH}$	$\bar{Q}^*$
	Q_{HH}	q_h^*	$\leq q_h^*$	αq_h^*	
	Q_{HL}	q_l^*	$\leq \bar{Q}_{HL}$	q_l^*	
	Q_{LL}	q_l^*	$\leq \bar{Q}_{HL}$	q_l^*	
$c_n > c_r$, $\alpha > \tilde{\alpha}$, $k > \bar{k}_3$	Q_{HL}	q_l^*	$\leq \bar{Q}_{HL}$	q_l^*	q_l^*
	Q_{LL}	q_l^*	$\leq \bar{Q}_{HL}$	q_l^*	

Table B6: Summary of the Comparison of the Firm's Profits

Region	$\pi_B^* - \pi_P^*$	Firm's preference	Region	$\pi_B^* - \pi_P^*$	Firm's preference
$B_{1H} \cap P_{1H}$	$= 0$	indifferent	$B_{1H} \cap P_{HH}$	≤ 0	percentage
$B_{MH} \cap P_{HH}$	≤ 0	percentage	$B'_{MH} \cap P_{HH}$	≤ 0	percentage
$(B_{ML} \cup B_{HL}) \cap P_{HH}$	≤ 0	percentage	$(B_{ML} \cup B_{HL}) \cap P_{LL}$	$= 0$	indifferent
$(B_{ML} \cup B_{HL}) \cap P_{1H}$	≤ 0	percentage	$B_{1L} \cap P_{1L}$	$= 0$	indifferent
$B'_{1L} \cap P_{1H}$	≤ 0	percentage	$B_{0L} \cap P_{0L}$	$= 0$	indifferent

Table B7: Summary of the Comparison of the NGO's Payoffs

Region	$\Pi_B^* - \Pi_P^*$	NGO's preference	Region	$\Pi_B^* - \Pi_P^*$	NGO's preference
$B_{1H} \cap P_{1H}$	$= 0$	indifferent	$B_{1H} \cap P_{HH}$	≥ 0	binary
$B_{MH} \cap P_{HH}$	≥ 0	binary	$B'_{MH} \cap P_{HH}$	≥ 0	binary
$B_{ML} \cap P_{HH}$	≥ 0	binary	$(B_{ML} \cup B_{HL}) \cap P_{LL}$	$= 0$	indifferent
$B_{HL} \cap P_{HH}$	≥ 0	binary	$(B_{ML} \cup B_{HL}) \cap P_{1H}$	≥ 0	binary
$B_{1L} \cap P_{1L}$	$= 0$	indifferent	$B'_{1L} \cap P_{1H}$	≥ 0	binary
$B_{0L} \cap P_{0L}$	$= 0$	indifferent			

References

Alev, I., Agrawal, V. V., and Atasu, A. (2020). Extended producer responsibility for durable products. *Manufacturing & Service Operations Management*, 22(2):364–382.

Amaran, S., Sahinidis, N. V., Sharda, B., and Bury, S. J. (2016). Simulation optimization: a review of algorithms and applications. *Annals of Operations Research*, 240(1):351–380.

Atasu, A. and Souza, G. C. (2013). How does product recovery affect quality choice? *Production and Operations Management*, 22(4):991–1010.

Atasu, A. and Subramanian, R. (2012). Extended producer responsibility for e-waste: Individual or collective producer responsibility? *Production and Operations Management*, 21(6):1042–1059.

Atasu, A. and Van Wassenhove, L. N. (2012). An operations perspective on product take-back legislation for e-waste: Theory, practice, and research needs. *Production and Operations Management*, 21(3):407–422.

Atasu, A., Van Wassenhove, L. N., and Sarvary, M. (2009). Efficient take-back legislation. *Production and Operations Management*, 18(3):243–258.

Bain & Company (2018). *Transforming Business for a Sustainable Economy*. https://www.bain.com/contentassets/d72f85af23564454970916d56eb4b5b4/bain_brief_transforming_business_for_a_sustainable_economy.pdf, accessed: January 12, 2022.

Benjaafar, S., Jiang, D., Li, X., and Li, X. (2022). Dynamic inventory repositioning in on-demand rental networks. *Management Science. Forthcoming.*

Biddle, D. (1993). Recycling for Profit: The New Green Business Frontier. *https:*

//hbr.org/1993/11/recycling-for-profit-the-new-green-business-frontier, accessed: December 30, 2020.

Bird (2020). Vehicle Payouts. https://help.bird.co/hc/en-us/articles/360024946572-Vehicle-Payouts/, accessed: January 27, 2022.

Birge, J. R. and Louveaux, F. (2011). Introduction to Stochastic Programming. *Springer.*

Boyacı, B., Zografos, K. G., and Geroliminis, N. (2015). An optimization framework for the development of efficient one-way car-sharing systems. European Journal of Operational Research, *240(3):718–733.*

Chang, J., Yu, M., Shen, S., and Xu, M. (2017). Location design and relocation of a mixed car-sharing fleet with a CO2 emission constraint. Service Science, *9(3):205–218.*

Chen, C. (2001). Design for the environment: A quality-based model for green product development. Management Science, *47(2):250–263.*

Chen, C. and Liu, L. Q. (2014). Pricing and quality decisions and financial incentives for sustainable product design with recycled material content under price leadership. International Journal of Production Economics, *147:666–677.*

Chen, L. and Lee, H. L. (2017). Sourcing under supplier responsibility risk: The effects of certification, audit, and contingency payment. Management Science, *63(9):2795–2812.*

Citi Bike (2021). https://citibikenyc.com/homepage. https://new.mta.info/agency/new-york-city-transit/subway-bus-ridership-2019, accessed: January 27, 2022.

Debo, L. G., Toktay, L. B., and Van Wassenhove, L. N. (2005). Market segmentation and product technology selection for remanufacturable products. Management Science, *51(8):1193–1205.*

Dell'Amico, M., Hadjicostantinou, E., Iori, M., and Novellani, S. (2014). The bike sharing rebalancing problem: Mathematical formulations and benchmark instances. Omega, *45:7–19.*

Drake, D. F. and Spinler, S. (2013). Om forum—sustainable operations manage-

ment: An enduring stream or a passing fancy? Manufacturing & Service Operations Management, *15(4):689–700.*

Esenduran, G. and Kemahlıoğlu-Ziya, E. (2015). A comparison of product take-back compliance schemes. Production and Operations Management, *24(1):71–88.*

Esenduran, G., Lin, Y.-T., Xiao, W., and Jin, M. (2020). Choice of electronic waste recycling standard under recovery channel competition. Manufacturing & Service Operations Management, *22(3):495–512.*

European Commision (2019). Report on the implementation of the Circular Economy Action Plan. *https://ec.europa.eu/transparency/regdoc/rep/1/2019/EN/COM-2019-190-F1-EN-MAIN-PART-1.PDF*, *accessed: September 1, 2020.*

Fatehi, S. and Wagner, M. R. (2022). Crowdsourcing last-mile deliveries. Manufacturing & Service Operations Management, *24(2):791–809.*

Feng, G., Kong, G., and Wang, Z. (2021). We are on the way: Analysis of on-demand ride-hailing systems. Manufacturing & Service Operations Management, *23(5):1237–1256.*

Fischer, C. and Lyon, T. P. (2014). Competing environmental labels. Journal of Economics & Management Strategy, *23(3):692–716.*

Fischer, C. and Lyon, T. P. (2019). A theory of multitier ecolabel competition. Journal of the Association of Environmental and Resource Economists, *6(3):461–501.*

Freund, D., Norouzi-Fard, A., Paul, A., Wang, C., Henderson, S. G., and Shmoys, D. B. (2020). Data-driven rebalancing methods for bike-share systems. In Analytics for the Sharing Economy: Mathematics, Engineering and Business Perspectives, *pages 255–278. Springer.*

Fricker, C. and Gast, N. (2016). Incentives and redistribution in homogeneous bike-sharing systems with stations of finite capacity. EURO Journal on Transportation and Logistics, *5(3):261–291.*

Fu, C., Zhu, N., Ma, S., and Liu, R. (2022). A two-stage robust approach to

integrated station location and rebalancing vehicle service design in bike-sharing systems. European Journal of Operational Research, *298(3):915–938.*

Garella, P. G. and Petrakis, E. (2008). Minimum quality standards and consumers' information. Economic Theory, *36(2):283–302.*

Goman, C. (2021). Guide to Recycling Aluminum for Businesses. *https://businessinsights.org/guide-to-recycling-aluminum-for-businesses/, accessed: December 30, 2021.*

Grahovac, J. and Chakravarty, A. (2001). Sharing and lateral transshipment of inventory in a supply chain with expensive low-demand items. Management Science, *47(4):579–594.*

GreenCircle Certified (2019). Recycled Content Certification. *http://www.greencirclecertified.com/recycled-content-certification, accessed: December 30, 2020.*

Gui, L., Atasu, A., Ergun, Ö., and Toktay, L. B. (2016). Efficient implementation of collective extended producer responsibility legislation. Management Science, *62(4):1098–1123.*

Hamilton, J. D. (2020). Time Series Analysis. *Princeton University Press.*

Harbaugh, R., Maxwell, J. W., and Roussillon, B. (2011). Label confusion: The groucho effect of uncertain standards. Management Science, *57(9):1512–1527.*

Hasija, S., Shen, Z.-J. M., and Teo, C.-P. (2020). Smart city operations: Modeling challenges and opportunities. Manufacturing & Service Operations Management, *22(1):203–213.*

He, L., Hu, Z., and Zhang, M. (2020). Robust repositioning for vehicle sharing. Manufacturing & Service Operations Management, *22(2):241–256.*

He, L., Mak, H.-Y., Rong, Y., and Shen, Z.-J. M. (2017). Service region design for urban electric vehicle sharing systems. Manufacturing & Service Operations Management, *19(2):309–327.*

He, Q.-C., Nie, T., Yang, Y., and Shen, Z.-J. (2021). Beyond repositioning: Crowdsourcing and geo-fencing for shared-mobility systems. Production and Operations Management, *30(10):3448–3466.*

Heyes, A. and Martin, S. (2016). Social labeling by competing ngos: A model with multiple issues and entry. Management Science, *63(6):1800–1813.*

Heyes, A. G. and Maxwell, J. W. (2004). Private vs. public regulation: political economy of the international environment. Journal of Environmental Economics and Management, *48(2):978–996.*

Horwitz, J. (2017). One of China's Top Bike-sharing Startups is Now Paying Users to Ride Its Bikes. *https://qz.com/942372/mobike-one-of-chinas-top-bike-sharing-startups-is-now-paying-users-to-ride-its-bikes/ One of China's Top Bike-sharing Startups is Now Paying Users to Ride Its Bikes, accessed: January 27, 2022.*

Huang, J., Chou, M. C., and Teo, C.-P. (2021). Bike-repositioning using volunteers: Crowd sourcing with choice restriction. In Proc. of the AAAI Conference on Artificial Intelligence, *pages 11844–11852.*

Huang, X., Atasu, A., and Toktay, L. B. (2019). Design implications of extended producer responsibility for durable products. Management Science, *65(6):2573–2590.*

Iyer, G. and Singh, S. (2018). Voluntary product safety certification. Management Science, *64(2):695–714.*

Jian, N., Freund, D., Wiberg, H. M., and Henderson, S. G. (2016). Simulation optimization for a large-scale bike-sharing system. In 2016 Winter Simulation Conference (WSC), *pages 602–613. IEEE.*

Judith Evans, M. P. and Hook, L. (2020). Pandemic sets back fight against single-use plastic. *https://www.ft.com/content/c479a718-36a6-48e2-8632-a77290fc223a, accessed: December 30, 2020.*

Kabra, A., Belavina, E., and Girotra, K. (2020). Bike-share systems: Accessibility and availability. Management Science, *66(9):3803–3824.*

Kafle, N., Zou, B., and Lin, J. (2017). Design and modeling of a crowdsource-enabled system for urban parcel relay and delivery. Transportation Research Part B: Methodological, *99:62–82.*

Kunz, N., Mayers, K., and Van Wassenhove, L. N. (2018). Stakeholder views on

extended producer responsibility and the circular economy. California Management Review, *60(3):45–70.*

Lee, H. L. and Tang, C. S. (2018). Socially and environmentally responsible value chain innovations: New operations management research opportunities. Management Science, *64(3):983–996.*

Li, Y. (2020). Competing eco-labels and product market competition. Resource and Energy Economics, *page 101149.*

Li, Y. and van 't Veld, K. (2015). Green, greener, greenest: Eco-label gradation and competition. Journal of Environmental Economics and Management, *72:164–176.*

Lim, M. K., Mak, H.-Y., and Park, S. J. (2019). Money well spent? operations, mainstreaming, and fairness of fair trade. Production and Operations Management, *28(12):3023–3041.*

Lizzeri, A. (1999). Information revelation and certification intermediaries. The RAND Journal of Economics, *pages 214–231.*

Lu, M., Chen, Z., and Shen, S. (2018). Optimizing the profitability and quality of service in carshare systems under demand uncertainty. Manufacturing & Service Operations Management, *20(2):162–180.*

Mak, H.-Y. (2022). Enabling smarter cities with operations management. Manufacturing & Service Operations Management, *24(1):24–39.*

Mason, C. F. (2011). Eco-labeling and market equilibria with noisy certification tests. Environmental and Resource Economics, *48(4):537–560.*

McKinsey (2019). Micromobility's 15,000-mile Checkup. *https://www.mckinsey.com/industries/automotive-and-assembly/our-insights/micromobilitys-15000-mile-checkup*, *accessed: January 27, 2022.*

McKinsey (2021). Why micromobility is here to stay. *https://www.mckinsey.com/industries/automotive-and-assembly/our-insights/why-micromobility-is-here-to-stay*, *accessed: January 27, 2022.*

MTA (2020). Subway and bus ridership for 2019. *https://new.mta.info/a*

gency/new-york-city-transit/subway-bus-ridership-2019, *accessed: January 27, 2022.*

Murali, K., Lim, M. K., and Petruzzi, N. C. (2019). The effects of ecolabels and environmental regulation on green product development. Manufacturing & Service Operations Management, *21(3):519–535.*

Murray, D. and Glidewell, S. (2019). An Analysis of the Operational Costs of Trucking: 2019 Update. https://truckingresearch.org/wp-content/uploads/2019/11/ATRI-Operational-Costs-of-Trucking-2019-1.pdf, *accessed: January 27, 2022.*

Nadar, E. and Ertürk, M. S. (2020). Eco-design of eco-labels with coarse grades. Omega, *page 102209.*

Nair, R. and Miller-Hooks, E. (2011). Fleet management for vehicle sharing operations. Transportation Science, *45(4):524–540.*

Nair, R. and Miller-Hooks, E. (2014). Equilibrium network design of shared-vehicle systems. European Journal of Operational Research, *235(1):47–61.*

Negahban, A. (2019). Simulation-based estimation of the real demand in bike-sharing systems in the presence of censoring. European Journal of Operational Research, *277(1):317–332.*

NYC DOT (2019). Mobility Report. NYC Department of Transportation. https://www1.nyc.gov/html/dot/downloads/pdf/mobility-report-2019-print.pdf, *accessed: January 27, 2022.*

O'Mahony, E. and Shmoys, D. (2015). Data analysis and optimization for (citi) bike sharing. In Proceedings of the AAAI Conference on Artificial Intelligence, *volume 29.*

Örsdemir, A., Kemahlıoğlu-Ziya, E., and Parlaktürk, A. K. (2014). Competitive quality choice and remanufacturing. Production and Operations Management, *23(1):48–64.*

PEFC Council (2008). PEFC Logo Usage Rules – Requirements. https://cdn.scsglobalservices.com/files/standards/pefc_st_2001-20

08_v2-0_en_pefclogousage_20101126.pdf, accessed: December 30, 2020.

Plambeck, E. L. and Taylor, T. A. (2016). Supplier evasion of a buyer's audit: Implications for motivating supplier social and environmental responsibility. Manufacturing & Service Operations Management*, 18(2):184–197.*

Qi, W., Li, L., Liu, S., and Shen, Z.-J. M. (2018). Shared mobility for last-mile delivery: Design, operational prescriptions, and environmental impact. Manuf. & Service Operations Management*, 20(4):737–751.*

Qi, W. and Shen, Z.-J. M. (2019). A smart-city scope of operations management. Production and Operations Management*, 28(2):393–406.*

Rahmani, M., Gui, L., and Atasu, A. (2021). The implications of recycling technology choice on extended producer responsibility. Production and Operations Management*, 30(2):522–542.*

Schlosser, R., Chenavaz, R. Y., and Dimitrov, S. (2021). Circular economy: Joint dynamic pricing and recycling investments. International Journal of Production Economics*, 236:108117.*

SCS Global Services (2014). Recycled Content Standard V7.0. *https://cdn.scsglobalservices.com/files/standards/scs_stn_recycledcontent_v7-0_070814.pdf, accessed: December 30, 2020.*

Shephard, R. W. and Färe, R. (1974). The law of diminishing returns. Zeitschrift für Nationalökonomie*, 34(1-2):69–90.*

Shu, J., Chou, M. C., Liu, Q., Teo, C.-P., and Wang, I.-L. (2013). Models for effective deployment and redistribution of bicycles within public bicycle-sharing systems. Operations Research*, 61(6):1346–1359.*

Simlett, J. and Møller, T. H. (2020). Micromobility: Moving Cities into a Sustainable Future. *https://assets.ey.com/content/dam/ey-sites/ey-com/en_gl/topics/automotive-and-transportation/automotive-transportation-pdfs/ey-micromobility-moving-cities-into-a-sustainable-future.pdf, accessed: January 27, 2022.*

Singla, A., Santoni, M., Bartók, G., Mukerji, P., Meenen, M., and Krause, A.

(2015). Incentivizing users for balancing bike sharing systems. In Proc. of the AAAI Conference on Artificial Intelligence*, pages 723–729.*

Soriguera, F., Casado, V., and Jiménez, E. (2018). A simulation model for public bike-sharing systems. Transportation Research Procedia*, 33:139–146.*

Souza, G. C. (2013). Closed-loop supply chains: A critical review, and future research. Decision Sciences*, 44(1):7–38.*

Stahl, K. and Strausz, R. (2017). Certification and market transparency. The Review of Economic Studies*, 84(4):1842–1868.*

Tagaras, G. and Cohen, M. A. (1992). Pooling in two-location inventory systems with non-negligible replenishment lead times. Management Science*, 38(8):1067–1083.*

UL (2019). Recycled Content Validation. https://www.ul.com/services/recycled-content-validation*, accessed: December 30, 2020.*

Verus Carbon Neutral (2019). Recycled Content Certification. http://www.verus-co2.com/RecycledContentCert.htm*, accessed: December 30, 2020.*

Yenipazarli, A. (2015). The economics of eco-labeling: Standards, costs and prices. International Journal of Production Economics*, 170:275–286.*

Youssef, A. B. and Lahmandi-Ayed, R. (2008). Eco-labelling, competition and environment: Endogenization of labelling criteria. Environmental and Resource Economics*, 41(2):133–154.*

Zapechelnyuk, A. (2020). Optimal quality certification. American Economic Review: Insights*, 2(2):161–76.*